

**SEISMIC VULNERABILITY ASSESSMENT OF MASONRY
INFILLED REINFORCED CONCRETE SCHOOL
BUILDING FRAMES IN SRI LANKA**

Mathavanayakam Sathurshan

(218112V)

Degree of Master of Science

Department of Civil Engineering

University of Moratuwa
Sri Lanka

November 2022

**SEISMIC VULNERABILITY ASSESSMENT OF MASONRY
INFILLED REINFORCED CONCRETE SCHOOL
BUILDING FRAMES IN SRI LANKA**

Mathavanayakam Sathurshan

(218112V)

Dissertation submitted in partial fulfillment of the requirement for the
degree of Master of Science in Structural Engineering

Department of Civil Engineering

University of Moratuwa
Sri Lanka

November 2022

DECLARATION

“I declare that this my own work and this dissertation does not incorporate without acknowledgement any material previously submitted for a Degree or Diploma in any other university or institute of higher learning and to the best of my knowledge and belief it does not contain any material previously published or written by other person except where the acknowledgement is made in the text.

Also, I hereby grant to University of Moratuwa the non-exclusive right to reproduce and distribute my dissertation, in whole or in part in print, electronic r other medium. I retain the right to use this content in whole or part in future works.”

Signature:.....

Date:...../...../.....
2023 03 18

The above candidate has carried out this research for the Master Dissertation under my supervision.

Name of the Supervisor: Prof. H. M. Y. C. Mallikarachchi

Signature of the supervisor:

Date:.....19../03../2023

Name of the Supervisor: Dr. J. A. Thamboo

Signature of the supervisor:

Date:..19...../03..../2023

Name of the supervisor: Prof. K. K. Wijesundara

Signature of the supervisor ***UOM Verified Signature*** te:...../...../.....

ACKNOWLEDGEMENT

I would like express my profound gratitude to **Prof. H. M. Y. C. Mallikarachchi** of the University of Moratuwa for accepting me as an MSc student and for his unfailing support throughout the wonderful trip. Also, the technical and administrative assistance he provided and his constant presence made it possible for me to fulfil aim of the study.

Also, I want to extent my sincere thanks to co-supervisor **Dr. J. A. Thamboo** at the South Eastern University of Sri Lanka for his guidance, for always standing as a true mentor throughout my research career, and for "opening the door for discussion" on any topic whenever I needed it and enlightened the contretemps. Equally, I would want to sincerely thank my co-supervisor **Prof. K. K. Wijesundara** at the University of Peradeniya, for his encouragement, untiring technical advice, constructively critical comments during the progress meetings and contributions significantly helped to achieve the aim of this study.

Next, I would also like to thank **Emeritus Prof. W. P. S. Dias** of the University of Moratuwa for serving as chairperson of the progress review committee and providing timely feedback on this project. I should also mention **Dr. T. M. N. Wijayaratna** for his support in the progress review meetings.

I wish to thank the Faculty of Graduate Studies, the University of Moratuwa for the opportunity to pursue my postgraduate studies. Also, I would like to acknowledge the financial assistance from the **National Academy of Sciences of Sri Lanka (NASSL)** in laying a foundation for my dream of a postgraduate research career. I also like to acknowledge that some of the school field surveys were funded by the **UK Global Challenge Research Fund project ReSCOOL** (Resilience of Schools to Extreme Coastal FLOODing Loads), awarded to **Prof. Tiziana Rossetto**, from University College London, by Research England; award No. 177813.

Moreover, I want to thank **Jonas Cels**, a doctoral candidate at University College London, for enlightening the OpenSees programme and clearing doubts at any time. The school building data acquisition would have been impossible without the help of E15 undergraduate students from the Department of Civil Engineering, South Eastern University of Sri Lanka: **B. M. N. D. Basnayaka, S. M. Faheem, A. Madursan, B. B. B. S. Bandara, D. G. H. S. Kalpage, D. M. N. S. Dasanayake**, and **T. P. A. Punyawardana**. I thank them all for their contributions to this study.

Last but far from least, I want to thank my family members and friends for their encouragement and immense patience until the end of this work.

ABSTRACT

Sri Lanka is considered as an aseismic country, hence the seismic risk is not explicitly considered in the planning and designing of critical structures. However, current studies indicate that the seismic risk cannot be completely omitted when designing buildings in Sri Lanka, particularly post-disaster structures like schools and hospitals that should be designed to withstand any potential seismic action. Meanwhile, assessing the seismic risk of all the critical structures in depth across Sri Lanka might not be an easy task, and therefore, the creation of a rapid assessment method would help to effectively screen the buildings which are seismically vulnerable.

Therefore, in this study, an attempt was made to assess the seismic vulnerability of school buildings in Sri Lanka in detail by incorporating possible variations and proposing an alternate Rapid Visual Screening method (RVS) for Sri Lankan conditions by incorporating FEMA P-154 guidance.

In order to study the existing school building typologies, detailed structural surveys were carried out across Sri Lanka in selected school buildings. The survey revealed that school buildings in Sri Lanka can be characterised as reinforced concrete (RC) frames, infilled with unreinforced masonry walls (MI). Based on the structural configurations, mainly two building typologies were found as (1) Type 01 and (2) Type 02. Nonetheless, in terms of MI arrangements, it was observed that significant variations exist among the school buildings. Therefore, those variabilities were explicitly taken to assess the seismic performance of MI-RC school buildings.

The seismic performance of the school buildings was analysed using the OpenSees (OS) finite element programme. The torsional effects and post-processing as shear capacity and stochastic material properties (concrete, steel, and masonry) from Monte-Carlo simulation were incorporated in this study. The modal analysis and non-linear static pushover analysis were carried out, in which a total of 640 building cases were analysed.

The analyses of pushover (PO) and seismic fragility revealed that the Type 02 buildings exhibit significantly better performance than the Type 01 buildings. Also, the variation in MI arrangements significantly influences the seismic resistance of the buildings. In addition, the application of the proposed RVS method is effective to carry out the seismic screening method of school buildings in Sri Lanka.

Keywords:

School buildings, Non-linear static pushover, Seismic performance assessment, Seismic Fragility assessment and Rapid visual screening method

TABLE OF CONTENTS

DECLARATION	II
ACKNOWLEDGEMENT	III
ABSTRACT.....	IV
TABLE OF CONTENTS.....	V
LIST OF FIGURES	IX
LIST OF TABLES	XII
LIST OF ABBREVIATIONS	XIV
1. INTRODUCTION.....	1
1.1 Background	1
1.2 Significant of the research	2
1.3 Aim and Objectives	2
1.4 Organisation of the thesis	3
2. LITERATURE REVIEW	4
2.1 Seismicity in and around Sri Lanka	4
2.2 Studies related seismic risk of infrastructure in Sri Lanka.....	6
2.2.1 Seismic assessment of school buildings - Local context.....	7
2.2.2 Seismic assessment of school buildings - Global context.....	8
2.3 Rapid seismic evaluation methods	11
2.3.1 The Regional based RVS - Guidelines	13
2.3.1.1 Unite States method (FEMA P-154).....	13
2.3.1.2 New Zealand method (NZSEE)	14
2.3.1.3 Canadian RVS (NRC92).....	15
2.3.1.4 Other RVS methods	16
2.4 Development of rapid visual screening method	24

2.4.1	Development of basic score and score modifiers	24
2.4.1.1	Basic score for RC-MI buildings (C3).....	24
2.4.1.2	Score modifiers for RC-MI buildings (C3).....	27
2.5	Summary	29
3.	METHODOLOGY	30
4.	SURVEY OF SELECTED SCHOOL BUILDINGS	32
4.1	List of Schools Surveyed.....	32
4.2	Identified typologies.....	33
4.2.1	Typologies based on the storey level.....	33
4.2.2	Typologies based on arrangements	34
4.3	Material and sectional properties	35
4.4	Infill (MI) configuration.....	37
4.5	Summary	39
5.	MODELING OF SCHOOL BUILDINGS TYPOLOGIES	40
5.1	Modeling using OpenSees.....	40
5.1.1	Defining beam and column section	41
5.1.2	Defining slabs (Multi-point constraints)	42
5.1.3	Defining foundation (Single point constraints)	43
5.2	Modelling of MI	44
5.3	Incorporating material variations	47
5.3.1	Material characteristics from survey	47
5.3.2	Material uncertainty characterisation	47
5.4	Pushover analysis and post processing of results.....	49
5.4.1	Pushover analysis (PO).....	49
5.4.2	Post processing	53
5.4.2.1	Sectional moment capacity validation	54

5.5 Seismic performances of the school buildings typologies	55
5.5.1 Transverse direction (Y-direction)	55
5.5.2 Longitudinal direction (X-direction)	56
5.5.2.1 Effects of OGS and FGS	56
5.5.2.2 Effects of typologies (T01 and T02)	57
5.5.2.3 Effects of MI configurations	59
5.5.2.4 Effects of material variations	61
5.6 Summary	63
6. DEVELOPING FRAGILITY CURVES	64
6.1 Defining the limit state for fragility functions.....	65
6.2 Development of fragility curves.....	67
6.3 Fragility curves.....	69
6.4 Damage matrices	72
6.5 Summary	74
7. RAPID VISUAL SCREENING (RVS) OF BUILDINGS FOR POTENTIAL SEISMIC HAZARDS	75
7.1 Concept of RVS for school buildings typologies.....	75
7.2 Establishment RVS method for local context	77
7.2.1 Development of Basic Score	78
7.2.2 Development of Score Modifiers	79
7.2.2.1 Open Ground Storey	80
7.2.2.2 Plan Irregularities (Horizontal)	81
7.2.2.3 Vertical Irregularities	83
7.2.2.4 Short-column effect	84
7.2.3 Minimum Score Evaluation.....	85
7.3 Assessment of proposed RVS method	86

7.3.1 Comparison between Proposed RVS and FEMA P-154	90
7.4 Summary	91
8. SUMMARY AND CONCLUSION	92
8.1 Summary of the study.....	92
8.2 Key findings	94
8.3 Future research	95
REFERENCES	97
A. Appendix A: selected surveyed school buildings details	108
B. Appendix B: ideal cases	117
C. Appendix C: opensees and monte carlo simulation coding	118
D. Appendix D: adaptation of score modifiers	128

LIST OF FIGURES

Figure 2-1. Seismicity in and around Sri Lanka.	5
Figure 2-2. (a) Longitudinal and (b) transverse fragility curves of immediate and collapse prevention of three-storey school building (Abey Siriwardena, 2018)	7
Figure 2-3. Short column formation due to strong MI.....	8
Figure 2-4. Summary of the RVS guidelines from different countries.....	12
Figure 2-5. FEMA P-154 Level 1 scoring evaluation table (Low seismicity region) 14	
Figure 2-6. IEP procedure to evaluate the NBS%	15
Figure 2-7. Canadian screening method (NRCC).....	16
Figure 2-8. Turkish (METU) RVS method.....	17
Figure 2-9. Indian probability and statistical based RVS	20
Figure 2-10. Procedure to adapt the basic score and Score modifiers	26
Figure 2-11. Irregularities in building for score modifiers adaption.....	28
Figure 3-1. Methodology of the study	31
Figure 4-1. Selected survey school buildings in Sri Lanka.....	32
Figure 4-2. Some of the surveyed school buildings (two and three storeys).....	33
Figure 4-3. Type-01 building with OGS and FGS illustration	34
Figure 4-4. Type-02 building with OGS illustration	35
Figure 4-5. RC section of T01 and T02	36
Figure 4-6. MI configuration (CW, QO, HO, and TO) in Sri Lankan school buildings	38
Figure 4-7. Summary of school building surveyed.....	39
Figure 5-1. Simplified analysis procedure of OS model.....	40
Figure 5-2. Reinforcement layer (confined and unconfined).....	41
Figure 5-3. Beam and column integration points.....	42
Figure 5-4. Multi Point constraints (MP constraints)	43
Figure 5-5. Single Point constraints (SP constraints)	43
Figure 5-6. Equivalent diagonal strut width of MI	44
Figure 5-7. 3D model of Type 01 (T01) three storey.....	46
Figure 5-8. 3D model of Type 02 (T02) three storey building with HO cases.....	46

Figure 5-9. The distribution of 1000 random samples (a) concrete – normal distribution, (b) steel – lognormal distribution and (c) masonry – normal distribution	48
Figure 5-10. Iterative pushover analysis procedure for the seismic performance assessment of MI frames incorporating shear demand parameters.....	50
Figure 5-11. Pushover graph of T01 and T02 of Bare frame (BF)	51
Figure 5-12. PO analysis results of torsional stiffness (TS) and non-torsional stiffness (NTS) of T01-S03-OGS-SW-CW cases	52
Figure 5-13. Moment-curvature comparison of OS and Response-2000 results of column section	54
Figure 5-14. Peak inter-storey drift ratio of T01-S03 cases with various MI configuration (CW, QO, HO, and TO) considering OGS and FGS	55
Figure 5-15. Y-direction PO curves of BF, QO and HO with different storey level.	56
Figure 5-16. Performance of T01-S03 building with different MI configurations along the along the <i>x</i> direction	57
Figure 5-17. Performance of T02-S03 building with different MI configurations along the <i>x</i> direction.....	58
Figure 5-18. Performance of T02-S02 building with different MI configurations along the <i>x</i> direction	60
Figure 5-19. PO curves of T01-S03-FGS-DW-QO buildings with different material properties.....	62
Figure 6-1. Flowchart of the fragility analysis procedure of the RC-MI school buildings.....	65
Figure 6-2. Variations in the school buildings considered (ideal cases and material uncertainty)	68
Figure 6-3. Fragility curve of the school buildings with respect to provinces – X direction (Western, South, Central, and Eastern provinces	70
Figure 6-4. Fragility curve of the school buildings with respect to provinces – Y direction (Western, South, Central, and Eastern provinces).....	71
Figure 6-5. Damage probability matrices with respect to provinces	73
Figure 7-1. Selected schools for rapid assessment methods	75

Figure 7-2. Seismic hazard map for 475 years of return periods (Uduweriya et al. (2020)).....	77
Figure 7-3. Basic score evaluation for Zone- I buildings	78
Figure 7-4. Open Ground Storey of T01 and T02 buildings.....	80
Figure 7-5. Plan irregularity of the school building.....	82
Figure 7-6. Vertical Irregularities in School buildings	83
Figure 7-7. Short column effect in school buildings.....	84
Figure 7-8. Minimum score evaluation (Worst case scenario)	85
Figure 7-9. Preliminary data collection portion in proposed RVS form.....	86
Figure 7-10. Photograph/ layout portion in proposed RVS form	87
Figure 7-11. Detailed data survey portion in proposed RVS form	87
Figure 7-12. Building risk score portion in proposed RVS form	88
Figure 7-13. Example of sample proposed RVS form.....	89
Figure 8-1. Summary of the study methods and findings	94

LIST OF TABLES

Table 2-1. Gravity loading condition designed school buildings - Global context ...	10
Table 2-2. Summary of RVS methods	23
Table 2-3. Collapse factor adapted from FEMA (2020)	27
Table 5-1. Mean material properties	47
Table 5-2. Material COV and the distribution used for the Monte Carlo simulation	48
Table 6-1. Definition of damage state of the school building for Sri Lanka	66
Table 7-1. Existing RVS scores/grades of school buildings	76
Table 7-2. Complete MI case (FW) - Basic score evaluation	79
Table 7-3. Open Ground Storey score modifiers	81
Table 7-4. Plan irregularities score modifiers	82
Table 7-5. Vertical irregularities score modifiers	83
Table 7-6. Score modifiers for short column effects	85
Table 7-7. Minimum score of the T01 and T02 buildings	86
Table 7-8. The proposed and FEMA P-154 results	90
Table A-1. Selected surveyed school buildings details.....	109
Table A-2. School building structural details	111
Table A-3. School building non-structural details	114
Table B-1. T01 building with MI configurations.....	117
Table D-1. Open Ground Storey effects	128
Table D-2. T01 Score modifiers for Open Ground Storey DW cases	128
Table D-3. T01 Score modifiers for Open Ground Storey SW cases	129
Table D-4. T02 Score modifiers for Open Ground Storey DW cases	129
Table D-5. T02 Score modifiers for Open Ground Storey DW cases	129
Table D-6. Plan Irregularity cases	130
Table D-7. T01 Score modifiers for plan irregularities DW cases	131
Table D-8. T01 Score modifiers for plan irregularities SW cases	131
Table D-9. T02 Score modifiers for plan irregularities DW cases	132
Table D-10. T02 Score modifiers for plan irregularities SW cases	132
Table D-11. Vertical Irregularity cases.....	133
Table D-12. T01 Score modifiers for Vertical irregularities DW cases	134

Table D-13. T01 Score modifiers for Vertical irregularities SW cases	135
Table D-14. T02 Score modifiers for Vertical irregularities DW cases	136
Table D-15. T02 Score modifiers for Vertical irregularities SW cases	137

LIST OF ABBREVIATIONS

<i>ADRS</i>	-	Acceleration Displacement Response Spectrum
<i>ATC</i>	-	Applied Technology Council
<i>CC</i>	-	Capacity Curve
<i>CDS</i>	-	Capacity Demand Spectrum method
<i>CF</i>	-	Collapse Factors
<i>CW</i>	-	Central Window
<i>d</i>	-	Displacement
<i>Du</i>	-	Ultimate displacement
<i>DW/SW</i>	-	Doubly or Single thickness masonry wall
<i>Dy</i>	-	Yield displacement
<i>FEMA</i>	-	Federal Emergency Management Agency
<i>FGS</i>	-	Fully closed Ground Storey
<i>HAZUS</i>	-	Hazard in United States
<i>HO</i>	-	Half Opening wall
<i>IEP</i>	-	Initial Evaluation Procedure
<i>ISA</i>	-	Initial Seismic Assessment
<i>JBDPA</i>	-	Japan Building Disaster Prevention Association
<i>MCS</i>	-	Monte-Carlo Simulation
<i>METU</i>	-	Metropolitan Municipality of Istanbul
<i>MI</i>	-	Masonry Infills
<i>NBS%</i>	-	New Building Standard percentage
<i>NLSPA</i>	-	Non-Linear Static Pushover Analysis
<i>NRCC</i>	-	National Building Council of Canada
<i>NSI</i>	-	Non-Structural Index
<i>OGS</i>	-	Open Ground Storey
<i>OS</i>	-	OpenSees
<i>PC</i>	-	Precast Concrete
<i>PO</i>	-	Pushover
<i>QO</i>	-	Quarter Opening wall
<i>RC</i>	-	Reinforced Concrete
<i>RC-MI</i>	-	Masonry Infilled Reinforced Concrete
<i>RM</i>	-	Reinforced Masonry
<i>RVS</i>	-	Rapid Visual Screening
<i>S02/S03</i>	-	Three or Two Storey
<i>Sa</i>	-	Spectral Acceleration
<i>Sd</i>	-	Spectral Displacement
<i>SI</i>	-	Structural Index
<i>T01/T02</i>	-	Type-01 or Type-02 buildings
<i>TO</i>	-	Three-quarter Opening wall
<i>URM</i>	-	Unreinforced Masonry
<i>V</i>	-	Base Shear

1. INTRODUCTION

1.1 Background

Sri Lanka is situated in the middle of the Indo-Australian plate; therefore, the seismic risk and related preparedness protocols are not generally included in designing the infrastructure systems. However, the historical earthquake records in and around Sri Lanka (Fernando & Kulasinghe, 1986; Seneviratne, Perera, et al., 2020) reveal, that the country cannot be considered as aseismic and occasional intra-plate earthquakes have occurred in the past. Recent studies stated that the failed Mannar Rift zone (Mannar Basin) and the Comorin Ridge are located closer to Sri Lanka (western coastal region of Sri Lanka), and they have the potential to trigger intra-plate earthquakes in magnitudes ranging from 6.5–6.9 Mw with a return period of 475 years (Seneviratne, Perera, et al., 2020; Seneviratne, Wijesundara, et al., 2020). Therefore, it is essential to conduct possible seismic risk assessments according to local contexts, especially for post-disaster structures such as schools and hospitals that are not planned in accordance with relevant seismic hazards in Sri Lanka. This study focused on assessing the seismic performance, vulnerability and damage probabilities of school buildings in Sri Lanka. Subsequently, attempts were made to (1) derive probabilistic damage states with respect to seismic fragility curves, and (2) develop a simplified seismic rapid visual screening method (RVS) for the existing school building typologies in Sri Lanka.

According to the Department of Census and Statistics in Sri Lanka (Ministry of Education, 2020), there are 10,155 schools functioning with 4,063,685 pupils and 249,494 teachers, accounting for nearly 20% of the total population of the country. However, Sri Lankan school buildings are designed only for the gravity loading combinations, and the possible seismic actions are not directly incorporated in the design stage (Abesiriwardena, 2018; Marasingha, 2013).

Generally, the school buildings in Sri Lanka can be classified as single to three-storey buildings, where the single-storey buildings are generally constructed with unreinforced masonry (URM) and the other categories are constructed of reinforced concrete (RC) frames with masonry infills (MI). This study focused on examining the

seismic performances of masonry infilled reinforced concrete (RC-MI) school buildings, as majority of the school buildings fall under this category. However, there are significant variations in terms of the arrangements and thicknesses of MI used in those RC-MI school buildings and their impact into the seismic responses should properly be assessed. It is well understood that the MI walls can interact with the surrounding RC frame during a seismic action; therefore, the contribution of MI walls should be taken into account in the design stage, which was not considered in the existing RC-MI school buildings in Sri Lanka. Consequently, systematic research studies are needed to assess the seismic risks of the RC-MI school buildings in Sri Lanka to establish suitable mitigation measures in the future.

1.2 Significant of the research

The significance of this study involves assessing the seismic risk of RC-MI school building typologies prevail across the country. In addition, fragility curves are developed using a performance-based approach to comprehend the overall damage probabilities under seismic scenarios. Finally, a simplified seismic rapid visual screening (RVS) method is proposed for the existing RC-MI building typologies, along with seismic structural scores to the school building typologies in different provinces of Sri Lanka.

1.3 Aim and Objectives

The aim of the study was to develop a simplified RVS method to evaluate the seismic risk of RC-MI school building typologies in Sri Lanka. The objectives set to achieve the aim of this study are given below:

- Conduct a detailed structural survey of selected school buildings to understand the structural and non-structural configurations used
- Assess the seismic performance of RC-MI school building typologies through a numerical approach
- Establish seismic fragility curves based on the damage sequences of the school building typologies
- Determine basic scores and score modifiers for the RC-MI school buildings, incorporating observed structural and non-structural attributes

- Propose a simplified RVS method to assess the seismic risk of RC-MI school buildings typologies

1.4 Organisation of the thesis

This thesis contains eight chapters:

Chapter 1: The brief background, significance, aim and objectives of this research study are presented.

Chapter 2: The possible earthquake hazards in Sri Lanka and previous studies related to seismic assessment of school buildings are highlighted in the literature review. Also, the available RVS methods of seismic risk assessments and their drawbacks in assessing the low-rise RC-MI buildings with irregularities in MI configurations and arrangements are emphasised.

Chapter 3: The methodology adopted in this research study to achieve the aim and objectives are outlined in this chapter.

Chapter 4: This chapter provides the summary of structural survey carried out in the selected school buildings. The common structural typologies and non-structural configurations used in the RC-MI school buildings surveyed are explained.

Chapter 5: The details of numerical modelling procedures implemented to assess the seismic performance of the RC-MI school building typologies using the Open System for Earthquake Engineering Simulation (OpenSees) programme are described in this chapter.

Chapter 6: The failure sequences of RC-MI school building typologies analysed and the method used to develop seismic fragility curves are discussed in this chapter. The definition of damage thresholds and damage matrices with regard to seismic hazards across the country are also provided.

Chapter 7: In this chapter, the development of seismic RVS procedure to evaluate the seismic risk of the RC-MI building typologies considered are explained.

Chapter 8: The summary and the key findings of this research study are given in this chapter. Also, the recommendation for future studies are mentioned.

2. LITERATURE REVIEW

The literature review was focused on understanding the seismic risk of Sri Lanka and the available assessment methods to determine seismic performance of RC-MI typological school buildings. The first sub-section (Section 2.1) provides information regarding the seismicity in and around Sri Lanka. Section 2.2 summarises the previous studies conducted on evaluating the seismic performance of different infrastructures and school buildings in Sri Lanka and other countries. Sections 2.3 and 2.4 provide the available rapid seismic evaluation methods and their limitation to assess the RC-MI buildings with variations in MI arrangements.

2.1 Seismicity in and around Sri Lanka

The Uniform Building Code (UBC, 1997) characterised Sri Lanka (Colombo) as zero on a scale of zero to four, seismic zone classifications, denoting as a lower seismic region. Meanwhile, past earthquake records reveal that intra-plate earthquakes are probable (Aluthapala, 2016; Dissanayake, 2005; Lewangamage & Kularathna, 2015) in and around Sri Lanka. The term "intra-plate earthquake" refers to an earthquake that occurs within the plate as opposed to the term "inter-plate earthquake," which refers to the earthquakes that occur at the plate borders. Additionally, it has been shown that the inter-plate earthquakes, induce higher corner frequencies and release more energy than the intra-plate earthquakes (Leyton et al., 2009).

The earthquakes recorded in and around Sri Lanka between year 1900 and 2021 are shown in Figure 2-1. Altogether around 1957 number of earthquake records were obtained from the numerous resources from past studies and the database (*Data Management Center, 2022; International Seismological Centre, 2022; Fernando & Kulasinghe, 1986; Seneviratne, Perera, et al., 2020; USGS-NEIC, 2020*) and plotted using ArcGIS software (ESRI, 2018). It can be observed from Figure 2-1, that the majority of the earthquakes were reported near Sunda subduction zones (Curry, 1989) and the Katrol Hill Fault (India-Kutch area in Gujarat) (Suribabu et al., 2022; Tiwari et al., 2021). In India, the high intensity earthquakes have been reported in north-east region to south-west, in Indian fault regions (Ongole to Kerala), and they possess no substantial impact to Sri Lanka, except in the northern region of the country

(Seneviratne, Perera, et al., 2020). The intra-plate seismicity around the country can be divided into three categories (marked in Figure 2-1): (1) South and Southeast regions (North Indian region and Bay of Bengal), (2) West of Sri Lanka (Laccadive Sea and Gulf of Mannar) and (3) North of Sri Lanka (South Indian Peninsula region) (Gamage, 2015). However, the western coastal area of Sri Lanka, where the Mannar Rift Zone and the Comorin Ridge Zone are the critical seismic inducers for Sri Lanka, and they can be the epicentre of intra-plate earthquakes in Sri Lanka according to Seneviratne et al. (2020).

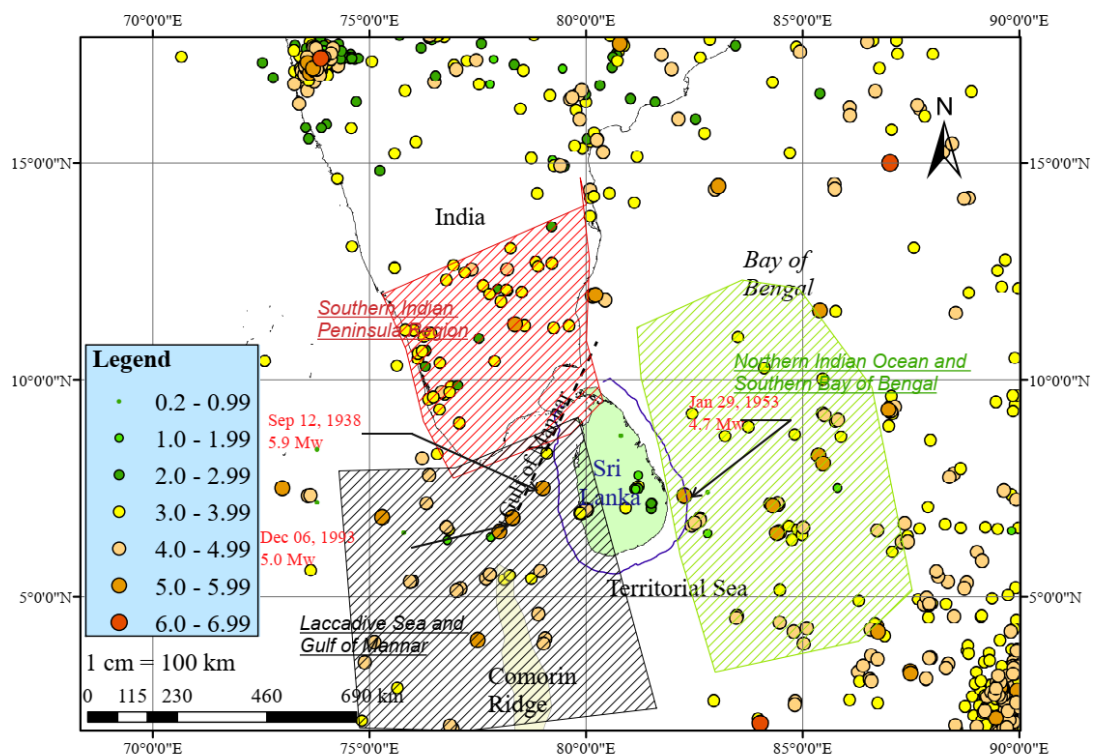


Figure 2-1. Seismicity in and around Sri Lanka.

There have also been several discussions about the separation of the Indo-Australian Plate (braking zone), which is approximately 1000 km from Southern edge of India (Van Orman et al., 1995). Consequently, Dissanayake (2005) stated that a new plate boundary is located 400-500 km away from Sri Lanka, therefore the country should be considered as “moderate earthquake prone region”. Additionally, Fernando & Kulasinghe, (1986) hypothesized that the Mahiyanganaya region and along Mahalweli shear zone are the potential micro seismic zones inside the country. Therefore, it can

be said that the seismic risks in Sri Lanka are clearly highlighted in the historical records and the past studies reported; therefore, it is crucial to conduct seismic risk assessments in the local terms. Therefore, proper efforts can be made to design infrastructures to withstand possible seismic hazards in the country.

2.2 Studies related seismic risk of infrastructure in Sri Lanka

The critical infrastructures in the country should be designed against probable seismic hazards. Therefore, it is important to ensure that infrastructures are seismically safe to provide services aftermath of any earthquake. The seismic performance of the buildings can be influenced by various factors such as soil condition, geometry of the buildings (irregularities), pounding effects, structural typologies, etc... The focus of this literature review was on the seismic performance evaluation of structures, particularly the school buildings.

Earlier, Jayasinghe et al. (1997) proposed an earthquake design technique for Sri Lanka from Australian AS 1170.4 (AS/NZS 1170.4, 2018) considering seismic activities are similar between Australia and Sri Lanka; additionally, the acceleration coefficient was declared as 0.04 for masonry infilled framed structures. Based on Eurocode 8 (EN 1998-1: 2004), IS 1893-1: 2002 and AS 1170.4: 2007, Lewangamage & Kularathna (2015) proposed national seismic analysis guideline for Sri Lankan buildings and stated that the peak ground acceleration (PGA) with 475 years of return period can be assumed to be 0.1 g and the IS 1893-1: 2002 elastic response spectra can be used for seismic analysis. Moreover, Prasanna (2016) compared different codes of practises to conduct the seismic analysis in local context, and the study recommended EN 1998-1: 2004, for seismic analyses in Sri Lanka.

Although Sri Lanka has no separate codes of practices for evaluating and designing structures against seismic actions, it should be highlighted that the National Building Research Organization (NBRO, 2015) has presented a national guidelines, where the planning against earthquakes is emphasised and then the structural design criteria of the buildings against earthquakes are suggested by the Society of Structural Engineers, Sri Lanka guidelines (SSESL, 2006).

2.2.1 Seismic assessment of school buildings - Local context

In Sri Lanka, relatively few research studies have been undertaken to assess the seismic performance of school buildings. A three story RC-MI school building was subjected to a seismic vulnerability assessment by Kularatne (2010). The study has considered the effect of the infill walls, which does not resist the horizontal forces also were taking into the account and the modified design was proposed based on the AS 1170.4 (AS/NZS 1170.4, 2018). Similarly, the importance of achieving the essential criteria based on the FEMA P-58 (ATC, 2018) guidelines to ensure the safety of the two-storey school buildings, which has low ductility and unfavourable drift ratio was discussed by Marasingha (2013). The two-story school building subjected to seismic actions revealed only minor structural damage, however a return period of 2475 years indicated unfavourable drift concentration on the building analysed. However, the study has certain limitation, as it did not include the effects of masonry infills in the school buildings (Marasingha, 2013). Based on the findings from the numerical and fragility analyses, Abey Siriwardena (2018) suggested improving the moment capacity of beams in the longitudinal direction of the school buildings to increase the seismic capacity of the buildings. The longitudinal fragility of three-storey school building obtained from incremental dynamic analysis is shown in Figure 2-2. As per the spectral acceleration value (i.e. 0.25g) for the first mode period of Sri Lanka, the probability of exceedances obtained were 40% and 2% for immediate occupancy and collapse prevention, respectively for the school building was examined.

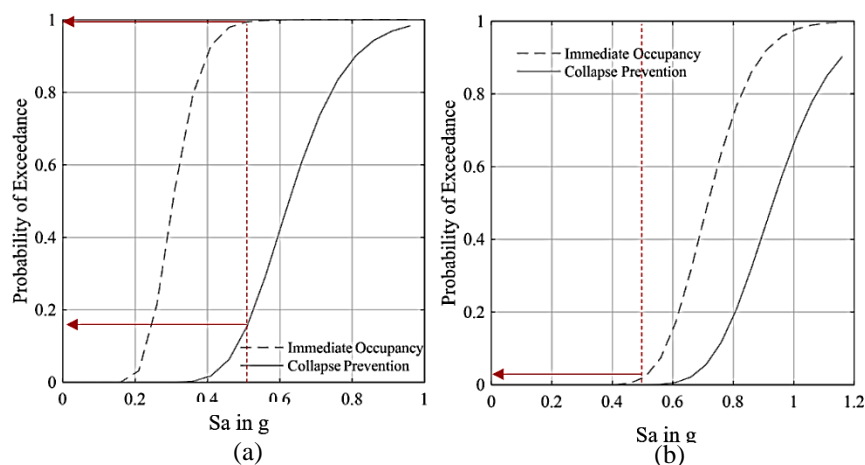


Figure 2-2. (a) Longitudinal and (b) transverse fragility curves of immediate and collapse prevention of three-storey school building (Abey Siriwardena, 2018)

2.2.2 Seismic assessment of school buildings - Global context

Several studies have been conducted on evaluating the seismic vulnerabilities of various school building typologies across the World. Table 2-1 gives a summary of past studies reported on assessing the seismic performance of school building typologies. The focus was given to retrieve the studies that assessed the building typologies designed only against gravity loading combinations. Most of the studies have been carried out to assess the seismic vulnerability through qualitative (Anelli et al., 2019) and quantitative viewpoints in countries with higher seismicity. O'Reilly et al. (2018) performed the seismic loss estimation of school buildings in Italy made of RC-MI, unreinforced masonry (URM), and precast concrete (PC) buildings, and the findings revealed that the URM types are more vulnerable, compared to RC-MI and PC school buildings. Similarly, the investigation revealed that the total drift capacity of the buildings was lower as a result of strong infill interactions, which resulted in short column development (shown in Figure 2-3) in the buildings, when shear capacity requirements were included in the analysis (O'Reilly & Sullivan, 2017). A seismic vulnerability assessment method for existing school buildings in Italy was proposed by Domaneschi et al. (2021), and the findings indicated that the seismic indices generated for the school buildings had a lower index for the cases analysed using the PGA, which was 10% lower than the spectral acceleration (S_a) cases.

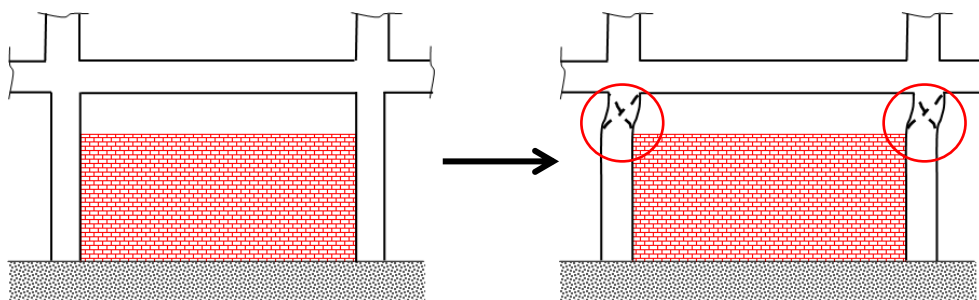


Figure 2-3. Short column formation due to strong MI

Adhikari & Gautam (2019) and Gautam et al. (2020) used the empirical framework to assess the seismic susceptibility of school buildings in Nepal, and the majority of the buildings were subjected to moderate to high earthquake risk. Similarly, 99% of the school buildings in Nepal were found to be not safe for the 9.0 Mw earthquakes, and

reported that about 80% of the buildings should be retrofitted to sustain against earthquakes (NSET, 2000). The RC-MI school buildings in Korea were evaluated to assess the economic effect of seismic retrofitting, where the non-retrofitted school buildings have shown 8–12% higher costs for the predicted earthquake damage than the retrofitted buildings (Dongwon et al., 2022). In Bangladesh, Alam & Haque (2020) evaluated the seismic vulnerability of school buildings through index-based approaches, and the assessment revealed that only 3.7% of buildings have shown to fall under low vulnerability category among 458 building cases considered. Rautela et al. (2020) revealed that 63.9% of the school buildings in the Himalayan provinces of India are located in the high seismic zone, and based on the earthquake hazard map, 78.5% of the buildings cannot be used after the earthquake occurred in that region.

It can be claimed that schools designed for gravity loading conditions are more vulnerable against seismic action. Although URM buildings are comparably more vulnerable (Vatteri et al., 2022), RC-MI buildings that are designed only for gravity loading are equally at risk under seismic loading (O'Reilly et al. 2018). Also, RC-MI buildings with stronger MI walls showed a reduction in the overall drift ratio, therefore higher strength properties of MI wall can induce relatively higher axial thrust to adjacent columns, thereby can cause short column failure (O'Reilly & Sullivan, 2017). In general, school buildings in the majority of developing countries demonstrated earthquake vulnerability due to a variety of factors, including irregularities in the structures, strong MI, which causes short column effects, soft storey mechanisms, poor construction quality and maintenance (Rodgers, 2012). These characteristics are also observed in Sri Lankan school buildings (Abey Siriwardena, 2018; Kularatne, 2010; Marasingha, 2013), demonstrating the need of carrying out thorough and affordable procedures to assess the seismic vulnerability of Sri Lankan school buildings. As a result, developing a RVS approach was the primary focus of this study to establish a simple and efficient way to comprehend the seismic risk of RC-MI school buildings in Sri Lanka.

Table 2-1. Gravity loading condition designed school buildings - Global context

Authors	Methods	Considerations	Remarks	Country
Dhungel et al. (2012)	1. Survey of schools	1. Physical facilities 2. School populations	1. Poor construction methods and materials 2. Limited resource	Nepal
Zain et al. (2019)	1. Survey of schools 2. Numerical analysis 3. Analytical fragility	1. Structural parameters 2. Intensity (peak ground acceleration and spectral acceleration)	1. Structural behaviours dominants by yielding	Pakistan (Zone 4)
O'Reilly & Sullivan (2017)	1. Numerical analysis 2. Loss estimation 3. Probabilistic seismic assessment 4. Shear behaviour of the columns	1. Expected demand 2. Overall collapse capacity	1. Structural and non-structural impacted on the overall performance	Italy
López et al. (2007)	1. Survey of schools 2. Non-linear static pushover (NLSP)	1. Old type of schools (50 years) 2. Box-type (20-30 years)	1. Old school buildings must be retrofitted 2. Box-type should be in the higher zone area	Venezuela
Gautam et al. (2020)	1. Survey of schools 2. Sensitivity analysis 3. Index based assessment	1. Structural and non-structural 2. Site condition 3. Seismic enhancement 4. Retrofitting 5. Workmanship	1. 90% of the building highly vulnerable	Nepal
(Tu et al., 2010)	1. Survey of schools 2. Non-linear static pushover (NLSP) 3. Capacity spectrum analysis	1. Failing behaviours (strong-beam-weak-column)	1. Damage states were defined 2. The analytical results undermine the for slight damage	Taiwan
Alam & Haque (2020)	1. RVS based survey of schools 3. Index based assessment	1. Expert opinions 2. Structural and systematic dimensions	1. Vulnerability map was developed 2. 23%, 46% and 27% buildings are high, moderate and moderate low vulnerability.	Bangladesh
Rautela et al. (2020)	1. RVS based survey of schools 2. Economical consideration	1. Structural and non-structural attributes 2. Pounding effect 3. Foundation 4. Damages	63.87% of the schools in Himalayan province in high earthquake risk zone	India

2.3 Rapid seismic evaluation methods

The seismic evaluation process can be categorised into three stages: (1) rapid visual assessment, (2) preliminary vulnerability assessment, and (3) detailed assessment (Nanda et al., 2019). The rapid visual screen (RVS) method is the simplest and quickest approach to evaluate the structural vulnerability of structures against earthquakes (Bektaş & Kegyes-Brassai, 2022). The RVS is generally conducted through a side-walk survey or from blueprints (ATC, 2015a). Therefore, RVS is the simplest method and can be used to assess the seismic risks of many buildings with limited time and resources (Harirchian et al., 2020). Following the RVS investigation, further assessments are required, such as detailed assessments and code-based assessments, can be performed to establish the seismic risk of structures. In this section, the existing RVS method to assess the seismic risk of structures are appraised.

The RVS for earthquakes was initially developed in the United States by the Applied Technical Council (ATC) along with the Federal Emergency Management Agency (FEMA) (ATC, 1988). Later, the second (ATC, 2002) and third (ATC, 2015a) editions were published including the parameters such as scoring development, ground motions selections, irregularity consideration, and pounding effects etc... Consequently, this RVS strategy was adapted by the various other nations such as India (NDMA, 2020), Canada (NRCC, 1992), New Zealand (NZSEE, 2006, 2017), and other countries with the modifications based on their local contexts. It can be seen from the Figure 2-5 that many countries have developed different RVS methods based on the structural and non-structural considerations and the local seismic hazards. In the following sections, brief summary of the available RVS methods are provided.

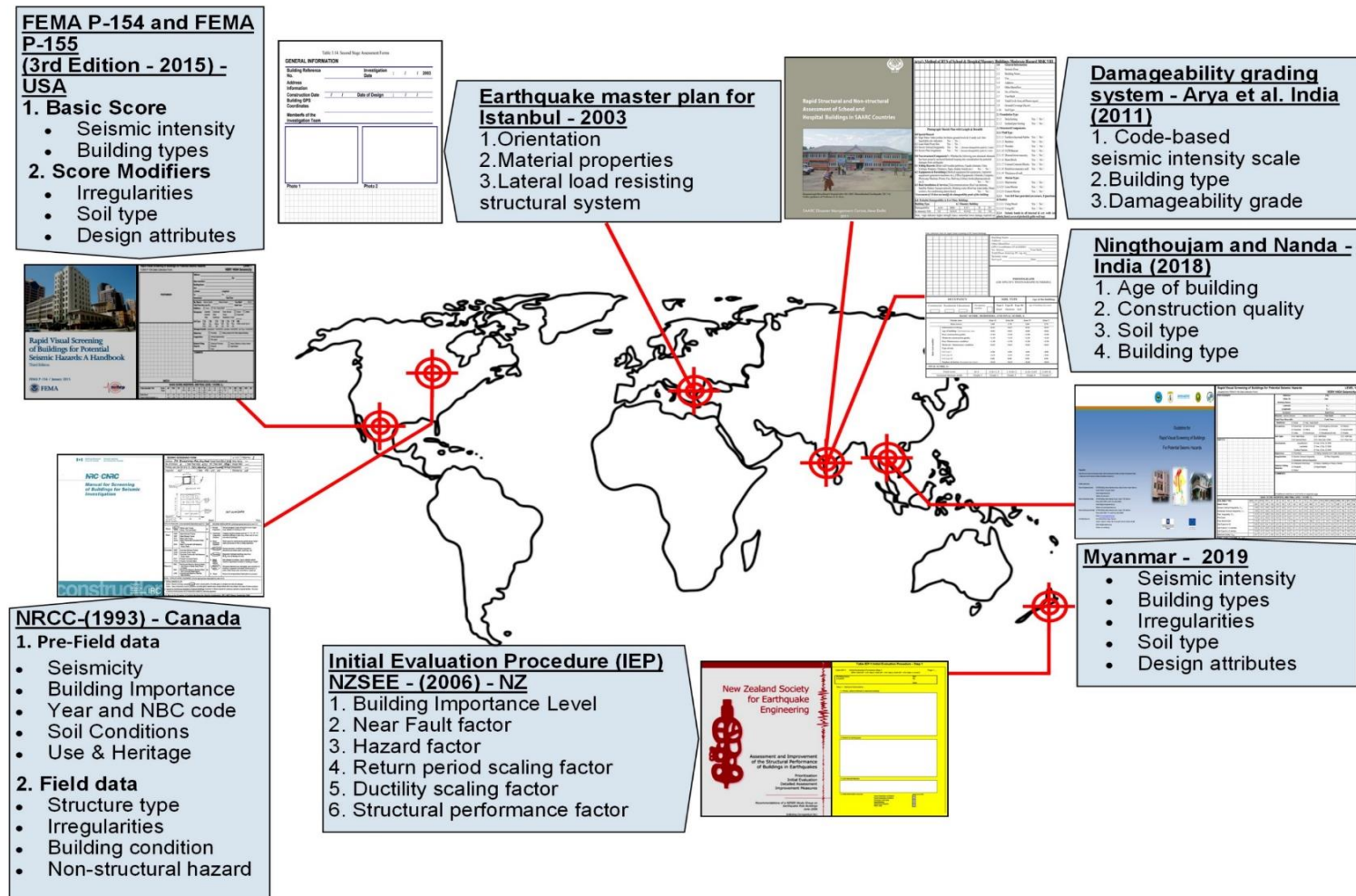


Figure 2-4. Summary of the RVS guidelines from different countries

2.3.1 The Regional based RVS - Guidelines

2.3.1.1 United States method (FEMA P-154)

The FEMA P-154 (ATC, 2015a, 2015b) guidelines provide the empirical approach to screen the seismically vulnerable buildings. It should be noted that the FEMA P-154 (ATC, 2015a) provides, two tiers of assessments, namely (1) Level -1 and (2) Level 2, in six different seismic regions in USA (low, moderate, moderate high, high, and very high) for seventeen building classes such as wood (W1, W1A, and W2), steel (S1, S2, and S3), concrete (C1, C2, and C3), precast (PC1 and PC2), and masonry (RM1, RM2, URM, and MH). Level 1 ratings are based on conservative values, however in Level 2 screening, which is an optional, imparts enhanced scores to buildings through analysing more detail structural features.

Figure 2-4 depicts the Level 1 score evaluation of the RC-MI building with moderate vertical irregularity and soil type E of the low-rise (1-3 story) building. The basic scores were formulated based on the seismic zone and the types of buildings. Score modifiers or performance modifiers are given for irregularities (vertical and plan which comes from the structural members), design factors, soil type, and number of storeys. It should be highlighted that the irregularities caused by the MI are not the primary aspect of the investigative work and require a separate investigation, since they can lead to structural collapse due to short column, soft storey and torsional effects. Afterwards, final scores have to be calculated by adding the positive and negative attributes. The negative values (shown in Figure 2-5) represent the unfavourable attributes of buildings during an earthquake. In order to sustain a building during the earthquake, the final Level 1 score must exceed the minimum score specified, which is determined by taking into account the worst conceivable combinations.

Level 2 assessment is divided into two sub-sections that include structural modifiers to alter the basic score (obtained from Level 1 assessment) as well as identifiable non-structural hazards in the buildings. In order to carry out the Level 2 assessment, the Level 1 irregularity modifier scores are deducted from the final Level 1 scores, and

comprehensive investigations on the irregularity (plan and vertical), pounding effects, recumbence, and lateral load resisting system are incorporated.

FEMA BUILDING TYPE	Do Not Know	W1	W1A	W2	S1 (MRF)	S2 (BR)	S3 (LM)	S4 (RC SW)	S5 (URM INF)	C1 (MRF)	C2 (SW)	C3 (URM INF)
Basic Score		6.2	5.9	5.7	3.8	3.9	4.4	4.1	4.5	3.3	4.2	3.5
Severe Vertical Irregularity, V_{1f}		-1.5	-1.5	-1.5	-1.4	-1.3	-1.6	-1.2	-1.3	-1.3	-1.2	-1.1
Moderate Vertical Irregularity, V_{1f}		-1.0	-0.9	-0.9	-0.9	-0.8	-1.0	-0.7	-0.7	-0.7	-0.7	-0.6
Plan Irregularity, P_{1f}		-1.6	-1.4	-1.3	-1.2	-1.1	-1.4	-1.0	-1.1	-1.0	-1.0	-0.9
Pre-Code		NA	NA	NA	NA	NA	NA	NA	NA	NA	NA	NA
Post-Benchmark		2.2	2.4	2.5	2.0	1.6	1.4	2.1	NA	2.3	2.2	NA
Soil Type A or B		0.9	1.1	1.3	1.0	1.2	0.8	1.3	1.4	0.9	1.2	1.2
Soil Type E (1-3 stories)		-1.2	-1.7	-2.3	-1.2	-1.4	-1.0	-1.7	-2.0	-1.4	-2.0	-1.6
Soil Type E (> 3 stories)		-1.7	-2.0	-2.2	-1.2	-1.4	NA	-1.7	-1.9	-1.3	-1.9	-1.6
Minimum Score, S_{MIN}		2.7	2.1	1.5	0.9	0.8	1.2	0.8	0.9	0.5	0.6	0.5
FINAL LEVEL 1 SCORE, $S_{L1} \geq S_{MIN}$												1.3

Appendix B, Table B-4

Appendix B, Table B-5

FEMA Building type and Basic score – Level 1 data collection
FEMA P-155
 (relates to the probability of the building collapse for a specified earthquake recurrence interval)
(HAZUS)

FEMA Building type and Score Modifiers – Level 1 data collection
FEMA P-155
 significant seismic-related defects

Considering worst possible combination of soil type, vertical and plan irregularities, and building age, all at once.

Figure 2-5. FEMA P-154 Level 1 scoring evaluation table (Low seismicity region)

2.3.1.2 New Zealand method (NZSEE)

The New Zealand version of RVS, which was initially named as the preliminary screening procedure and published in 1996 (NZSEE, 1996). Later it was modified as the Initial Evaluation Procedure (IEP), published in 2006 (NZSEE, 2006), and then refined in 2014 (NZSEE, 2014). It is proposed based on the FEMA 154 (ATC, 1988) procedure (Idham, 2011); nevertheless, the scoring system and building type were factored with a detailed assessment method via graphs that differentiate, this approach from FEMA 154 (ATC, 1988). The identification and qualitative evaluation of the impacts of any structural elements are key components of the IEP, and those will be considered in the first step of the initial seismic assessment (ISA) approach.

The IEP largely focused on structural irregularities in terms of torsion and weak storey effects of the buildings (Ningthoujam & Nanda, 2018) caused by irregular mass distribution (Furtado et al., 2017). The procedure entails doing a preliminary evaluation of building in comparison to the standard requirement for a new building as the NBS% (percentage to new building standard). The procedure to evaluate the NBS% of the buildings is shown in Figure 2-6; where the baseline NBS% $((NBS\%)_b)$ of the building has to be evaluated, then the performance achievement ratio (PAR) has

to be evaluated through the irregularity and site characteristics. The NBS% values are finally evaluated by multiplying the PAR and (NBS%)_b.

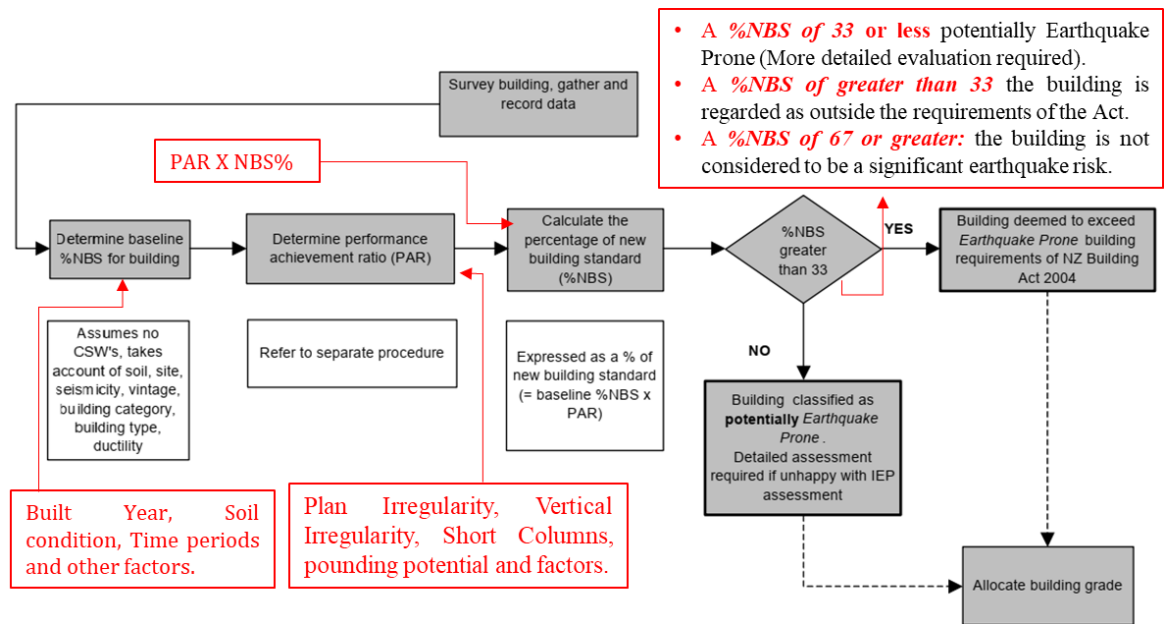


Figure 2-6. IEP procedure to evaluate the NBS%

2.3.1.3 Canadian RVS (NRC92)

The National Building Council of Canada (NRCC) released a RVS method under the name "Manual for screening of buildings for seismic investigation" in 1992 (NRCC, 1992). The purpose of this document is to establish the Seismic Priority Index (SPI) with the consideration of the structural and non-structural indices, whereas the fifteen building typologies based on the materials of the constructed buildings and the irregularities are considered. It should be noted that the NRCC (NRCC, 1992) method is largely based on the concept of the FEMA 154 (ATC, 1988) method and the final cut-off score of the building is proposed as a priority indication for detailed assessment (Tischer, 2012).

The framework of the NRCC method to evaluate the seismic priority index can be seen in Figures 2-7. The seismic hazard, local soil conditions, irregularities of the building, importance classes, and structural typologies were five characteristics associated to the code of practises that were multiplied to determine the structural index (SI) of the building. The non-structural index (NSI) is based on the soil condition, building

occupancy and the non-structural hazards. According to NRCC (NRCC, 1992), the SPI of 10 for a building is considered as low priority for any intervention, while SPI score higher than 30, is recommended for a detailed seismic analysis.

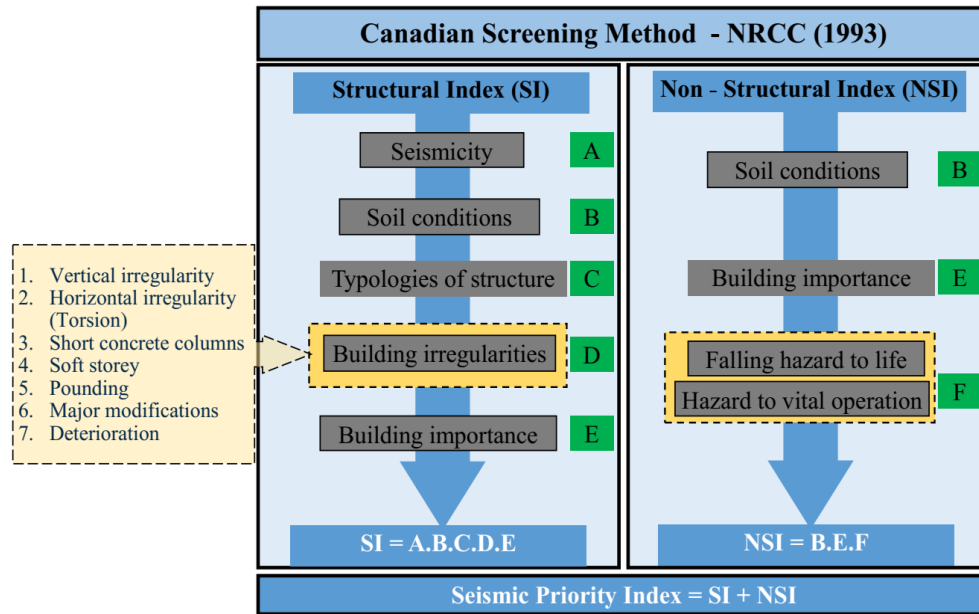


Figure 2-7, Canadian screening method (NRCC)

2.3.1.4 Other RVS methods

I. RVS in Japan

The Japan Building Disaster Prevention Association (JBDPA) (JBDPA, 2001) developed a RVS in 1977 to evaluate the Seismic Index Method of low and mid-rise RC structures under the theme of "Standard for Seismic Evaluation of Existing Reinforced Concrete Structures" (Bektaş & Kegyes-Brassai, 2022). The building inspection has to be carried out in three phases, during the first phase: primary inspection, first level inspection, and second level inspection are being considered. The seismic index (I_s) of the building is determined by multiplying of basic seismic index, irregularity index and time index (JBDPA, 2001). However, this technique provides less clarity than other methods for calculating scores and ranking of the buildings (Bhalkikar & Pradeep Kumar, 2021). Because the Japanese code of practise requires large columns and shear walls to provide the lateral-load resisting system in the construction, and their loading conditions vary significantly on each floor, since

the JBDPA (JBDPA, 2001) screening technique was developed based on each storey shear demand in the building (Aftabur & Shajib, 2013).

II. RVS in Turkey

In Turkey, a RVS method was proposed in 2003 as part of the "Earthquake Master Plan for Istanbul" by the Metropolitan Municipality of Istanbul to evaluate the basic capacity index of the building (METU, 2003). The approach was established using the data obtained from damage surveys performed after the earthquakes occurred in Turkey. The capacity index of the building, such as material properties, the orientation of the building, and later load-resisting systems in the building were considered. As it can be seen in Figure 2-8, the METU (METU, 2003) method proposed, three levels of assessments. In the first stage, the RVS method is performed without entering into a building (using blueprints). The second stage (performance modifiers stage) is a detailed investigation required to enter the building and perform the structural and non-structural assessments. In the final stage, the topographical effect has to be considered, detail structural analyses have to be performed.

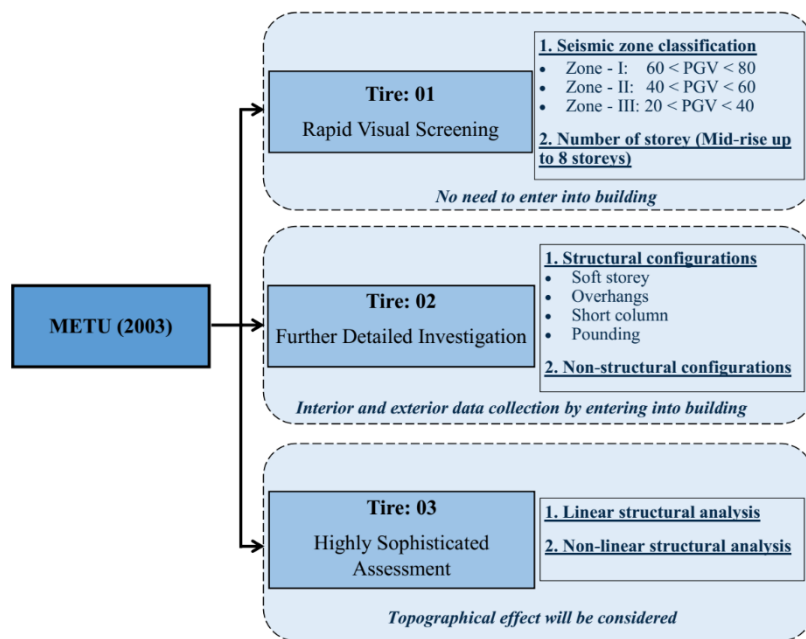


Figure 2-8. Turkish (METU) RVS method

Sucuoğlu et al. (2007) proposed a statistic based RVS grading method for Turkey metropolitan regions that considers building quality, soft story effects, overhangs, and

the number of storeys for homogeneous soil conditions. The basic score was suggested using the PGA and the damage level, while the modifiers are suggested using the irregularities. However, this method is similar to METU (2003) and ATC (2002) RVS methods.

III. RVS in Greece

The RVS method for the Greece was developed in 2000 by the Greek Earthquake Planning and Protection Organization as “Provisions for Pre-Earthquake Vulnerability Assessment of Public Buildings (Part A)” (OASP, 2000) based on the FEMA 154 (ATC, 1988). This method was developed based on two features: building lateral load resisting system and the material properties of the building, considering the three states of assessments. The first stage, which is mentioned as the initial structural hazard score (ISH) is evaluated with the consideration of the eighteen building classifications. Following the ISH, the score was modified as the basic structural hazard score (BSH), with the consideration of the masonry arrangement, soft storey effect, short column and the seismic zoning classification found in Greece. In the final step, BSH was further modified to evaluate the final score regarding the performance attributes. The final score (FSH) should be more than 2 ($FSH > 2$) and the building with less or equal to 2 (≤ 2) should be analysed in detailed. In addition, Fuzzy based RVS (FL-RVSP) was proposed by Demartinis & Dritsos (2006) for Greece, which can be categorised into five different damage states related to evaluate the structural capacity of the building. The FL-RVSP method reduced the number of buildings to be analysed in detail by 20% compared to the OASP (OASP, 2000) method.

IV. RVS in Italy

No specific RVS general are available in Italy, (Bektaş & Kegyes-Brassai, 2022; Sangiorgio et al., 2020). However, the research studies were conducted in the past to perform expert surveys to assess the seismic risk of masonry and RC structures in Italy. In 1988, Angeletti et al. (1988) proposed the damage-vulnerability method with different seismic zones, incorporating eleven factors such as structural consideration (lateral resisting system, diaphragms, safety factor, irregularities and foundations),

non-structural features (roof and walls, and other non-structural elements), and decay of the structure were proposed to be considered in the RVS assessment.

Perrone et al. (2015) and Ruggieri et al. (2020) developed RVS methods to evaluate the seismic risk index/safety index (SI) of the RC hospital and school buildings, respectively, by considering the structural (I_{STR}), non-structural (I_{NSTR}), emergency preparedness (I_{ORG}), occupancies (EXP) and the seismic zone (HAZ). The SI can be evaluated from the following equation 2-1:

$$SI = VULN \cdot \frac{HAZ}{1.67} \cdot \frac{EXP}{1.25} \quad (2-1)$$

Where, $VULN$ will be obtained using I_{STR} , I_{NSTR} , and I_{ORG} parameters from the survey.

In addition, analytic hierarchy process (AHP) based method was proposed by Sangiorgio et al. (2020) to assess the robust risk index (I_{RISK}) following RVS with 80 parameters. The study was performed with consideration of the non-structural attributes in the building with multi-criteria analysis. The results showed that the RVS and AHP based methods exhibited the same ranking for the building, though RVS has some limitation, involving large number of data and the technical persons for the assessment.

V. RVS in India

In 2002, Structural Engineering Research Centre (SERC, 2002) proposed a RVS method to assess the performance of the masonry and multi-storey RC structures, which was modified from FEMA 154 (ATC, 1988) to the local context. Similar to FEMA 154 (ATC, 1988), the basic structural score and the structural score modifiers were evaluated with consideration of soil types, age of the buildings, foundation types, seismicity zone, eccentricity and storey level (Rai, 2005). Recently, the National Disaster Management Authority of India released a RVS method to assess the safety of the buildings (NDMA, 2020). The earthquake risk index was introduced with the consideration of the seismic zonation in India and a colour code (red, green and yellow) was proposed based on the importance of the structures. It was assumed that, if the building attributes come under the red tag, the building is prone to damage under an earthquake. The life-threatening parameters such as siting condition, foundation

condition, and structural aspects were considered. However, this method is regarded as a qualitative procedure. Conversely, the recommendations did not specifically address the detrimental consequences of MI arrangements in the buildings.

Figure 2-9 illustrates the two distinct types of RVS developments, namely, probability (Sinha & Goyal, 2004) and statistical regression based method (Ningthoujam & Nanda, 2018) to provide the grade to the building based on the expected damages. Probability based RVS (Sinha & Goyal, 2004) was developed based on FEMA 154 (ATC, 2002) and it considers the seismicity and the building typologies (masonry, wood, RC and steel), while for score modifiers, storey level, soil type, vertical irregularity, plan irregularity and design code consideration were considered.

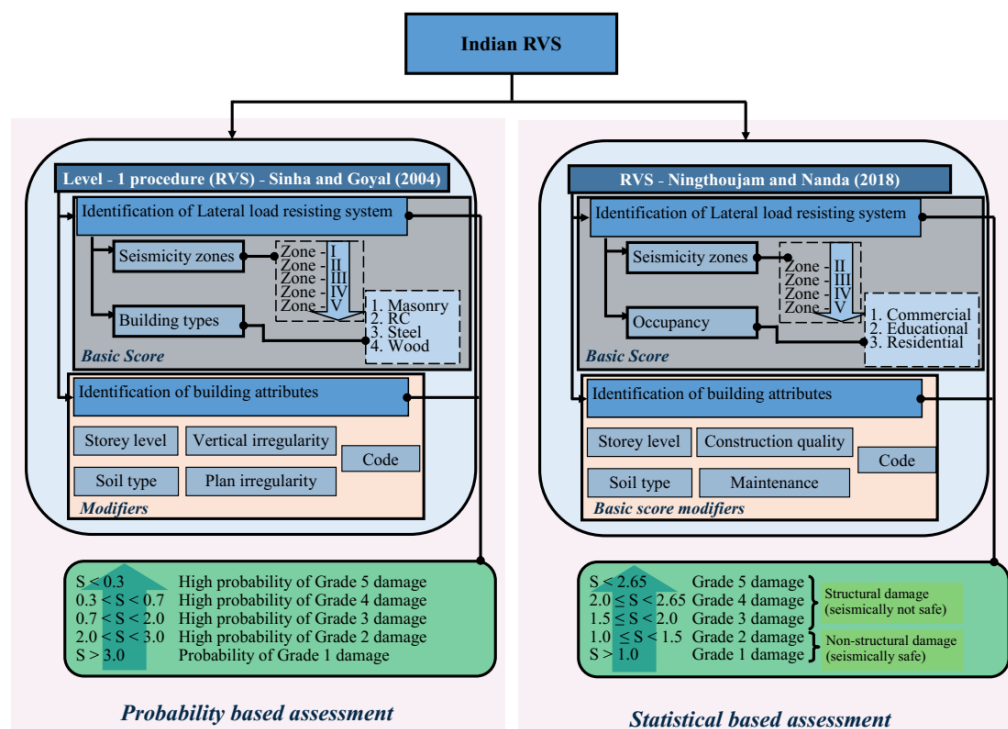


Figure 2-9. Indian probability and statistical based RVS

A statistical regression assessment method was performed using the 2016 Manipur earthquake damage data, where 396 buildings were analysed. The damage data analysis was carried out by considering ten variables, which were substantial overhang, soft storey, floating column, maintenance, soil types, re-entrant corners (plan irregularity) construction quality, staircase location and age of the buildings.

Among the ten variables, six variables (soil types, construction quality, maintenance, age of the building, substantial overhang and storey level) have considerably influenced the damage grade of the building. In addition, it should be noted that the region based RVSs were also proposed in India (Sarmah & Das, 2018; Siddharth & Sinha, 2022).

Furthermore, Arya (2011) presented a RVS method in accordance with FEMA 154 (ATC, 2002) by taking into account the primary lateral-load resisting system and modifiers based on irregularities (plan and vertical), building type, non-structural threats, and seismic intensity to generate damageability ratings based on previous earthquake observations. Consequently, Jain et al. (2010) developed a RVS for RC buildings with grading systems from G1-G5 (slight to severe) to evaluate the Expected Performance Score (EPS). The defined vulnerability parameters were, number of storeys, maintenance, re-entrant corners, basement, open ground storey and short column effects. In addition, the performance modifiers were defined by considering the purpose of the building, seismic zone and soil type.

VI. RVS in Thailand

In Thailand, a rapid assessment framework was developed by modifying FEMA 154 (ATC, 2002; DeMasi, 2006). Rupakheti & Apichayakul (2019) developed a RVS method based on the Nepal 2015 earthquake damage data through ordinal logistic regression to evaluate the damage grade in Thailand. The RVS method considers, various attributes such as the floor type, height of the building, surface condition, location, plinth area, age, roof types, foundation types and building conditions. The study revealed that the damage grade is preliminary depending on the age, roof type, plinth area and the foundation type.

VII. RVS in Malaysia

Various research projects have been conducted to develop RVS methods in the last ten years, based on FEMA 154 (ATC, 2002, 2015a, 2015b) with modifications based on the Malaysian context (Ghafar et al., 2015; Jainih & Harith, 2020; Kassem et al., 2021; Mohamad et al., 2019). The Geographic Information System (GIS) based RVS was performed by Mohamad et al. (2019) to assess the building vulnerability as a grading

system (G1-G3) through FEMA 154 (ATC, 2015a). The results stated that most of the buildings were not designed for earthquakes. Kassem et al. (2021) generated the web-based RVS by modifying FAMA 154 (ATC, 2002). The lateral-load resisting system, irregularities, age, soil type and the building height were considered to generate the performance modifiers/ score modifiers with the aid of Google earth and Google map.

2.3.3 Summary of RVS

Table 2-2 shows the summary of the attributes that have been considered in various countries to generate the RVS. It can be seen that most countries focused primarily on local seismicity, vertical and plan irregularities, and less on infill effects. However, Greek (OASP, 2000) and Italian studies (Angeletti et al., 1988; Ruggieri et al., 2020) concentrated on detail of MI with consideration to falling hazard perspectives. Usually, Sri Lankan school buildings possess MI irregularities in terms of thickness and opening configurations, and they can influence the seismic performance of the buildings by causing shear failure of columns (Cavaleri et al., 2017; Celarec & Dolšek, 2013).

The RVS methods of evaluating the seismic risks of building have evolved over the years,; nevertheless, they have limitations because the survey must be conducted by professionals in the field (NDMA, 2020). It can be mentioned that the consideration of the attributes is significantly similar across RVS methods available, though some of the local contexts of the buildings/physical conditions (e.g. seismicity and soil types) are generally incorporated. Though the FEMA (ATC, 2015a) predicted the vulnerability of the building greater than the actual; most of the country-based guidelines and the studies followed the FEMA 154 (ATC, 1988, 2002, 2015a, 2015b) guidelines. FEMA P-154 (ATC, 2015a) method is widely accepted approach to perform the seismic risk assessment of the building (Palagala & Singhal, 2021). Meanwhile, the need for separate RVS in Sri Lanka to assess the seismic vulnerability of school building is essential and in this study emphasis was made to developed a RVS based on FEMA P-154 (ATC, 2015a) for RC-MI school building typologies with local variations.

Table 2-2. Summary of RVS methods

Attributes	USA	New Zealand	Canada	Japan	Turkey	Greece	Italy		India			Malaysia
	FEMA P-154	NZSEE (2006)	NRCC, (1992)	JBDPA (2001)	METU (2003)	OASP (2000)	Angeletti et al. (1988)	Ruggieri et al. (2020)	(SERC, 2002)	(Jain et al., 2010)	Ningthoujam & Nanda (2018)	Kassem et al. (2021)
Soil types	✓	✓	✓	✗	✗	✓	✗	✓	✓	✓	✓	✓
Seismicity	✓	✓	✓	✗	✓	✓	✓	✓	✓	✓	✓	✓
Foundation	✗	✓	✓	✓	✗	✗	✓	✓	✓	✓	✗	✗
Year of construction	✓	✓	✓	✓	✓	✓	✗	✓	✓		✓	✓
Building types	✓	✓	✓	✓	✓	✓	✓	✗	✓	✓		✓
No. of Storeys	✓	✓	✓	✓	✓	✓	✗	✓	✓	✓	✓	✓
Vertical irregularity	✓	✓	✓	✓	✓	✓	✓	✓	✗	✓	✓	✓
Plan irregularity	✓	✓	✓	✓	✓	✓	✓	✓	✗	✗	✓	✓
Pounding effects	✓	✓	✓	✗	✓	✓	✗	✗	✗	✗	✗	✓
Code consideration	✓	✓	✓	✓	✗	✗	✓	✓	✗	✗	✓	✓
Damages/Deterioration	✗	✗	✗	✓	✗	✓	✓	✓	✗	✗	✗	✗
Falling hazard/ Non-structural	✓	✗	✓	✗	✓	✗	✓	✓	✗	✗	✗	✓
Lateral-resisting system	✓	✓	✓	✓	✗	✗	✓	✓	✗	✗	✗	✓
Infill/wall	✗	✗	✗	✗	✗	✓	✓	✓	✗	✗	✗	✗

✓ - Considered ✗ - Not considered

2.4 Development of rapid visual screening method

To date, FEMA 154 has released the third edition, as FEMA P-154 (ATC, 2015a), with FEMA P-155 (ATC, 2015b) as the supporting document. In this document, an approach described to establish RVS method is outlined. The "Multi-hazard Loss Estimation Methodology, HAZUS-MH MR4 Technical Manual" (FEMA, 2002, 2020) and the "California Office of Statewide Health Planning and Development (OSHPD)" (CAC, 2010), also known as "HAZUS methodology," are combined to create the FEMA P-154 (ATC, 2015b) procedure to develop RVS methods. The basic scores and score modifiers in the third edition of FEMA P-154 (ATC, 2015a) are defined based on the building capacity and fragility parameters, they are computed based on performance of the building and building characteristics in FEMA P-154 RVS (ATC, 2015a) method.

2.4.1 Development of basic score and score modifiers

2.4.1.1 Basic score for RC-MI buildings (C3)

The basic score of building typologies is defined by assuming the basic lateral load resisting system with no irregularities for the specific earthquake ground motion. The basic score in the FEMA P-154 (ATC, 2015a) is obtained for the low-rise building in six seismic regions and seventeen building typologies as specified in Section 2.3. Figure 2-10 depicts the procedure of adopting the basic score of a building typology. Following the numerical analysis procedure, the pushover curve (PO) and capacity curve (CC) have to be derived, as shown in Fig 2-10. In order to compare the capacity of the building with respect to an earthquake demand, the base shear (V) and displacement (d) are converted to the spectral acceleration (S_a) and spectral displacement (S_d), respectively, by applying model parameters, those are acquired during the PO analyses (FEMA, 2013). Then, the yield (D_y) and ultimate (D_u) displacement are obtained from CC (Figure 2-10 (c)). The structure is considered to be elastic until it reaches D_y , and then it gains maximum capacity, when it reaches D_u . HAZUS (FEMA, 2002, 2020) assumes that the plastic region is reached after it attains D_u . The equations 2-2 to 2-5 can be used to convert PO curve to CC curve for the analysis (ATC-40, 1996; Chopra & Goel, 1999):

$$S_a = \frac{V/W}{\alpha_1} \quad (2-2)$$

$$S_d = \frac{\Delta_{\text{roof}}}{PF_1 \cdot \phi_{1 \cdot \text{roof}}} \quad (2-3)$$

$$\alpha_1 = \frac{\left[\sum_{i=0}^N \frac{(w_i \cdot \phi_{i1})}{g} \right]^2}{\left[\sum_{i=0}^N \frac{w_i}{g} \right] \left[\sum_{i=0}^N \frac{(w_i \cdot \phi_{i1}^2)}{g} \right]} \quad (2-4)$$

$$PF_1 = \left[\frac{\sum_{i=0}^N \frac{(w_i \cdot \phi_{i1})}{g}}{\sum_{i=0}^N \frac{(w_i \cdot \phi_{i1}^2)}{g}} \right] \quad (2-5)$$

Where V: base shear; W: dead weight + live loads; α_1 : model mass coefficient (1st mode); Δ_{roof} : roof displacement N: upper most level of the building; w_i/g : mass assigned to level i; ϕ_{i1} : amplitude of mode 1 at level i; PF_1 : model participation factor for mode 1

Additionally, the 5% damped elastic response spectrum has to be constructed based on the parameters of the ground motion and it have to be converted as the Acceleration-Displacement Response Spectrum (ADRS). When building capacity is increased, effective damping improves as well, resulting in a lower elastic response demand to inelastic response demand fraction in the spectrum (Palagala & Singhal, 2021), the inelastic response spectrum is represented in terms of hysteric behaviour of the structure (Figure 2-10 (e)). Subsequently, the performance point of the building, i.e. the peak response of the building to a particular earthquake scenario, is determined by combining the response spectrum and the capacity spectrum, which is known as the Capacity Demand Spectrum method (CDS) in ADRS.

The threshold limits are defined based on the damage states (Figure 2-10 (d)), that are already defined in the HAZUS (FEMA, 2002, 2020). Fragility curves of the buildings are the lognormal probability functions, which are defined as the probability of exceeding specific structural and non-structural damage thresholds for a given peak building response (performance point). However, FEMA P-154 (ATC, 2015a) proposes the total damage probability based on the collapse state condition. The collapse state is defined as a partial or complete structure that loses its capacity to resist gravitational loading condition. Therefore, the probability of complete damage fragility (Figure 2-10 (f)) is determined based on the collapse state of the building. In

order to develop the basic score, complete damage fragility curves are required. It should be noted that the fragility parameters are associated to three sources: CC variability of the building, demand spectrum variability, and the damage states threshold. The probabilities of complete damage thresholds to develop fragility are computed using equation 2-6 (i.e. at collapse state):

$$P[\text{complete damage}] = \varphi \left[\frac{1}{\beta_{S,C}} \ln \left(\frac{D}{S_{d,c}} \right) \right] \quad (2-6)$$

Where, $P[\text{Collapse}]$: probability of collapse; φ : standard normal cumulative distribution functions, D : performance point (peak point); $\beta_{S,C}$: standard deviation of spectral displacement natural logarithm of the collapse damage state and $S_{d,c}$: median value of the spectral displacement at the collapse damage state. $S_{d,c}$ and $\beta_{S,C}$ are suggested in the HAZUS guidelines.

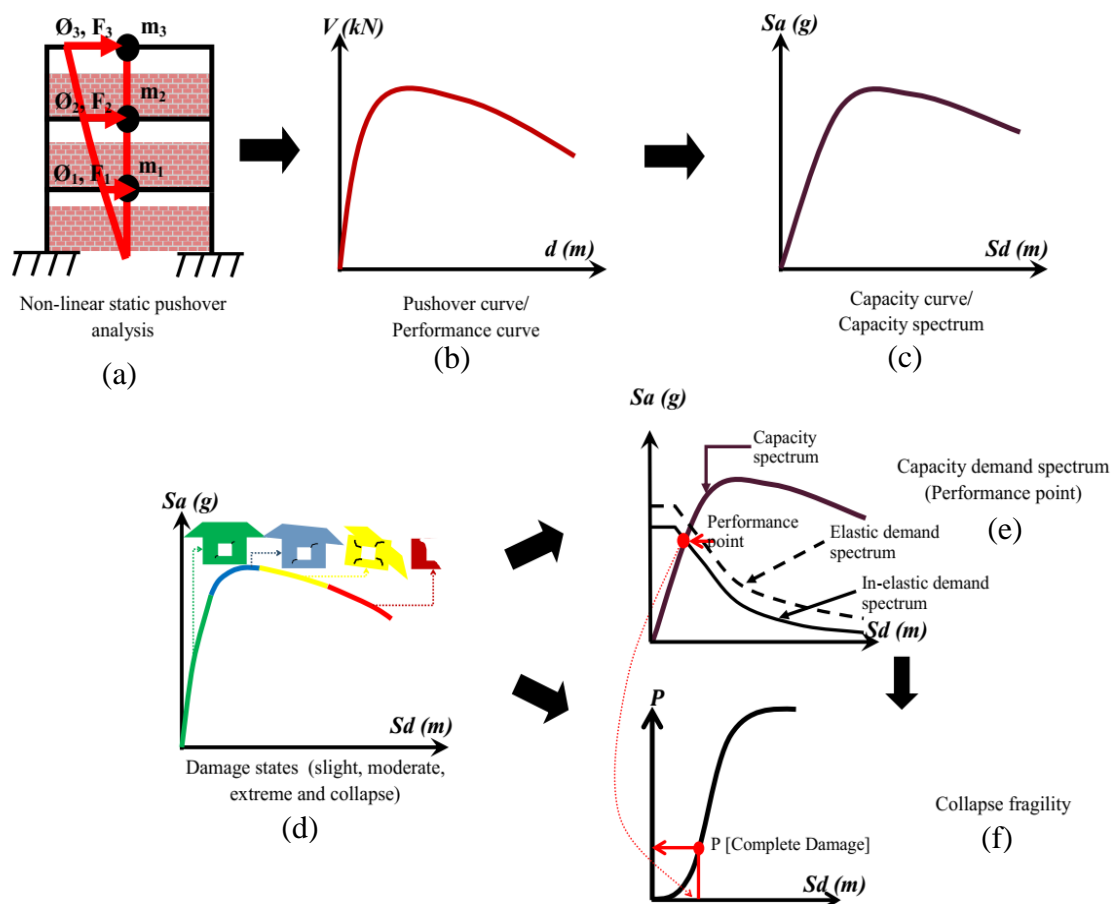


Figure 2-10. Procedure to adapt the basic score and Score modifiers

Once the collapse probability is obtained for the particular building type, the basic scores can be obtained by incorporating the collapse factors (CF) for baseline factors, which are pre-defined in the HAZUS (FEMA, 2002, 2020) as can be seen in Table 2-3. The basic score of the building can be evaluated using equations 2-7 and 2-8:

$$P[\text{collapse}] = CF \cdot P[\text{complete damage}] \quad (2-7)$$

$$\text{Basic score} = -\log_{10}(P[\text{collapse}]) \quad (2-8)$$

Table 2-3. Collapse factor adapted from FEMA (2020)

Performance level	Collapse factor (CF)
Baseline (Basic score)	0.13
Sub-baseline (moderate irregularities)	0.25
Ultra- Sub-baseline (severe irregularities)	0.50

2.4.1.2 Score modifiers for RC-MI buildings (C3)

The score modifiers are integrated with the basic score, to account the irregularities in buildings that may affect the performance during earthquakes. The score modifiers could be negative values indicating irrelevant or redundant features that reduced the performance of the building, or positive values indicating advantageous characteristics during the earthquake. The possible irregularities that are suggested by FEMA P-154 (ATC, 2015a) are shown in Figure 2-11. Vertical irregularities are caused by the sloping site, split level, short column, weak storey, and setbacks in buildings, whereas plan irregularities are caused by torsional effects, an irregular shape, and an opening in the diaphragm, as descriptively illustrated in Figure 2-11. The calculations of the score modifiers are also similar to the basic score evaluation procedure (as can be seen in Figure 2-10) and the attributes that affect the performance of the building during an earthquake should be considered. Following steps are given to compute the score modifier based on the irregularities identified:

- i. Probability of the complete damage state is considered based on the irregularities of the building ($P[\text{complete damage}]$)
- ii. The equivalent score to complete damage state is determined $\{\text{Equivalent score} = -\log_{10}(P[\text{collapse}])\}$

iii. The SModifier is calculated by deducting from the basic score

$$(Modifier = Equivalent\ score - Basic\ score)$$

Additionally, the minimum score of the building should not be zero, and if the complete damage condition is 100% or less, it means that the collapse probability is inferred as a percentage of the complete damage probability. The following equations 2-9 and 2-10 are used to calculate the minimum score of the building (S_{min}) based on the collapse factor (CF) and collapse condition, where the damage level is considered to be 100%:

$$P[\text{collapse}] = CF \cdot 100\% \quad (2-9)$$

$$\text{Minimum score } (S_{min}) = -\log_{10}(P[\text{collapse}]) \quad (2-10)$$

Where P[collapse]: probability of collapse; CF: collapse factor (defined in HAZUS)

The final structural score (S) of the building has to be calculated by combining the basic score and the score modifiers for the building, and if the score is greater than the minimum score, the building is considered safe for the specific earthquake. If the final structural score is 2, it indicates that the probability of collapse is 1 in 100, and if it is 3, it implies that the probability is 1 in 1000. Therefore, the greater the final structural score, the safer it will be during that specific earthquake.

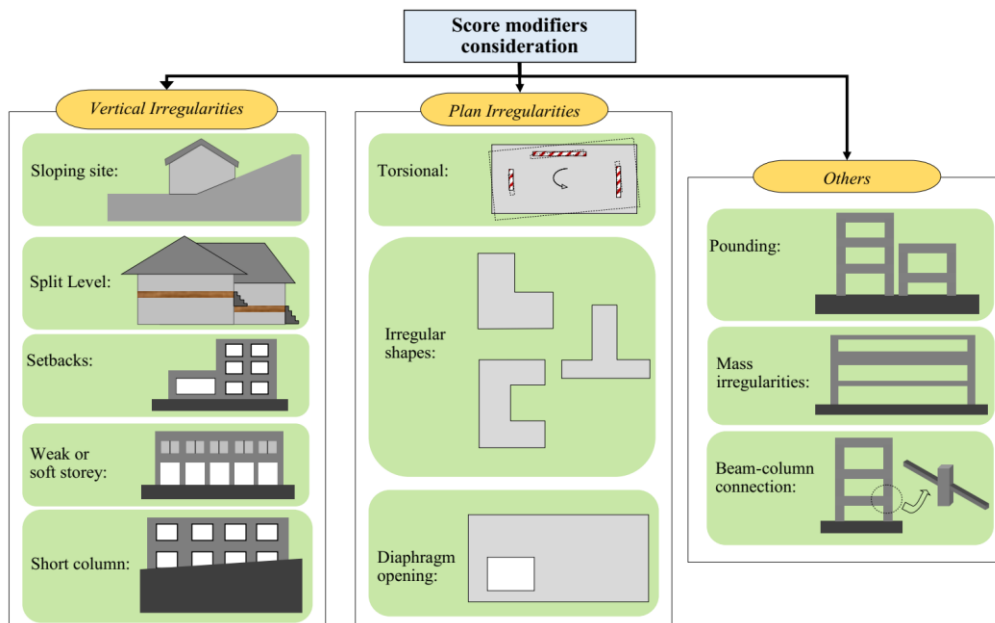


Figure 2-11. Irregularities in building for score modifiers adaption

2.5 Summary

The literature review reveals that Sri Lanka cannot be considered an aseismic country, particularly in the western coastal region, where Mannar failure drift and Comorin ridge are the seismic inducers to Sri Lanka. The studies related to assessing seismic performances of school buildings in Sri Lanka are limited, and meantime the school buildings in Sri Lanka are not designed for seismic hazards. Meanwhile, there is a wealth of literature on the earthquake safety of school buildings; yet, lightly reinforced RC-MI based school building typologies with various MI configurations have received little attention, and majority of the Sri Lankan RC-MI school buildings fall were under this category. Therefore, the seismic evaluation of school buildings in the Sri Lankan context is essential to implement any seismic mitigation measures. In this context, the seismic performances of the school buildings have to be investigated, and RVS approach suggested in FEMA (ATC, 2015a) is useful to develop a separate RVS method to assess the large number of RC-MI typological school buildings exist in Sri Lanka.

3. METHODOLOGY

The methodology followed to achieve the objectives and aim of this research study are outlined in this Chapter. Figure 3-1 illustrates the methodology adopted in this study, by indicating the steps taken to achieve the objectives and aim of this research study. Initially, detailed structural surveys were conducted in selected school buildings to identify the structural and non-structural attributes in those buildings. The survey results were examined to determine the possible structural typologies existing among the school buildings. Meanwhile, non-structural attributes with regard to the MI opening configurations and thickness were also acquired in detail, as they significantly vary within and between the buildings (explained in Section 4.1 and Section 4.4)

The aim of this study was to develop an appropriate RVS method to assess the seismic risks of typological RC-MI school buildings; therefore, RVS methods from the literature were reviewed to measure the seismic risk of Sri Lankan RC-MI school buildings. However, similar seismic risk grades/rating of the school buildings have been encountered due to a lack of prominence on accounting irregularities in MI configurations in the existing RVS methods. In order to address this issue, the objectives were set to modify the RVS approach defined in FEMA 154 and 155 (ATC, 2015b, 2015a) to assess the seismic risk of typological RC-MI school buildings in Sri Lanka.

The numerical models of the RC-MI school buildings were developed using OpenSees (OS) (OpenSees, 2021) by considering the possible variation in structural (RC frame arrangements) and non-structural features (MI configurations) observed during the survey. The nonlinear static pushover (PO) method was adapted to analyse the performance of the buildings under seismic action. Subsequently, the numerical analysis results were further processed to examine the failure mechanisms, and then PO graphs were generated for different typologies of the school buildings. In total, 640 building cases were analysed incorporating different typologies, MI configurations and stochastic variations of material properties.

Furthermore, damage thresholds for the school building were defined based on the failure sequences of these RC-MI school buildings from the numerical analyses and

later used to develop seismic fragility curves of those buildings. Later, damage matrices for each building typology in relation to the regional seismic hazards were developed. The collapse fragility was extracted from the combined fragility curves and later used to calculate the basic score and score modifiers for the building typologies considered, while taking into account irregularities in those buildings. Eventually, structural scores (S) for the building typologies were derived and a new RVS method is proposed to evaluate the seismic risk of typological RC-MI school buildings.

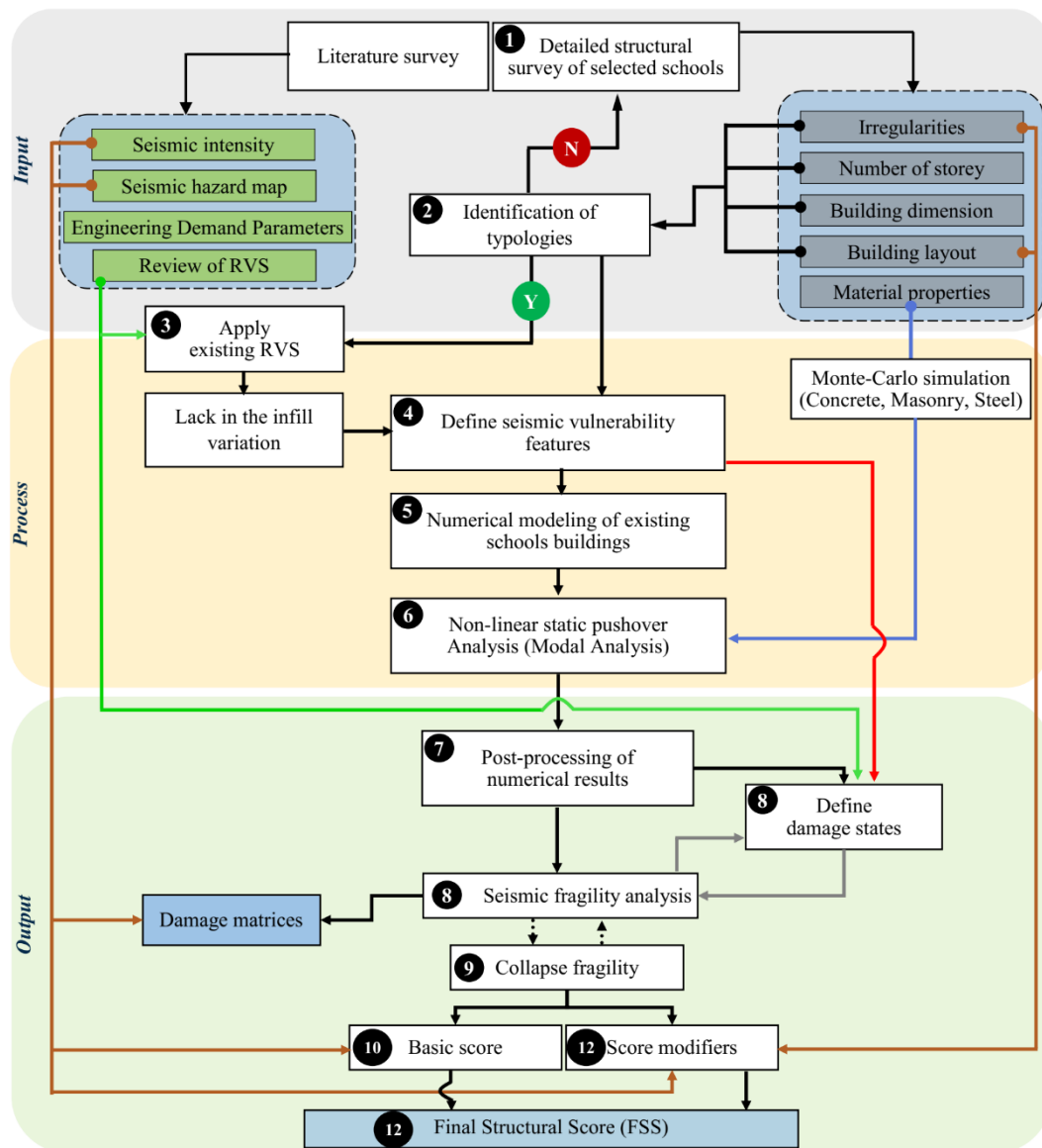


Figure 3-1. Methodology of the study

4. SURVEY OF SELECTED SCHOOL BUILDINGS

A detail survey was carried out to identify the structural and non-structural attributes among the school buildings. The survey forms used to acquire the details of the school buildings are given in *Appendix A-1*. The following sub-sections will provide the details of the schools surveyed, structural typologies identified and non-structural features prevailing in the selected school buildings.

4.1 List of Schools Surveyed

The survey was conducted to measure the structural and non-structural attributes of the school buildings. In total, 40 school buildings (from twenty schools) were chosen from eight districts in Sri Lanka. The surveys were not conducted in all the districts in the country, as similar typologies were repetitively identified among the schools surveyed and due to time and financial constraints. However, one may extend the survey to other districts in future to further verify the findings made in this study. Meanwhile, the focus was given to acquire the details of RC-MI school buildings with two and three storeys, as majority of the buildings are built with this RC-MI typology. Figure 4-1 shows the selected school buildings and their locations in each district. The list of surveyed school buildings can be referred from *Appendix A-2*.

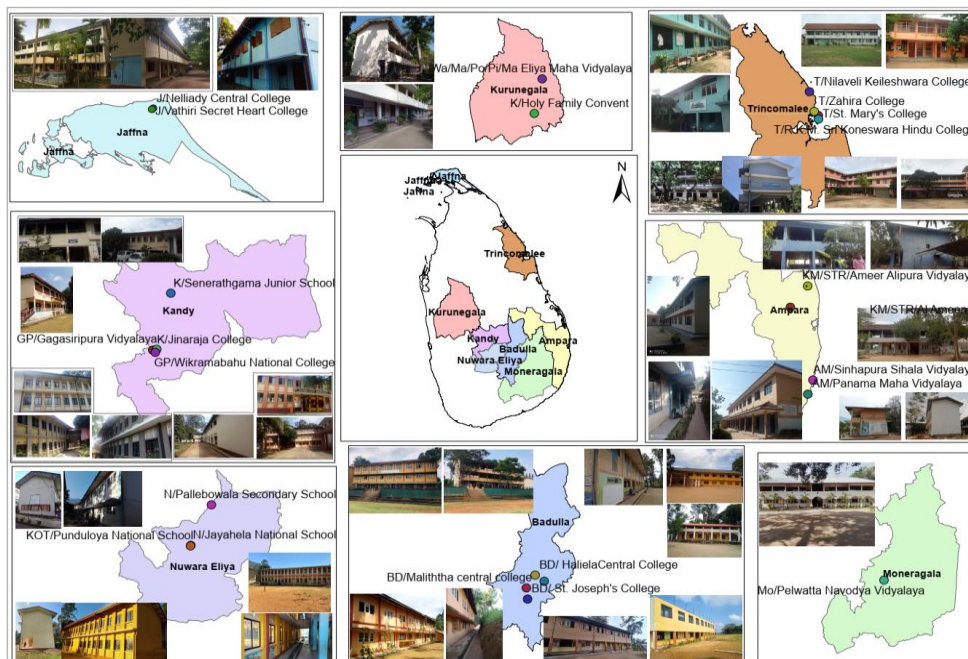


Figure 4-1. Selected survey school buildings in Sri Lanka

4.2 Identified typologies

4.2.1 Typologies based on the storey level

Primarily two RC-MI school building typologies exist among the school buildings surveyed. They are generally classified as two and three storey classroom buildings. However, the number of class rooms may vary within those buildings, when additional facilities such as a laboratory, office, or staff rooms have to be included.

Figure 4-2 represents some of the school buildings surveyed. It can be seen that the school buildings have different structural and non-structural outlook. In order to further assess the buildings, the details column location and dimensions, beam dimensions and orientation, thickness of the MI wall, window and door sizes were obtained. The survey revealed that the different of structural and non-structural attributes that exist among those buildings surveyed. Subsequently, each building layout was examined to differentiate the typologies exist.



Figure 4-2. Some of the surveyed school buildings (two and three storeys)

4.2.2 Typologies based on arrangements

Among the two (S02) and three (S03) story buildings surveyed, two comparable structural attributes were identified. The existence of varied numbers of column layout (rows) distinguishes the typologies identified, as shown in Figures 4-3 and 4-4. The buildings were further categorised, in terms of structural arrangements, as seen in Figure 4-3, which has two rows of columns, it is denoted as Type-01 (T01), whereas building typologies in Figure 4-4 are labelled as Type-02 (T02). Typically, the floor plan of the T01 is comprised of 27 m and 7.5 m of length and width, respectively, and the T02 consists of 27 m and 7.7 m of length and width, respectively. The average floor height of the buildings is 3 m. The chosen dimension of the school buildings considered were based on the most common typological dimensions observed in the survey, although it is worth noting that other dimensions and bays were observed during the survey. Nevertheless, most of the buildings in the X-direction had nine bays, whereas the Y-direction possessed only one bay for T01 buildings and two bays for T02 buildings. Therefore, the study was conducted to assess the most common school building typologies in Sri Lanka.

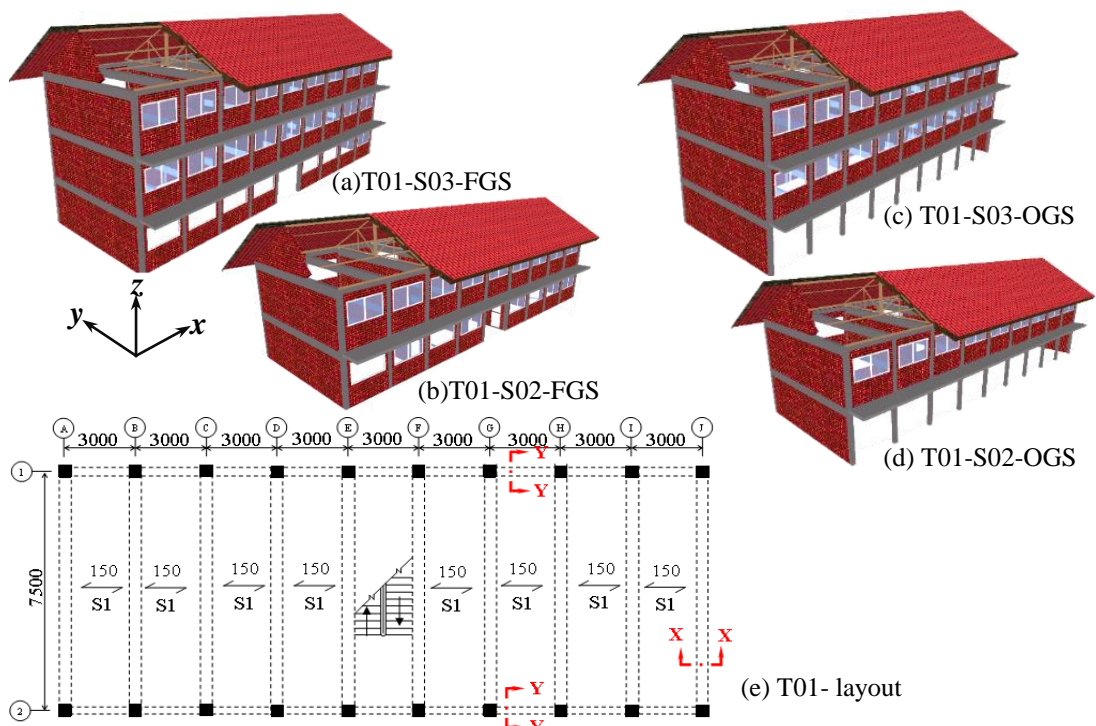


Figure 4-3. Type-01 building with OGS and FGS illustration

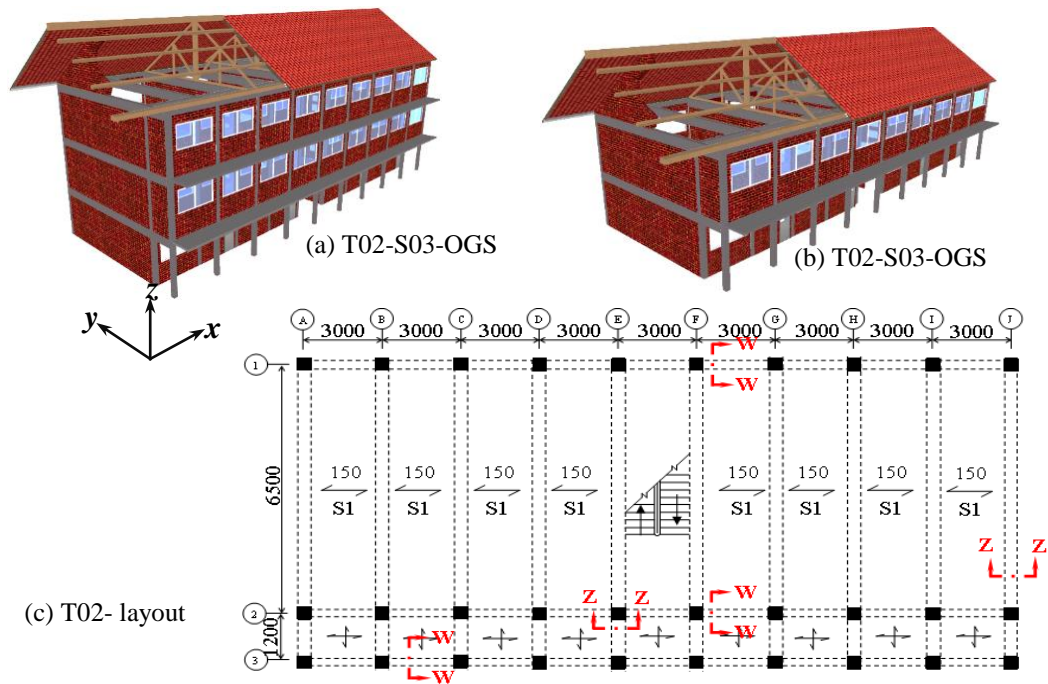


Figure 4-4. Type-02 building with OGS illustration

However, significant variances were observed in MI configurations and arrangements used in the school buildings surveyed, as shown in Figures 4-3 (a-d). As a result, those variations have to be incorporated in the analyses of the buildings against seismic actions. The presence of MI at the GF was designated as the full ground storey (FGS), otherwise denoted as open ground storey (OGS) for those typologies. Remarkably, T01 typologies of S02 and S03 contained two sub typologies, while T02 buildings had only OGS. Nevertheless, the sub typology as in the middle frame, which has the central window (denoted as OGS cases) and half openings (denoted as MHO cases), were observed in T02 buildings.

4.3 Material and sectional properties

Figure 4-5 shows the sectional details of the beams and columns of the T01 and T02 building typologies. The average beam size measured in T01 buildings in X- and Y- directions are 300 mm \times 225 mm with 16 mm diameter bars in the corners, and 525 mm \times 225 mm with three 25 mm- diameter bars at bottom and two 16 mm diameter bars at top, respectively. In the T02, the X-direction section was similar to the T01, however the Y-direction beam was 450 mm \times 225 mm with three 20 mm bars at the

bottom and two 16 mm bars at the top. The column dimension was similar for both typologies, which were 225 mm × 225 mm with 20 mm and 16 mm diameter bars at corners for T01 and T02, respectively. The stirrups are generally made of 6 mm diameters bars with 150 mm of spacing. Meanwhile, the average RC slab thickness was obtained as 150 mm, and the roof of the buildings are made of clay tiles, concrete slab, etc.... The detailed dimensions of the school buildings can be seen in **Appendix A-3**. In addition, the material strength properties used in the school buildings were referred from past studies (Abey Siriwardena, 2018; Marasingha, 2013; Thamboo & Dhanasekar, 2019a). Generally, the compressive strengths of concrete and masonry used in the school building construction are 20 MPa and 1.5 MPa respectively. Conventional TMT steel bars are used as reinforcement, where the yield strength of those steel bars can be taken as 460-500 MPa.

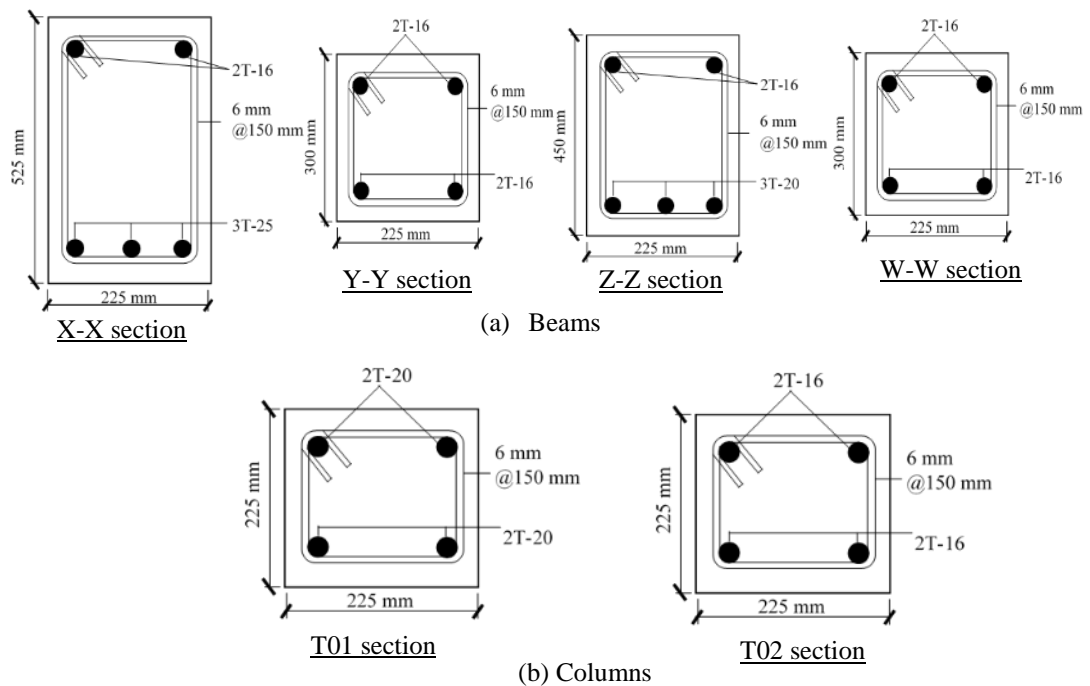


Figure 4-5. RC section of T01 and T02

4.4 Infill (MI) configuration

The presence of the MI in the buildings influences the performance of the building during a seismic action. Past studies conducted in Sri Lanka (Abeywardena, 2018; Marasingha, 2013), did not assess the irregularities of MI configurations and arrangement in the school buildings against the performance under seismic loading. However, the survey data revealed different MI configurations in Sri Lankan school buildings exist, that are depicted in Figures 4-6. The detail dimension and the non-structural configuration can be seen in *Appendix A-4*. There were primarily four MI configurations observed in the X-direction of the school buildings surveyed: they are (1) central window (CW), (2) quarter opening (QO), (3) half opening (HO), and (4) three quarter openings (1 m height wall) (TO), while the full wall (FW) is used in the Y-direction. Also, thickness of the MI wall with 225 mm could be made of double bonded brick (DW) masonry arrangement, otherwise thickness of 115 mm could be made of single bonded (SW) brick masonry assemblage. Only FW configuration is used to separate the classrooms in the school buildings.

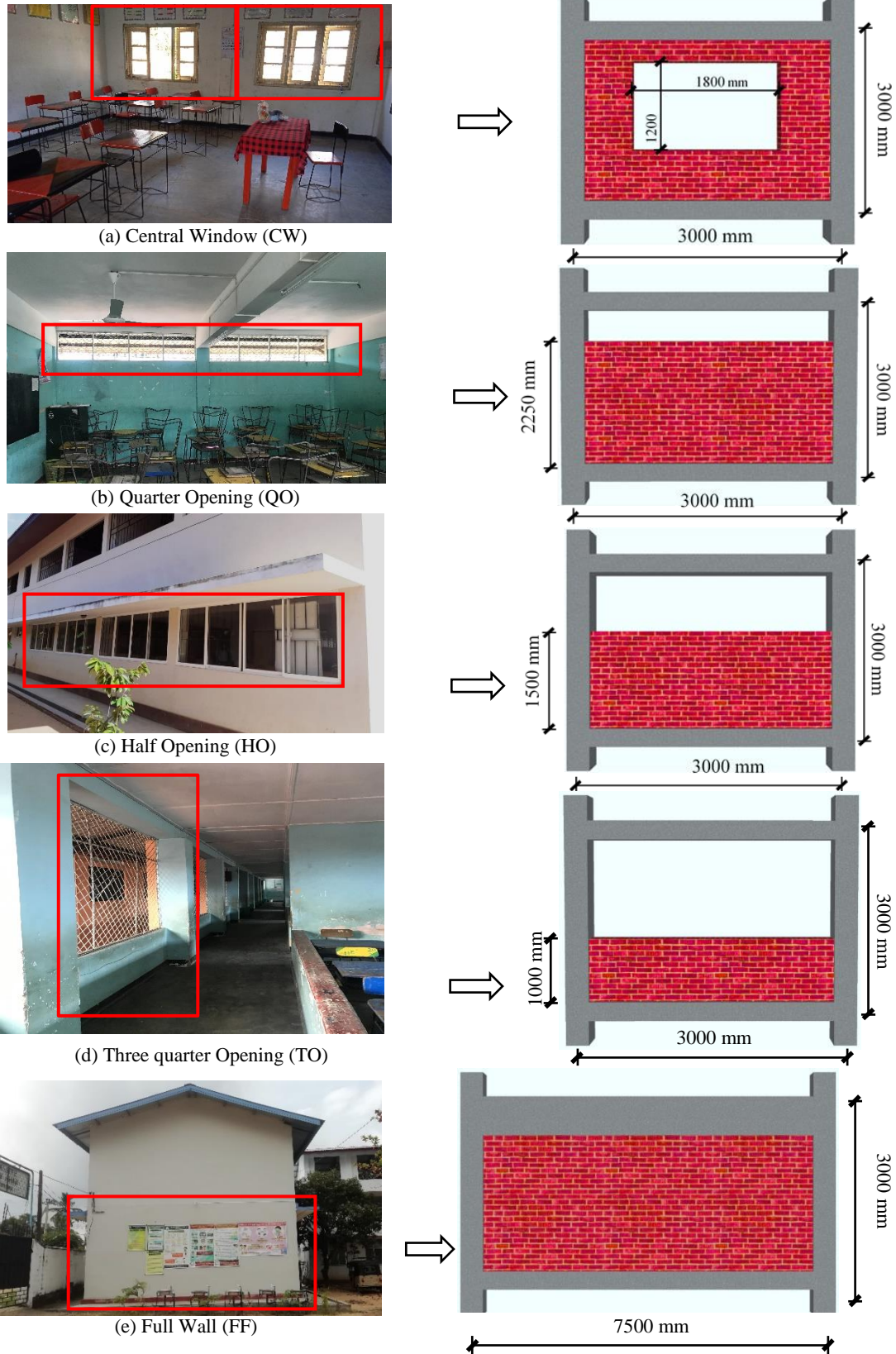


Figure 4-6. MI configuration (CW, QO, HO, and TO) in Sri Lankan school buildings

4.5 Summary

Altogether 40 school buildings were surveyed to determine the structural and non-structural attributes prevailing in the Sri Lankan school buildings. The survey showed two typologies exist in terms of structural layouts referred, as shown in Figure 4-7. Notably, in terms of RC-MI classifications, two and three storey buildings were predominantly observed. However, the structural typologies of the study were considered to be vary in terms of rows of columns present in the layout and was defined as T01 (two rows of columns) and T02 (three rows of columns). Remarkably, the presence of MI in the GF resulted in the creation of new sub-types such as OGS and FGS, and the FGS sub-type was only witnessed in T01 buildings. Furthermore, many MI configurations in terms of opening sizes such as CW, QO, HO, and TO were seen, notably in the X-direction with different thicknesses such as SW and DW, whereas FW was discernible in the Y-direction with DW.

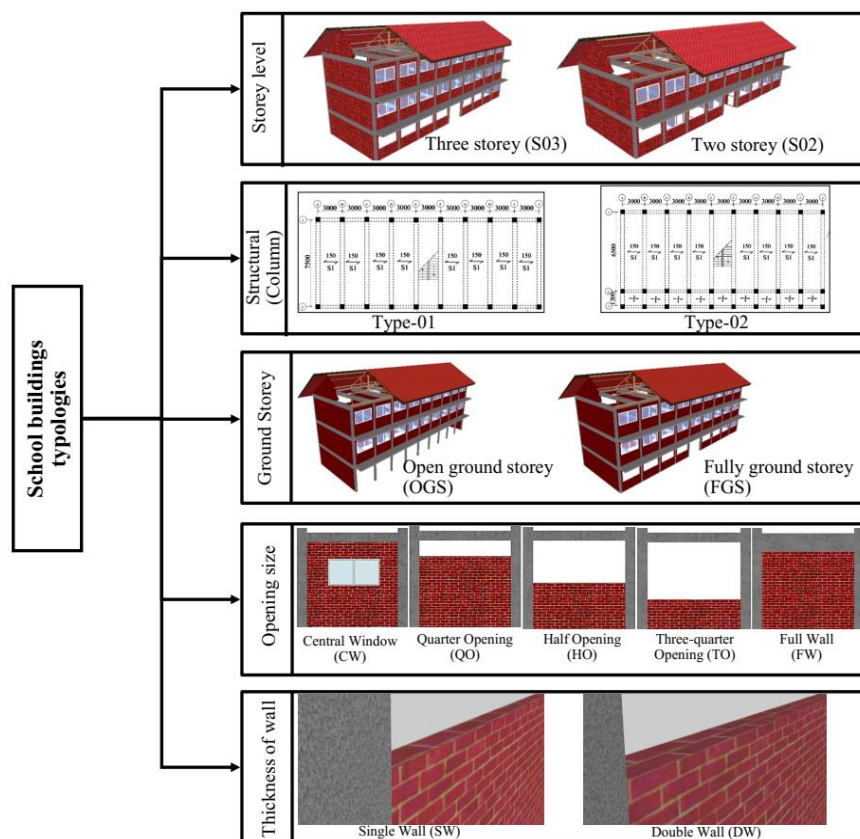


Figure 4-7. Summary of school building surveyed

5. MODELING OF SCHOOL BUILDINGS TYPOLOGIES

In order to assess the seismic performances of the school buildings in Sri Lanka, their numerical models were developed using finite element (FE) framework and the performances were analysed. The numerical analyses were carried out by considering all the possible structural and non-structural variations observed in the survey. In this section, the numerical modelling procedure, the method of incorporating MI into the modelling, and post processing techniques used to effectively analyse the buildings under seismic loading are explained.

5.1 Modeling using OpenSees

OpenSees (OS) is an open system earthquake engineering simulation framework developed by Pacific Earthquake Engineering Research (PEER) to analyse the performances of structures subjected to earthquakes (Mazzoni et al., 2006; McKenna et al., 2000). All two and three storey buildings typologies identified in the survey were modelled by incorporating the potential variations in the buildings as stated in Chapter 4. The procedure followed to create OS models of the buildings is shown in Figure 5-1 (The TCL code for T01-S03-FGS-DW-CW case can be seen in *Appendix-C*). The details of each modelling attribute are explained in following sub-sections.

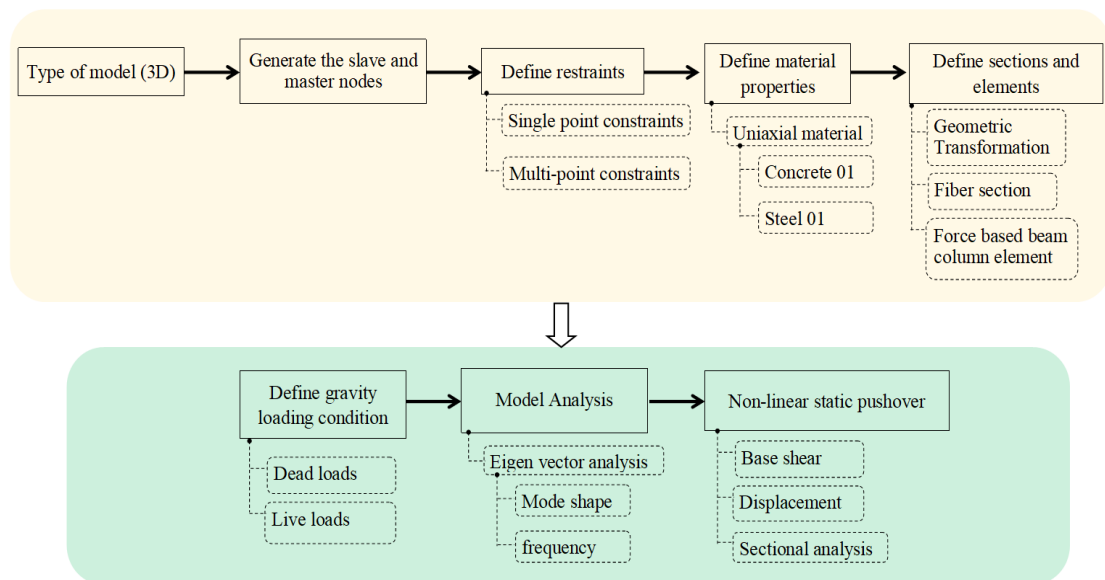


Figure 5-1. Simplified analysis procedure of OS model

5.1.1 Defining beam and column section

The beam and column elements were generated as the quadrilateral patch fiber section. The fiber sections that were assigned to the columns are shown in Figure 5-2, where the confined and unconfined areas of the sections were separately assigned.

A fiber section was defined as having its geometric center as the origin of a 2D local coordinate system of y and z for the section. The confined area was divided as 10×10 fiber sections, whereas the unconfined area was divided into 10×3 fiber sections. It should be noted that the uniaxial stress-strain relationship of concrete (confined and unconfined) was assigned to each fiber. The start and end positions of the steel layers as well as the four corner points of the concrete patch have been specified. The cross-sectional area and number of bars of each reinforcement layer (bottom and top) were also defined as shown Figure 5-2.

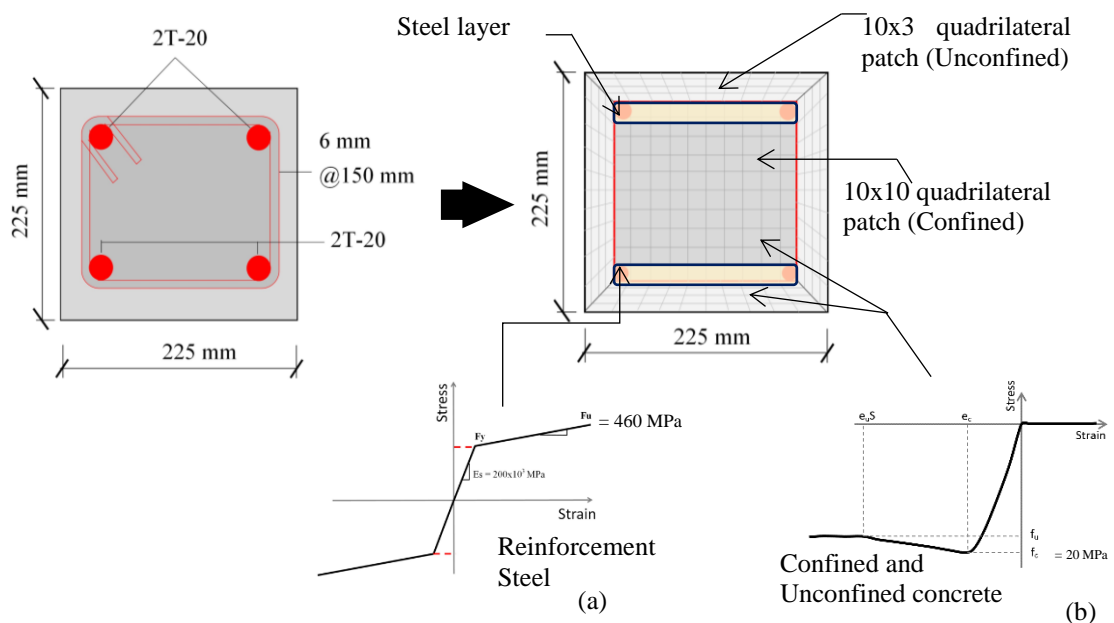


Figure 5-2. Reinforcement layer (confined and unconfined)

The beam and columns were modelled using force-based nonlinear beam column element, which is provided in OS (OpenSees, 2021), with five integration points, as shown in Figure 5-2. This element enables to determine the curvature distribution of each single element with sufficient precision by acquiring the necessary integration

points. The element nodal deformations were determined based Gauss-Lobatto integration along the element (OpenSees, 2021). Each sectional response of the members was recorded and analysed to assess the shear demand of the columns in this study (explained in Section 5.5). The effects of geometric transformation were considered by the corotational transformation method, using OS (OpenSees, 2021), as it is an accurate method of transforming the geometrical sections.

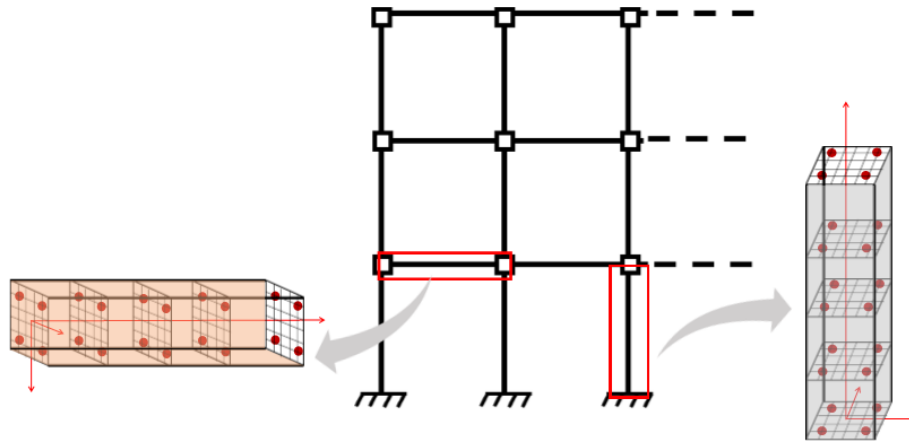


Figure 5-3. Beam and column integration points

5.1.2 Defining slabs (Multi-point constraints)

The RC slabs were defined as rigid diaphragms to account for in-plane stiffness of the floors. A RC building subjected to lateral loading, has infinite in-plane stiffness (own plane) and behaves like a rigid body that restricts the action of shear, bending and axial forces on the diaphragm (Aydenlou, 2020). Figure 5-4 shows the modelling approach of the slab, with each adjacent node introduced as a slave node and the node at the middle of the structure as the master node. The master and slave nodes on each floor were rigidly connected using the multi-point constraints provided in OS (OpenSees, 2021), allowing for translation in the x and y directions and rotation in the z direction. In addition, changes in slab stiffness were not incorporated in the study. However this assumption would anyway allow to conservatively predict the seismic performance of the buildings (Shanthika et al., 2022).

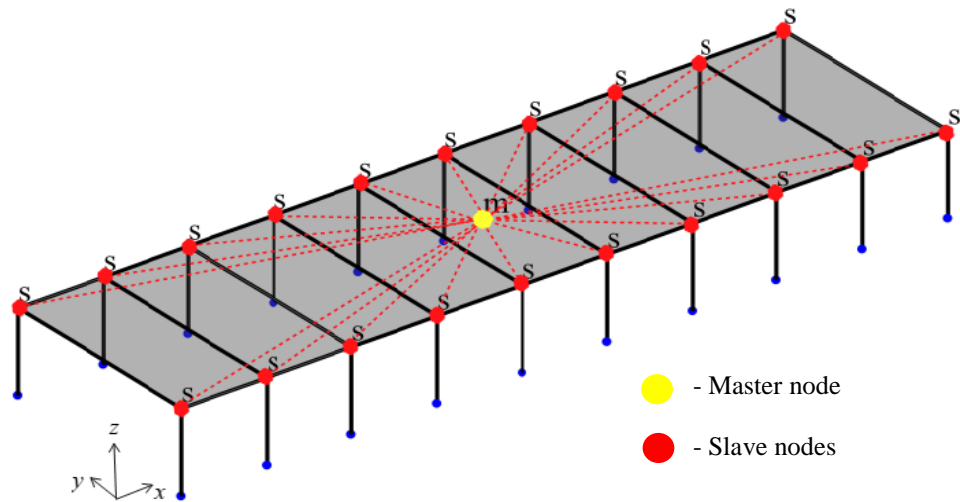


Figure 5-4. Multi Point constraints (MP constraints)

5.1.3 Defining foundation (Single point constraints)

In order to incorporate the foundation support condition, single point constraints (SP) was adapted in OS (OpenSees, 2021). The SPs were assigned at the supports (ground floor nodes) as fixed support conditions. It is due to the assumption that these school buildings are provided with single pad footing, and the effect was not incorporated as it would sufficiently stiffness to the buildings. Similarly, in the master node, X and Y (global coordinate) rotational degree of freedom were restricted. Figure 5-5 shows the assigned SP constraints at column base and master node.

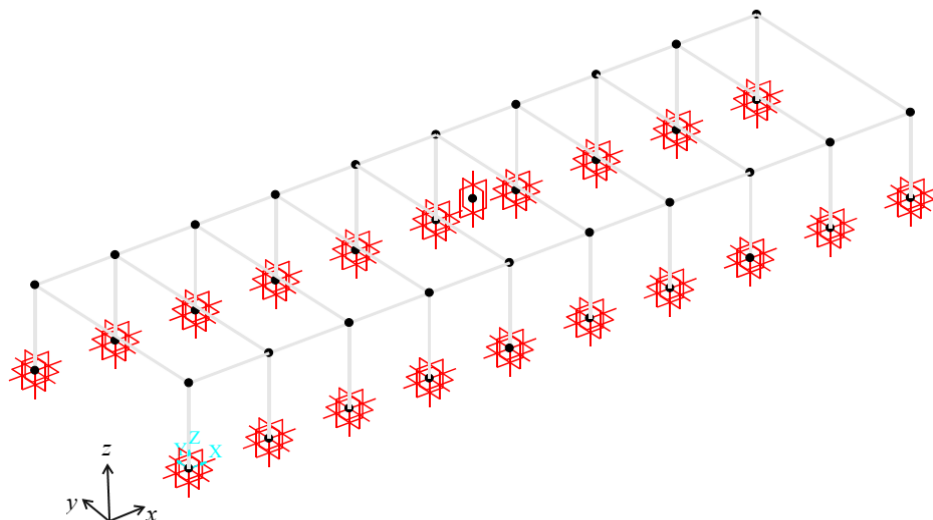


Figure 5-5. Single Point constraints (SP constraints)

5.2 Modelling of MI

The MI walls were modelled by considering the existing variation in the buildings, those are CW, QO, HO, TO, and FW with different thicknesses (SW and DW) as observed in the survey (Figure 4-6). The equivalent diagonal strut model is a widely used method of modelling MI in frames to analyse against lateral forces. MI walls can be modelled as equivalent diagonal struts in the frame to perform nonlinear pushover analysis. In this study, the MI was modelled as a single strut using the approach proposed in FEMA 356 (FEMA-356, 2000). In this study, the MI was modelled as a single strut using the approach proposed in FEMA 356 (FEMA-356, 2000). The single strut method simplifies the analysis of MI exposed to in-plane lateral loads. The wall is designed to function like a single strut in this method, supported by two perpendicular compression lines running from the ends of the wall to the centre of the base. Also, it should be highlighted that, to capture the behaviour of MI accurately, non-linear modelling was considered using truss element in OS.

Figure 5-6 depicts the equivalent diagonal single strut of a MI, where width is denoted by a . MIs with larger openings (i.e., greater than 70% opening ratio), particularly where doors and windows exist in bays, were not modelled as they do not produce sufficient strut action in the frame. The corotational truss element available in the OS (OpenSees, 2021) was used to model the MI. The stiffness and strength of the diagonal struts were reduced as per the opening configurations (i.e., opening ratio) of MIs found. In addition, the MIs in both directions (longitudinal and transverse) were explicitly modelled; they imply primary contribution to the stiffness and strength in their own direction rather than the other direction of the building.

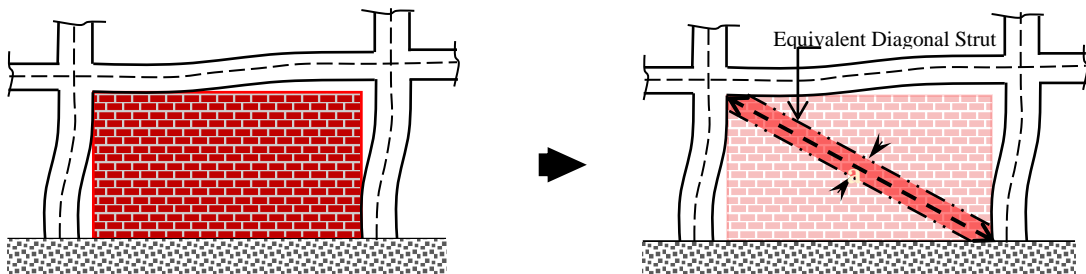


Figure 5-6. Equivalent diagonal strut width of MI

The following equations (5-1) and (5-2) were used to evaluate the strut width (a) of the MI, and then it was multiplied by the thickness of the wall to compensate for the equivalent diagonal single strut (FEMA-356, 2000) in the model:

$$a = 0.175 (\lambda_1 \cdot h_{col})^{-0.4} \cdot r_{inf} \quad (5-1)$$

$$\lambda_1 = \left[\frac{E_{me} \cdot t_{inf} \cdot \sin 2\theta}{4 \cdot E_{fe} \cdot I_{col} \cdot h_{inf}} \right]^{0.25} \quad (5-2)$$

Where, h_{col} and h_{inf} are the heights of column and MI, respectively. r_{inf} is the length of the MI, E_{fe} and E_{me} are the modulus of elasticity of frame and MI, respectively. I_{col} is the moment of inertia of the column and t_{inf} is the thickness of MI.

However, when the openings are presented in the walls, the reduction factor R should be applied, and the following equation (5-3) was used to calculate the factor R based on the based on the study reported by Al-Chaar et al. (2002):

$$R_1 = 0.6 \left(\frac{A_{open}}{A_{panel}} \right)^2 - 1.6 \left(\frac{A_{open}}{A_{panel}} \right) + 1 \quad (5-3)$$

where A_{open} is the area of the openings and A_{panel} is the gross area of the MI.

Figures 5-7 and 5-8 (a and b) show the numerical models of school buildings created and each model has been named as per the variations obtained during the survey (Figure 4-7). For an example, T01-S03-FGS-DW-HO implies Type 01, three storey (S03), fully ground storey (FGS), double thickness (DW) wall with half wall opening (HO) case. Consequently, 64 combinations (see **Appendix-B**) were analysed in this study to assess the seismic performance of schools.

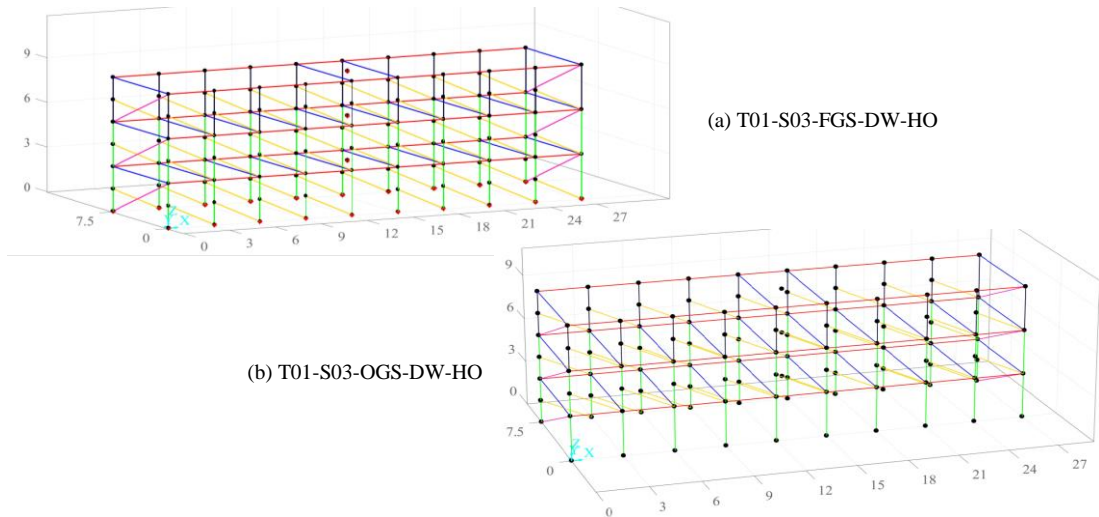


Figure 5-7. 3D model of Type 01 (T01) three storey

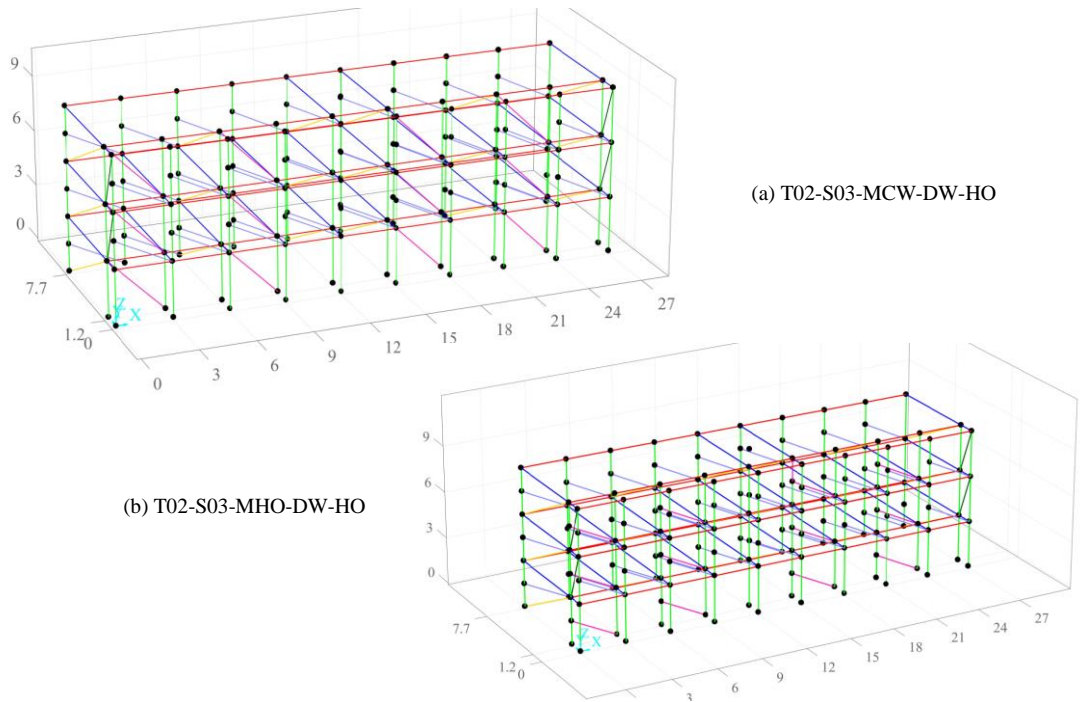


Figure 5-8. 3D model of Type 02 (T02) three storey building with HO cases

The 64 combinations analysed were from T01 (OGS and FGS) and T02 (Middle frame with CW (MCW) and HO (MHO) variations), two storey levels (S02 and S03), two IMW thickness (SW and DW), and four IMW configurations in x direction (CW, QO,

HO and TO). Consequently, the 32 cases were analysed for each typology (T01 and T02) leading to 64 cases ($2 \times 2 \times 2 \times 4 = 32$ and $32 \times 2 = 64$).

5.3 Incorporating material variations

5.3.1 Material characteristics from survey

The concrete properties assigned in the numerical models were obtained from the literature (Abey Siriwardena, 2018; Marasingha, 2013). The default Concrete04 model from the material portfolio of OS (OpenSees, 2021) was employed to assign the non-linear behaviour of concrete. It represents the uniaxial confined behaviour of concrete according to Popovic (Popovics, 1973), taking into account diminishment due to cyclic loading according to model Karsan & Jirsa, (1969) model. Then, the steel reinforcement bars were given the Steel 01 classification according to the elasto-plastic stress-strain model specified in OS (McKenna et al., 2000). Similarly, the masonry properties were adapted from the study conducted by Thamboo & Dhanasekar (2019). The mean material properties of confined and unconfined concrete and steel used in this study can be seen in Table 5-1.

Table 5-1. Mean material properties

Material	Properties	Values	Reference
Unconfined Concrete	Compressive strength (f_c)	20.0 MPa	Marasingha (2013) and Abey Siriwardena (2016)
	Peak strain (ϵ_c)	0.0025	
	Modulus of Elasticity (E_c)	22000 MPa	
Confined Concrete	Compressive strength (f_{cc})	22.0 MPa	
	Peak strain (ϵ_{cc})	0.003	
	Modulus of Elasticity (E_{cc})	24500 MPa	
Steel	Yield Strength (f_y)	460 MPa	
	Hardening Ratio (b)	0.001	
	Modulus of Elasticity (E_s)	200000 MPa	
Masonry	Compressive Strength (f_m)	1.5 MPa	Thamboo & Dhanasekar (2019)
	Strain (ϵ_{mp})	0.003	
	Modulus of Elasticity (E_m)	2000	

5.3.2 Material uncertainty characterisation

In order to predict material uncertainty for the analysis of fragility functions (Chapter 6), the probabilistic material variation of concrete (unconfined), masonry and steel were incorporated in this study. The coefficient of variations (COV) considered for the strength properties of the material are given in Table 5-2.

Table 5-2. Material COV and the distribution used for the Monte Carlo simulation

Material	Properties	COV (%)	Distribution
Unconfined Concrete	Compressive strength	15	Normal
Steel	Yield Strength	5	Lognormal
Masonry	Compressive Strength	30	Normal

The normal probability distribution function was assigned for compressive strength characteristics of the masonry and the concrete, whereas the lognormal probability distribution function was selected for the steel as can be seen in Figure 5-9. In order to generate the random combination of the material uncertainty with defined COV, the Monte Carlo simulation (MCS) approach was used for the building cases considered.

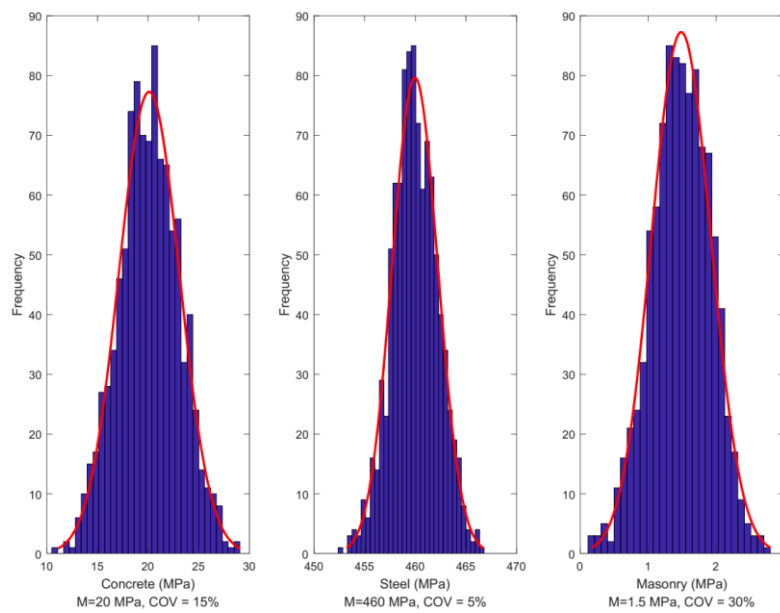


Figure 5-9. The distribution of 1000 random samples (a) concrete – normal distribution, (b) steel – lognormal distribution and (c) masonry – normal distribution

The random samples of compressive strengths of unconfined concrete and masonry, and yield strength of reinforcement were only obtained in MCS. Meanwhile, uncertainty in the Young's modules and the shear modulus parameters were assumed to depend on the compressive strength or the yield strength. However, corresponding mechanical properties of the materials were obtained from the analytical formations given in the literature. The confined strength of concrete and the corresponding mechanical properties were determined from Mander et al. (1989) and EN:1992-1-1:2004-(E), (2004) as per the formulations given in equations (5-4) to (5-6). The peak

strain and elastic modulus of the concrete were computed from the compressive strength of concrete (confined or unconfined) as per equations (5-5) and (5-6) (Mander et al., 1989). Additionally, the only the compressive strength of the masonry was randomised in the MCS, whereas, the corresponding peak strains and elastic moduli of the randomised masonry compressive strengths were determined from the formulations suggested in Thamboo & Dhanasekar (2019), as given in equations (5-7) and (5-8). Subsequently, whole stochastic material data were generated using a purposely written MATLAB, (2017a) script (see *Appendix C*) and then integrated into the OS (OpenSees, 2021) models. Consequently, for each building case considered, ten randomised sets of material properties, leading to 640 building cases (64×10), to analyse and generate fragility curves of the three major building typologies considered (T01-OGS, T01-FGS, and T02-OGS).

$$f_{cc} = f_{ck} \left[1000 + 5 \left(\frac{\sigma_2}{f_c} \right) \right] \quad (5-4)$$

$$\varepsilon_{cp} = 0.0007f_c^{0.31} \quad (5-5)$$

$$E_{cm} = \left[\frac{f_c}{10} \right]^{0.3} \quad (5-6)$$

$$\varepsilon_{mp} = 0.0025f_m^{0.29} \quad (5-7)$$

$$E_m = 550f_m \quad (5-8)$$

Where f_{ck} , f_{cc} and f_c are the concrete characteristic compressive strength, confined strength of confined and unconfined concrete, respectively. Also, σ_2 is the effective lateral compressive stress. ε_{cp} is the strain at peak stress of concrete, and then E_c is the elastic modulus of concrete. f_m , ε_{mp} and E_m are the compressive strength, strain at peak stress and elastic modulus of masonry.

5.4 Pushover analysis and post processing of results

5.4.1 Pushover analysis (PO)

The PO was introduced by ATC-40 (1996) and FEMA 273 (1997) to carry out the performance based earthquake engineering assessment and has been used for more than two decades (Maziligüney, 2020), due to its simplicity and consideration of the post-elastic behaviour of the structure. The monotonic lateral loads are applied to the structure with a step-by-step increment until it reaches ultimate failure, at which point

the degradation of progressive stiffness is considered. In general, multi-degree of freedom (MDOF) systems are transformed to single degree of freedom (SDOF), and the fundamental mode of vibration of the MDOF structural system is considered to be the equivalent mode of SDOF in the analysis (Saiidi & Sozen, 1981). The conventional PO analysis procedure of the building incorporating MI can be seen in Figure 5-10 (Steps 1-3). The obtained modal parameters are used to evaluate the distribution of equivalent static load conditions under constant gravity load conditions (Hasan et al., 2002). Therefore, PO-based assessment and design approaches are recommended for low- to mid-rise regular buildings (Maziligüney, 2020). Therefore, it was adopted in this study.

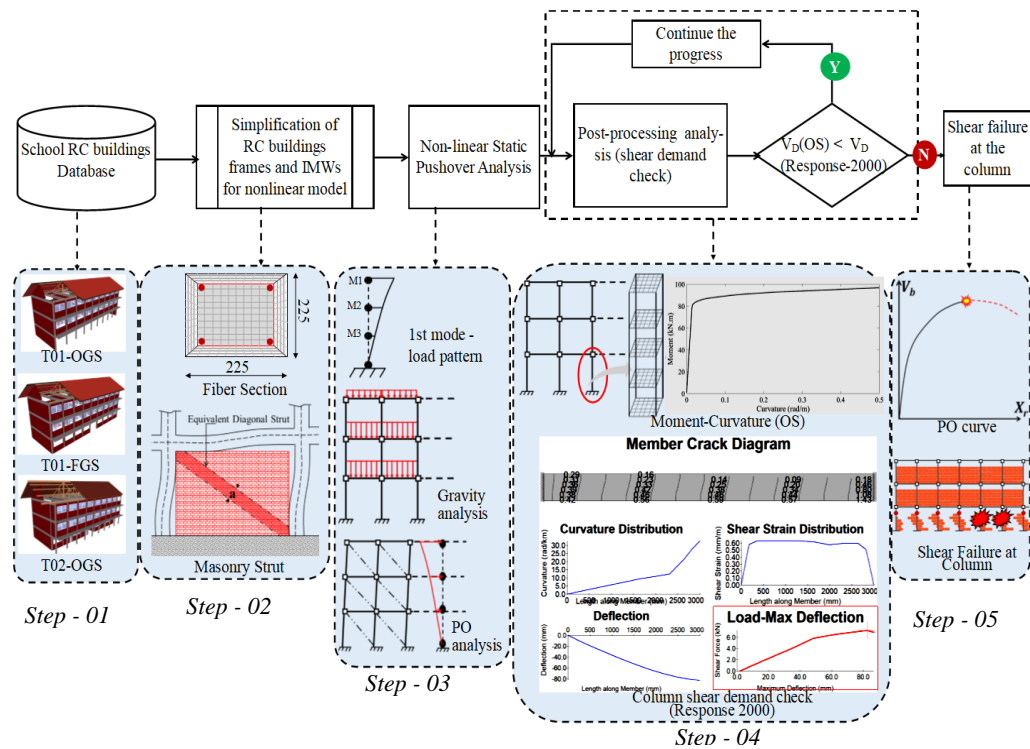


Figure 5-10. Iterative pushover analysis procedure for the seismic performance assessment of MI frames incorporating shear demand parameters

To assess the seismic performance and fragility assessment (Chapter 6) of school buildings in Sri Lanka, a nonlinear static pushover (PO) procedure was employed. The pushover graphs and capacity graphs of the buildings in both orthogonal direction (X- and Y-directions) were obtained in the analyses. The PO assessment was performed for 64 different building cases, including T01 and T02 structures with S02 and S03

storey levels. In addition, bare frames (BF) of the typological buildings were also analysed for comparison purpose. To perform the analysis, the latest version of OpenSees 3.3.0 (OpenSees, 2021) was used, and the master node deformation, base shear, and the element responses were recorded.

The gravity action acting on each element were determined and applied on the elements. Permanent actions were assigned by integrating with slab, beam, columns, and MI self-weight. The variable actions were obtained as per EN:1992-1-1:2004-(E), (2004) and assigned as 3 kN/m^3 . To calculate the permanent action, the self-weight of the RC section was assumed to be 25 kN/m^3 . Furthermore, the lumped mass of the storey was calculated by integrating each storey mass and applied to the center of the structures, where the master nodes were allocated. Preliminary Eigen vector analysis was carried out to obtain the model parameters of the particular building. Consequently, the gravity analysis was performed prior to the PO analysis to obtain the elastic forces and the displacement. After analysing the buildings against gravity loads, nonlinear pushover analyses were performed in two primary directions (X and Y) to determine the seismic performances of the RC-IMW building typologies considered. The PO procedure was applied as triangular-shaped linear displacement increments through the master nodes assigned, incorporating modal parameters. The PO analysis results of the bare frame (BF) of T01 and T02 buildings in both X and Y directions can be seen in Figure 5-11.

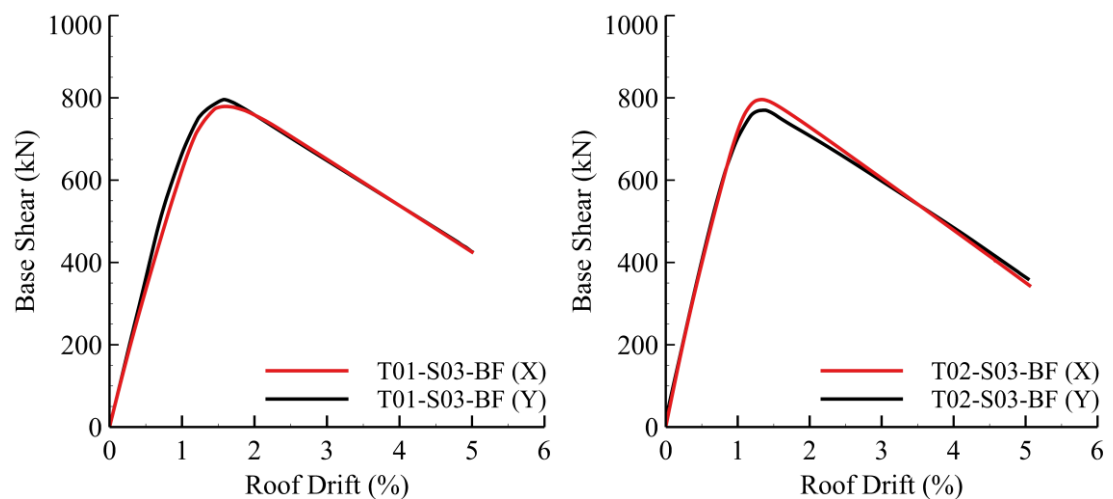


Figure 5-11. Pushover graph of T01 and T02 of Bare frame (BF)

If a building is not symmetric in plan, the building can experience the torsional effect and create additional shear forces to the elements. Therefore, torsional effect of the building that can occur due to the asymmetry of the structure due to MI was incorporated into this study. The torsional stiffness modulus of each member was computed and applied during the analysis phase. Figure 5-12 shows the PO curves of results of torsional stiffness and non-torsional stiffness integrated into the analysis, and it can be observed that the incorporation into the torsional effect reduced the overall capacity of the building. The following equation (5-9) was used to compute the torsional rigidity of the members:

$$\text{Torsional Rigidity} = GJ \quad (5-9)$$

Where G and J denote the modulus of rigidity and torsional constant respectively. J and G was calculated as per equations (5-10) and (5-11), respectively (Young et al., 2012, p. 401):

$$J = \left[ab^3 - 3.36 \frac{b}{a} \left(1 - \frac{b^4}{12a^4} \right) \right] \text{ for } a \geq b \quad (5-10)$$

$$G = \frac{E}{2(1+\nu)} \quad (5-11)$$

Where a and b are the half of the length and width of the members. E is Young's modulus of the uniaxial material and ν is Poisson's ratio.

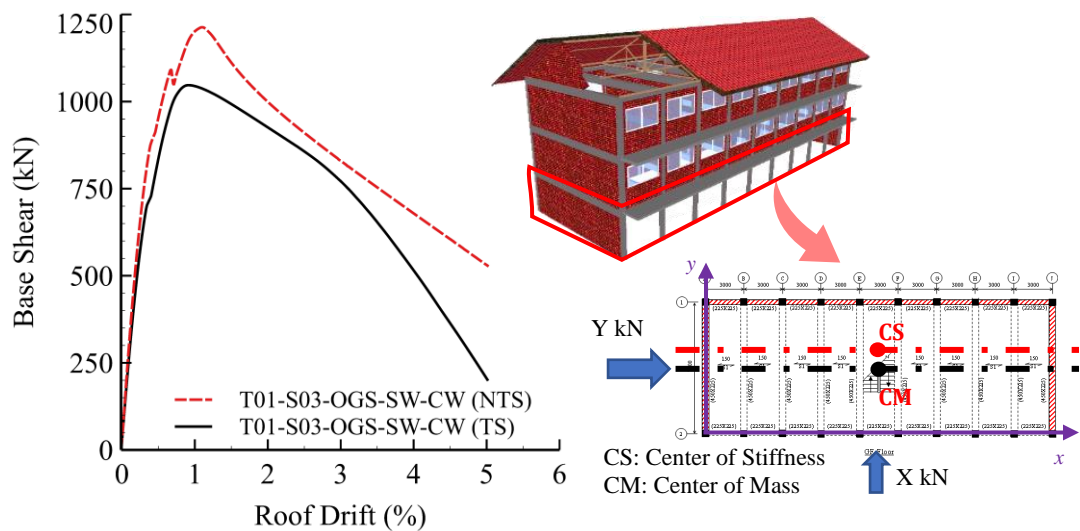


Figure 5-12. PO analysis results of torsional stiffness (TS) and non-torsional stiffness (NTS) of T01-S03-OGS-SW-CW cases

5.4.2 Post processing

The school buildings to be analysed against seismic loading are designed only against gravity actions. However, MI in these buildings would interact with the adjacent columns or frame during the seismic action and cause shear failure of these column elements. Nonetheless, the shear force-deformation constitutive response is not available in the OS (McKenna et al., 2000) force-based beam-column elements to explicitly capture the shear failure of the elements. Therefore, to incorporate the axial-shear and axial-moment interactions in the columns, a simplified approach was followed in this study. Subsequently, during the pushover analyses, the axial-shear and axial-moment interactions of the column elements were monitored from the OS (McKenna et al., 2000) output data and the shear failure of the columns were explicitly accounted by verifying the predicted shear resistance of the column elements using Response-2000 software (Bentz, 2000; Bentz et al., 2006). Fig 5-10 (Steps 4 and 5) shows the iterative process adopted to account for the shear failure of the columns in the analyses and the adjustment of the PO graphs based on the shear failure.

Response-2000 (Bentz, 2000) is a sectional analysis tool developed by incorporating Modified Compression Field Theory (MCFT) to compute the shear resistance of RC elements incorporating the axial load of the members, material properties, and sectional dimensions (Bentz, 2000; Bentz et al., 2006). Response-2000 (Bentz, 2000) provides accurate depictions of the shear behaviour of reinforced concrete members, including the development of crack patterns. The axial forces were computed from the gravitational actions applied to the column sections created (only the edge and intermediate columns), before performing PO analyses to verify the shear resistances of the sections. Then, during the analysis of each building, the shear forces developed in those columns were monitored against the resistances obtained in Response-2000 (Bentz, 2000) to verify the shear failure of the columns. This process was iterated until both the OS (McKenna et al., 2000) output and Response-2000 (Bentz, 2000) axial-shear interaction response convergence was achieved in each building case analysed, as illustrated in Figure 5-10. Then, the PO curve was cut off at the point, where the shear failure of the column (at the GF level) was detected and further process was carried out.

The technique implemented was similar to practice oriented column shear failure analyses methods suggested for RC-MI buildings by Celarec & Dolšek, (2013) and Cavaleri et al., (2017). However, it has to be mentioned that this procedure has some limitations, as it ignores the redundancy and redistribution of forces during the collapse mechanism of the buildings. Nonetheless, it can be said that this technique is comparatively simple and effective for assessing a large number of structural variabilities, particularly to develop fragility functions.

5.4.2.1 Sectional moment capacity validation

Figure 5-13 shows the comparison of the moment curvature of GF column obtained from OS (OpenSees, 2021) and Response 2000 (Bentz, 2001). During the analysis of OS (OpenSees, 2021), the GF column moment curvature parameters were recorded for the column section, and for the same column, the axial load was obtained and analysed with the Response 2000 (Bentz, 2001). The moment capacity obtained from OS (OpenSees, 2021) showed 62 kN.m, whereas the Response 2000 (Bentz, 2001) displayed 58 kN.m. The slight difference in the results occurred because the OS (OpenSees, 2021) generated the moment-curvature relationship with varying axial load parameters, while the Response 2000 (Bentz, 2001) performed with constant axial load parameters.

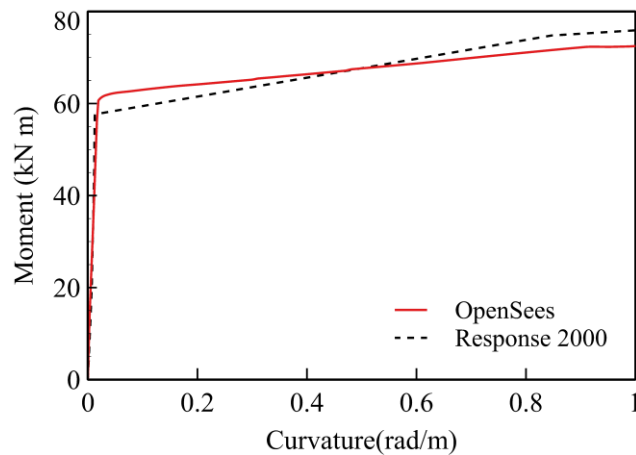


Figure 5-13. Moment-curvature comparison of OS and Response-2000 results of column section

5.5 Seismic performances of the school buildings typologies

The seismic performance of school building typologies in Sri Lanka is presented and discussed in terms of failure mechanisms and PO curves obtained. Furthermore, instead of overall drift ratio (roof drift ratio), the GF inter-storey drift ratio (IDR%) was used in the analyses, because the failure mechanisms of the buildings (due to their low rise) were concentrated at the ground floor elements (IMWs and columns). Also, as shown in Figure 5-14, the drift ratio at GF was found to be higher than that at the other storey levels. In total, 64 cases were examined, including MI configurations (CW, QO, HO, and TO) and thickness (SW and DW), typologies (T01 and T02), and the influence of the OGS and FGS (Section 4.4 and 4.5). The lateral load-displacement responses (X and Y direction) of the three and two storey building cases analysed are shown in Figures 5-15, 5-16, 5-17 and 5-18, respectively. The PO analysis was carried out in both directions of the buildings (X and Y), and the results will be discussed in details in the following sections.

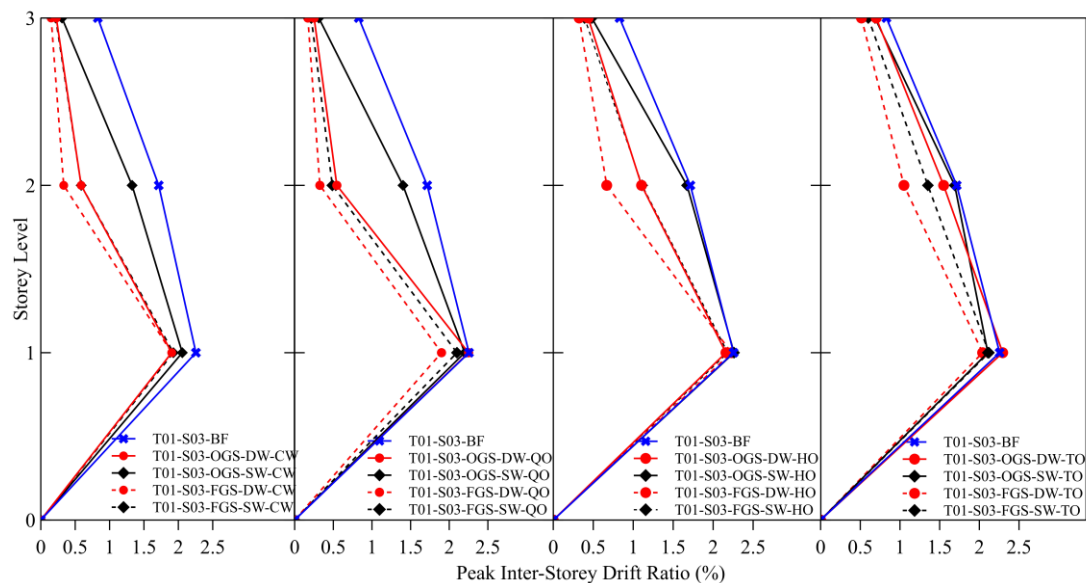


Figure 5-14. Peak inter-storey drift ratio of T01-S03 cases with various MI configuration (CW, QO, HO, and TO) considering OGS and FGS

5.5.1 Transverse direction (Y-direction)

It was mainly observed from Fig 5-15, that the performance of the building in the Y-direction demonstrated a similar performance for all types of buildings, even for varied MI configurations located in the Y-direction. The BF was also analysed for

comparison purposes. This is because all typologies have identical MI configurations in the Y-direction as observed in the survey (see Figure 4-6 (e)), nonetheless significant variation was found in the X-direction. In general, the Y-direction walls were built as DW-MI, with no openings. Therefore, the main focus was given to verify the X-direction responses of the buildings.

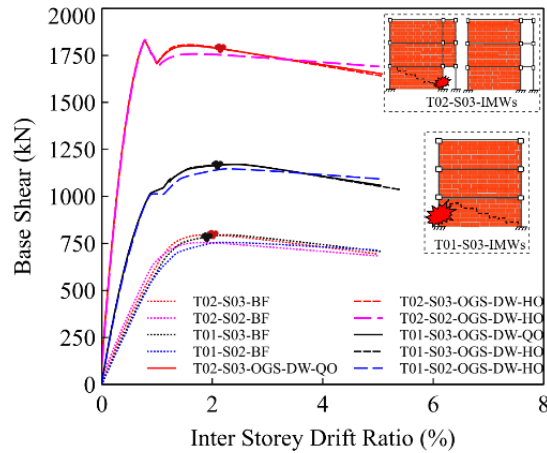


Figure 5-15. Y-direction PO curves of BF, QO and HO with different storey level

5.5.2 Longitudinal direction (X-direction)

The performances of the s in terms of the typologies, MI configurations (CW, QO, HO, and TO) and thickness of MI were varied significantly and influence of these parameters are discussed below.

5.5.2.1 Effects of OGS and FGS

As described in sections 4-4 and 4-5, for sub-types OGS and FGS, the performance and the failure mechanism of SW and DW of S03 and S02 buildings are represented in Figures 5-16, 5-17 and 5-18, respectively. The primary variation in the FGS and OGS is the presence of MI at GF for FGS, which influences the overall stiffness of the buildings. The lack of MI in the GF causes the first floor (FF) to be more flexible and increases the drift ratio, ultimately leading to form soft-storey mechanism. However, the shear failure was delayed in T02-S03-OGS (IDR% of SW-2.9% and DW-3.1%) compared to T01-S03-FGS (IDR% of SW-2.8% and DW-3.0%), and T01-S03-OGS (IDR% of SW-2.2% and DW-2.5%) for the CW cases.

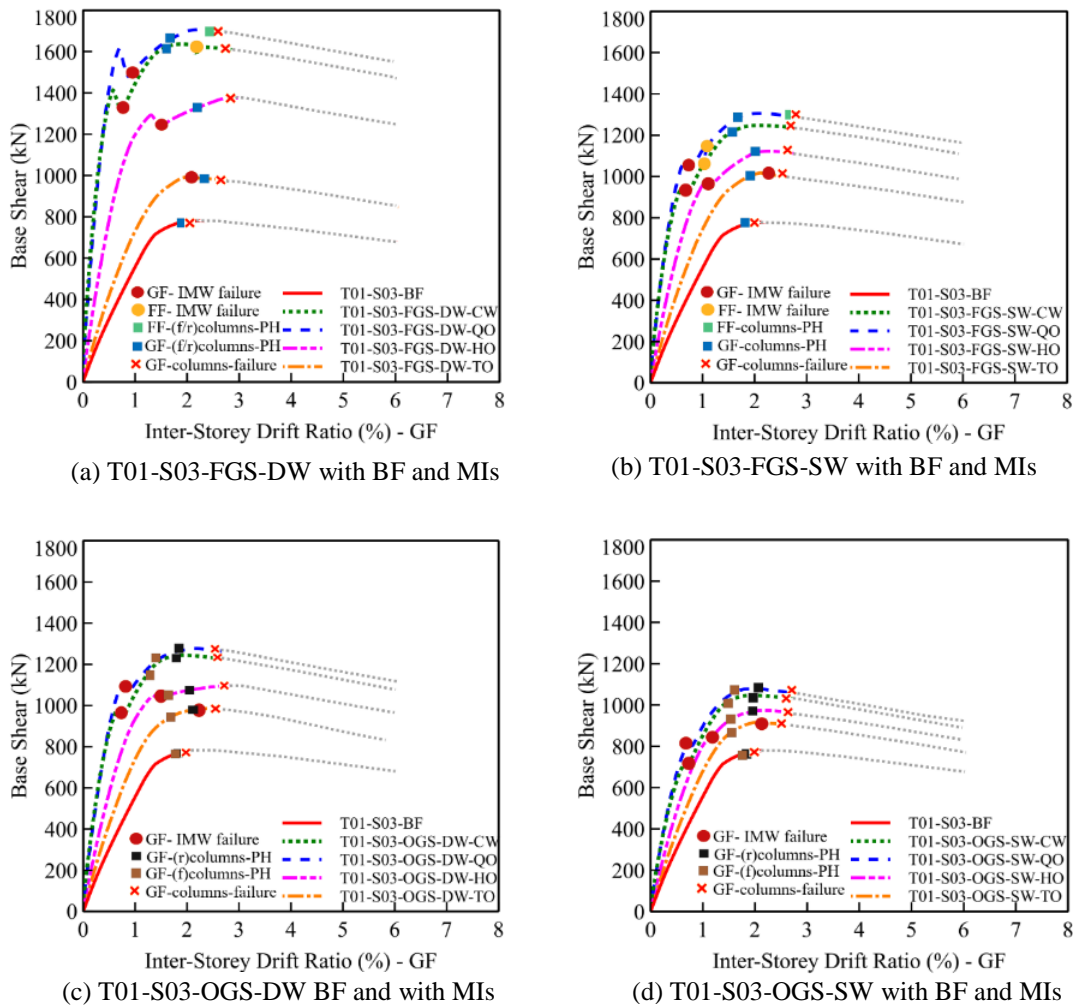


Figure 5-16. Performance of T01-S03 building with different MI configurations along the along the x direction

5.5.2.2 Effects of typologies (T01 and T02)

The seismic performances of S03 and S02 of different typologies (T01 and T02) can be seen in Figures 5-16, 5-17, and 5-18. Initially, it can be observed that the S02 and S03 storeys of T02 buildings (from the BF and MI cases) exhibit significantly larger peak lateral load capacity than T01 buildings. In terms of deformity, T02 shows slightly better performances than T01 cases, where the ultimate column shear failures of T02-S03 cases occurred around IDRs 2.8% and 3.5%, respectively. However, the IDRs corresponding to the shear failures of T01-OGS-S03 and T01-FGS-S03 cases varied between 2.4% to 2.9% and 2.6% to 3.2%, respectively.

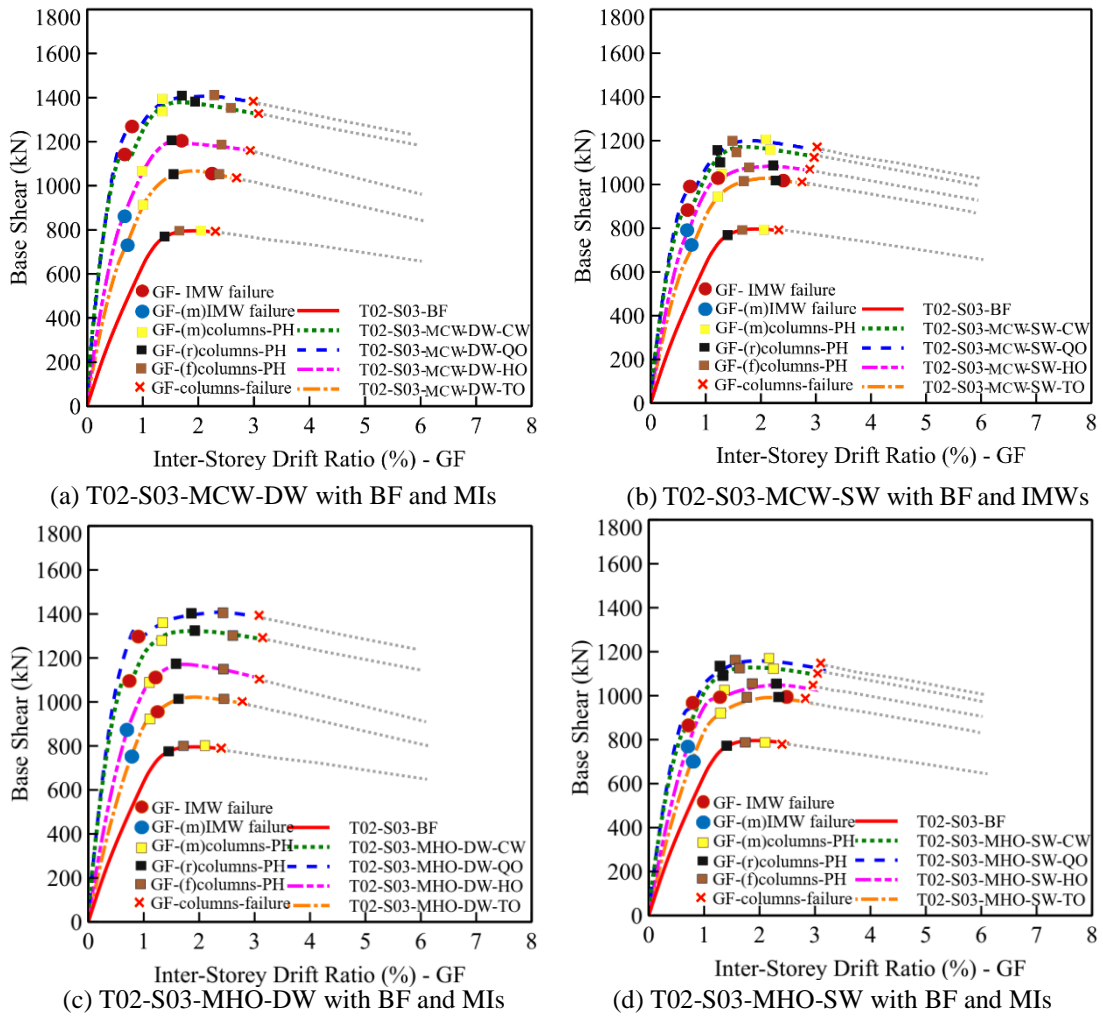


Figure 5-17. Performance of T02-S03 building with different MI configurations along the x direction

The presence of the additional frame (Figure 4-4) in the building distinctly enhanced the performance of the building in both directions. The majority of school structures in Sri Lanka have strong beams and weak column connections, because these structures were only intended to withstand gravity forces and the presence of MI transfers additional shear force (the required shear demand will increase); the most common type of failure that can occur under dynamic loads is brittle failure (Cavaleri et al., 2017). As can be seen from Figures 5-16, 5-17, and 5-18, the plastic hinge (PH) formations and shear failure conditions were obtained mostly in the GF region for all typologies of building. It should be noted that the failure initiation (PH formation in the columns) was observed during the pseudo-elastic phase of the pushover curve (Haldar et al., 2013), whereas the T02 delayed the shear failure by increasing

displacement and load carrying capacities due to the additional frame. Furthermore, the shear failure in the column was attained, when the column was subjected to the least axial load in the ultimate condition (TO cases). Conversely, the columns that were subjected to higher axial loads (CW and QO cases) failed in shear, which has a lower drift ratio and consistent with the findings of the previous studies (Cavaleri et al., 2017; Elwood & Moehle, 2008).

5.5.2.3 Effects of MI configurations

The variation in the seismic performances due to the presence of different MI configurations can be seen for the S03 buildings in Figures 5-16 and 5-17 and for the S02 buildings in Figure 5-18. Also, the PO curves of corresponding BF are presented for comparison. Apparently, it can be noted that the MI configurations are greatly influencing the failure patterns and lateral resistance of the buildings.

Remarkably, the buildings with DW-MIs cases showed higher lateral resistances than the SW-MIs cases as thickness enhanced the overall stiffness of the building. In terms of the MI configuration considered, the buildings with QO showed better deformity, while possessing lower lateral resistance than the other configurations considered. The buildings with SW-QO show a marginal contribution to the lateral resistance, due to relatively lower strut-action exerted by the SW-TO configuration.

It can be seen in Figures 5-16, 5-17, and 5-18, the MIs have failed prior to failure in the frame elements, despite different MI configurations. Among the cases analysed, IDRs corresponding to MI failure varied from 0.5% to 2.2%. T01-FGS building cases, in particular, showed slightly delayed MI failure compared to the other cases; this phenomenon could be attributed to the uniform distribution of MI in this typology. Afterward, PH in the GF columns were detected, leading to the MI failures in the frames (the PHs were formed between 1.2% and 2.1% IDRs). Typically, in OGS-HO and OGS-TO cases, the PHs were formed prior to the failure of MIs in some cases. Finally, the shear failures in the GF columns were noted in all the building cases between the IDRs of 2.4% to 3.5%. The typologies with HO-DW and TO-DW exhibited slightly better performances, in terms of IDRs (2.7%–3.2%), corresponding to ultimate shear failure in the columns, than the other configurations. Also, the

buildings with QO-DW cases showed the ultimate shear failure earlier (2.4% to 3.3%) than the other cases (2.8% to 3.5%). This phenomenon was due to the short column effect created by the QO-DW MI walls in the frames.

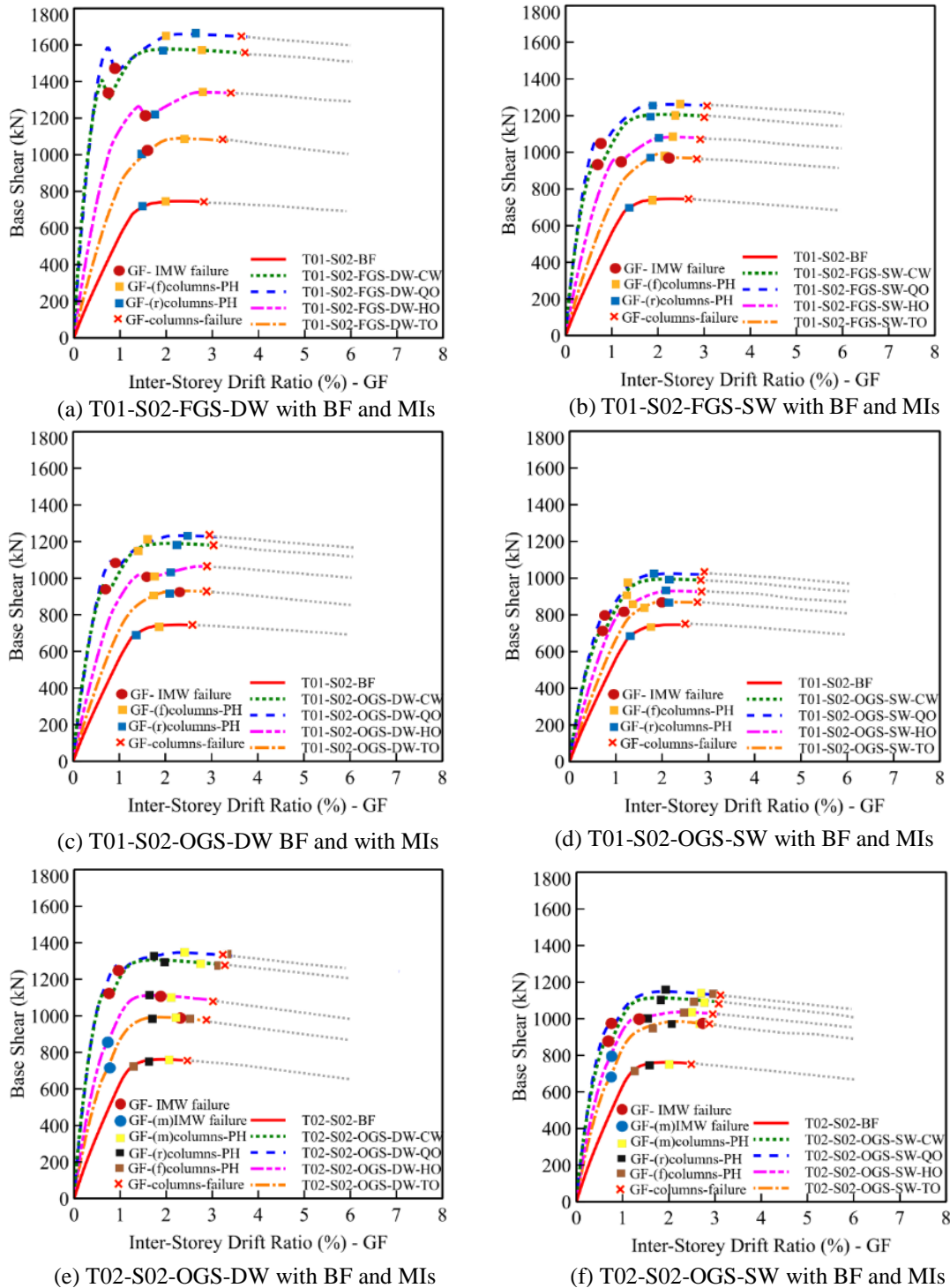
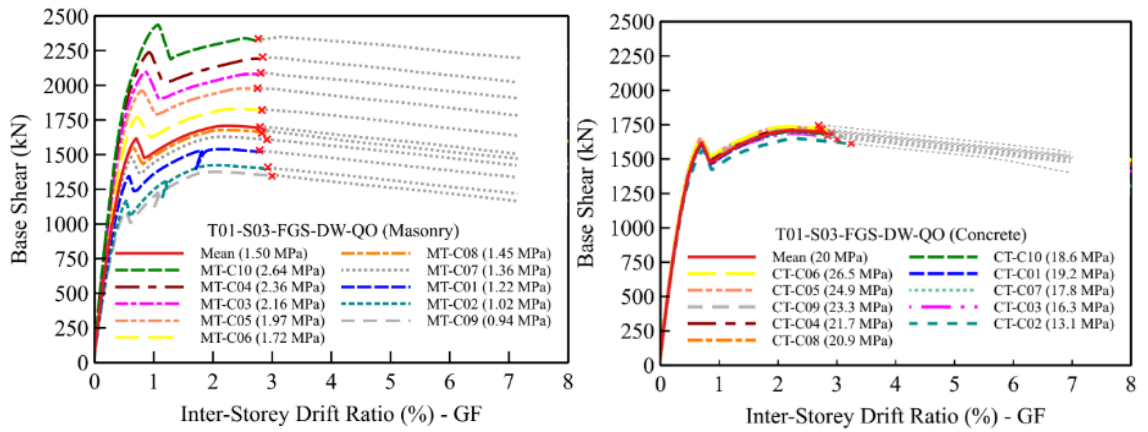


Figure 5-18. Performance of T02-S02 building with different MI configurations along the x direction

5.5.2.4 Effects of material variations

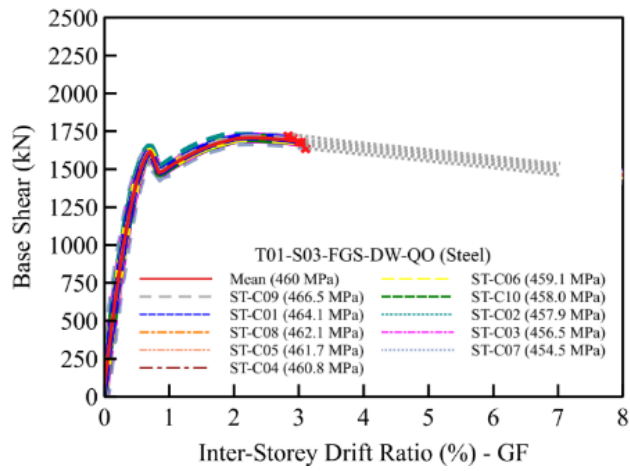
The material properties of the buildings can influence the seismic performance of the buildings. As stated in the section 5.3.2, In order to comprehend the seismic responses of the typologies in terms of the stochastic material properties, the PO analyses were carried out for varied material properties and results are presented in this section. The MCS was used to generate the random samples and the ten randomly picked samples were incorporated into PO analysis. Figure 5-19 depicts the PO graphs along with the failure mechanism of the T01-S03-FGS-DW-QO building typology with various material properties in terms of concrete, masonry and the steel. As the MI configuration of QO-DW has been found to considerably impact the seismic response of the buildings, only three-story T01 typological buildings with the QO-DW configuration were chosen for comparison. Although unconfined concrete and masonry compressive strengths were altered in the studies, their corresponding material characteristics were also changed in accordance with the formulas shown in equations (5-4) to (5-8).

The lateral resistance and failure patterns of the structures are greatly influenced by the strengths of MI, as seen in Figure 5-19 (a). For instance, increasing the MI strength from 0.94 MPa to 2.36 MPa increased the lateral resistance of building by 23%, whereas the IDRs that correspond to ultimate shear failure of the GF columns changed from 2.5% to 3.7% (for T01-S03-FGS-DW-QO cases). However, the changes in the unconfined concrete properties (13.1-26.5 MPa) have minimal influence on the overall seismic performance of the building cases as shown in Figure 5-19 (b). Although, the yield strength of steel can influence the moment capacity of the elements (especially the columns), the change in the steel strength in the range of 5% COV (also due to lognormal distribution considered) was not significantly influenced the lateral resistance of the building. Therefore, it can be said that the variations in MI (i.e. masonry) properties can considerably influence the seismic performance of the building than the variations in concrete and steel properties in the buildings.



(a) T01-S03-FGS-DW-QO (Masonry)

(b) T01-S03-FGS-DW-QO (Concrete)



(c) T01-S03-FGS-DW-QO (Steel)

Figure 5-19. PO curves of T01-S03-FGS-DW-QO buildings with different material properties

5.6 Summary

The seismic performances of the school building typologies in Sri Lanka were assessed through a set of numerical analysis procedures developed using the OS (McKenna et al., 2000) and the Response 2000 (Bentz, 2001). The study incorporated the various MI configurations (CW, QO, HO, and TO) and typologies (T01 and T02), as well as the presences of MI at GF (FGS and OGS) observed in the survey. It was found that the MIs in the buildings have a profound influence, enhancing the performance of the building as its overall stiffness increased. Nevertheless, the strong MI showed the earlier failure in the building due to the formation of short columns. In addition, the absence of the MI in GF increased the flexibility of the upper floor and led to early failure due to soft storey mechanisms. Notably, the presence of the additional frames (i.e. T02 typology) enhanced the performance of the building during the analysis. However, the performance of the building during an earthquake can be evaluated using PO analysis; the expectable damage of the building (probability of the damage) at the particular earthquake scenario can be obtained from fragility-based study. As a result, the following section will concentrate on defining the damage threshold and the probability of damage occurring at a specific earthquake scenario.

6. DEVELOPING FRAGILITY CURVES

Seismic fragility curves characterise the probabilistic seismic responses of structural systems relative to defined structural damage thresholds, therefore the fragility curves represent the probability of attaining certain damage thresholds of the structural system against earthquakes. The term "fragility" can generally be defined as "the quality of easily being broken or damaged," whereas in structural engineering it is defined as the expression of the probability of damage to the assets (Maziligüney, 2020; Porter, 2021). Meanwhile, fragility and vulnerability are not the same, and fragility expresses the probability of damage, while vulnerability reveals the loss aspect of a system (Maziligüney, 2020).

When earthquakes of varying magnitude occur, a significant number of infrastructure and the populated metropolitan region may be affected with various damage states, and some structures may be completely destroyed. The aim of this chapter is to derive the analytical fragility curves of the T01-OGS, T01-FGS, and T02-OGS RC-MI school building typologies in Sri Lanka based on the consequence damage threshold limits. Because damages in school buildings have a greater impact on society, when an earthquake occurs compared to other types of structures, it is critical to develop a realistic description of their fragility functions.

Damage thresholds are assessed based on the seismic responses of the analysed systems. The identified damage thresholds are then applied to the structural responses to confirm the performance levels of the systems considered, and the probabilities are then assessed to confirm the attainment of the damage thresholds as a function of the seismic activity considered. However, there are different definitions and approaches to describing the structural damage thresholds for a system. These include empirical observations and parameters from numerical analyses (e.g. base shear, IDR, spectral accelerations, etc...) (Porter, 2021; Rajkumari et al., 2022). In this study, the damage state threshold limit was defined by considering the structural performance of the building based on the Sri Lankan school building attributes. The following sections will detail the steps followed to generate the fragility curve and the performance of the building.

6.1 Defining the limit state for fragility functions

There are different damage threshold limit states are suggested for the RC buildings (ATC, 2015b; CEN, 2004; FEMA, 2002) in literature. These damage states are not suitable for the Sri Lankan school buildings. Therefore, the thresholds were defined in this study based on the performances of the buildings based on the nonlinear PO analysis method (Chapter 5) presented, incorporating HAZUS guidelines (FEMA, 2013). Out of the different concepts established in the literature to assign the damage thresholds of RC-MI buildings under seismic actions (Rajkumari et al., 2022), this study uses the damage thresholds that are linked to the failure sequence of the buildings correlated to the IDR values at ground storey level. As shown in Figure 6-1 (stage 3), four damage states: (1) slight damage (SD), (2) moderate damage (MD), (3) extensive damage (ED), and (4) collapse (CD) were established to develop the seismic fragility curves of the RC-MI typological school buildings in Sri Lanka.

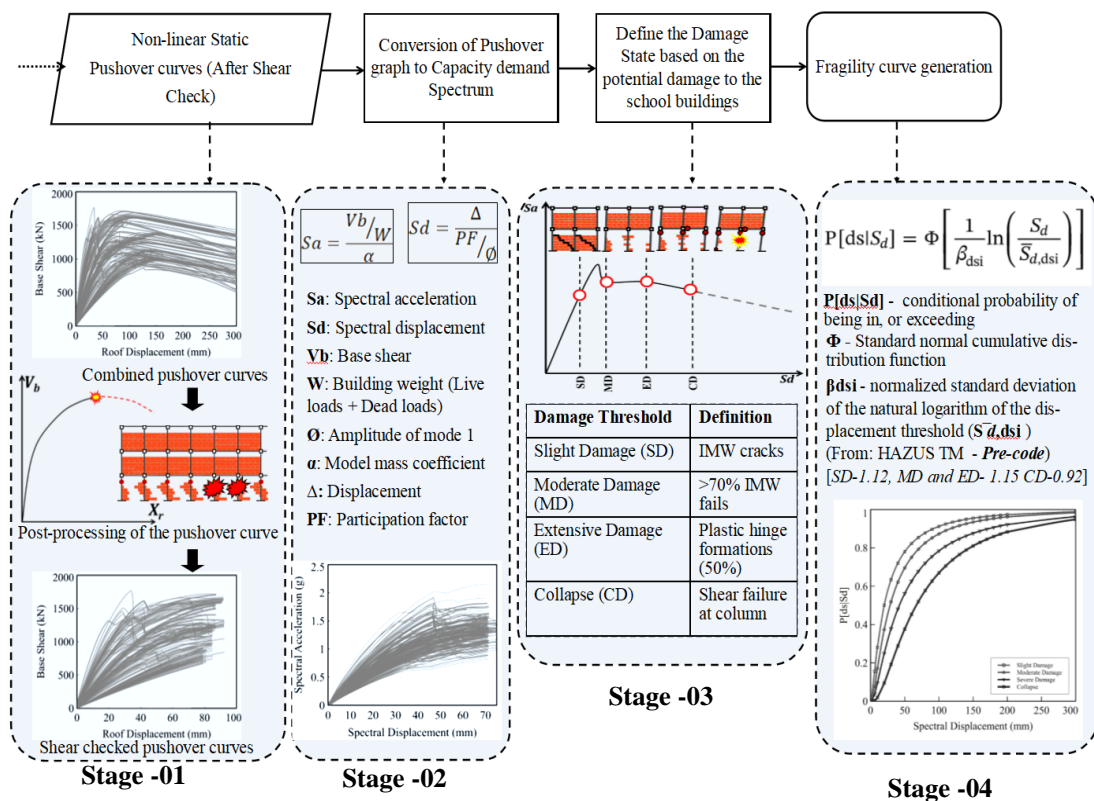


Figure 6-1. Flowchart of the fragility analysis procedure of the RC-MI school buildings

Table 6-1 illustrates the damage states and threshold limit defined in this study incorporating HAZUS guidelines (FEMA, 2013). The graphical representation of the damage states integrated with the capacity curve can be seen in Figure 6-1 (Stage-03). The SD damage condition, which was defined as the beginning of MI cracking at the ground storey bays, was deemed to have been achieved, if more than 50% of the MIs had reached the cracking limit. The cracking limit of MIs was evaluated, when the force in MIs reached 70% of the maximum masonry strength specified. When more than 50% of MIs at the ground story were entirely failed, a building was said to be in MD condition, meaning that its masonry strength had been depleted. Consequently, the ED limit is reached, when more than 50% of the ground storey columns possess PHs. In contrast, the structure had attained its maximal strength, and negative stiffness was about to begin. Finally, the CD limit is the IDR, where more than 50% of the ground storey columns have reached their shear resistance. It was presumed that, when shear failure of the columns is recorded, the building has gone beyond the recovery stage; therefore, it could either collapse or have to be demolished.

Table 6-1. Definition of damage state of the school building for Sri Lanka

Damage states	Definition	Threshold	HAZUS (FEMA, 2013)
<i>SD</i> - Slight damage	Minor MI crack development at GF up to less than 50% (around corners and openings)	Elastic region: strength is increased and reduction in the initial stiffness	Slight
<i>MD</i> - Moderate damage	More than 50% of the MI at GF is completely damaged, and the remaining wall is subject to shear and flexural cracks (reaching maximum masonry strength)	Maximum masonry strength is reached (initiation of yield limit)	Moderate
<i>ED</i> - Extensive damage	Plastic hinge formation reaches more than 50% of the GF columns	Peak capacity is achieved and negative stiffness formation/initiation of plastic region	Extensive
<i>CD</i> - Collapse damage state	Around 50% of the GF columns reaches shear capacity	Rapid degradation in strength is reached, negative stiffness is reached, a quick increment is made in the IDR, and the additional lateral load condition causes the complete collapse	Complete

6.2 Development of fragility curves

The fragility curves were created using the approach provided in the ATC-40 (ATC-40, 1996) and HAZUS (FEMA, 2013) guidelines. The findings of the PO analysis were combined, taking into account both the ideal scenarios and the material uncertainty, to create the fragility curve. The graphical illustration of the considered cases can be seen in Figure 6-2. Also, Figure 6-1 shows the methodology used in this study to generate the fragility curves of school buildings. This procedure can be mainly divided into four stages. Firstly, the PO curves (adjusted by verifying the shear failure of the columns) were grouped by the building typologies analysed. Secondly, the PO curves were converted to capacity demand spectra as per the formulations (provided in Fig 2-10) given in HAZUS (FEMA, 2013). Then, based on the displacement limits (i.e., IDR at the ground storey level), the four damage states (SD, MD, ED, and CD) of the threshold were developed.

The probability of exceedance ($P[ds|S_d]$) was then computed using the natural logarithm function based on the normalised standard deviation of damage thresholds (i.e. IDR) as per the equation provided in Figure 6-1 (Stage-04). The detailed explanation of the equation can be seen in Section 2.4 (equation (2-6)). It should be noted that the standard deviation of natural logarithm of the S_d for the damage state (β_{dsi}) primarily depends on the three lognormal standard deviation parameters: variability of the capacity curve (β_c), variability in demand spectra (β_D) and discrete threshold of each damage state ($\beta_{M(Sds)}$) as defined in equation (6-1).

$$\beta_{Sds} = \sqrt{(\text{CONV}[\beta_c, \beta_D, \bar{S}_{d,Sds}])^2 + (\beta_{M(Sds)})^2} \quad (6-1)$$

Although, distinct, β_{Sds} could be used to establish fragility curves for the typological building cases analysed in this study, β_{Sds} values suggested in HAZUS (FEMA, 2013) were used. It should be noted that, Sri Lanka does not possess separate seismic codes and therefore, the school buildings were not designed for the seismic provisions. Meanwhile, historical records of the seismicity are not well documented in the country, therefore the accurate computation of β_{Sds} is a challenging task. Subsequently, due to these limitations, the values recommended in HAZUS (FEMA, 2013) were used.

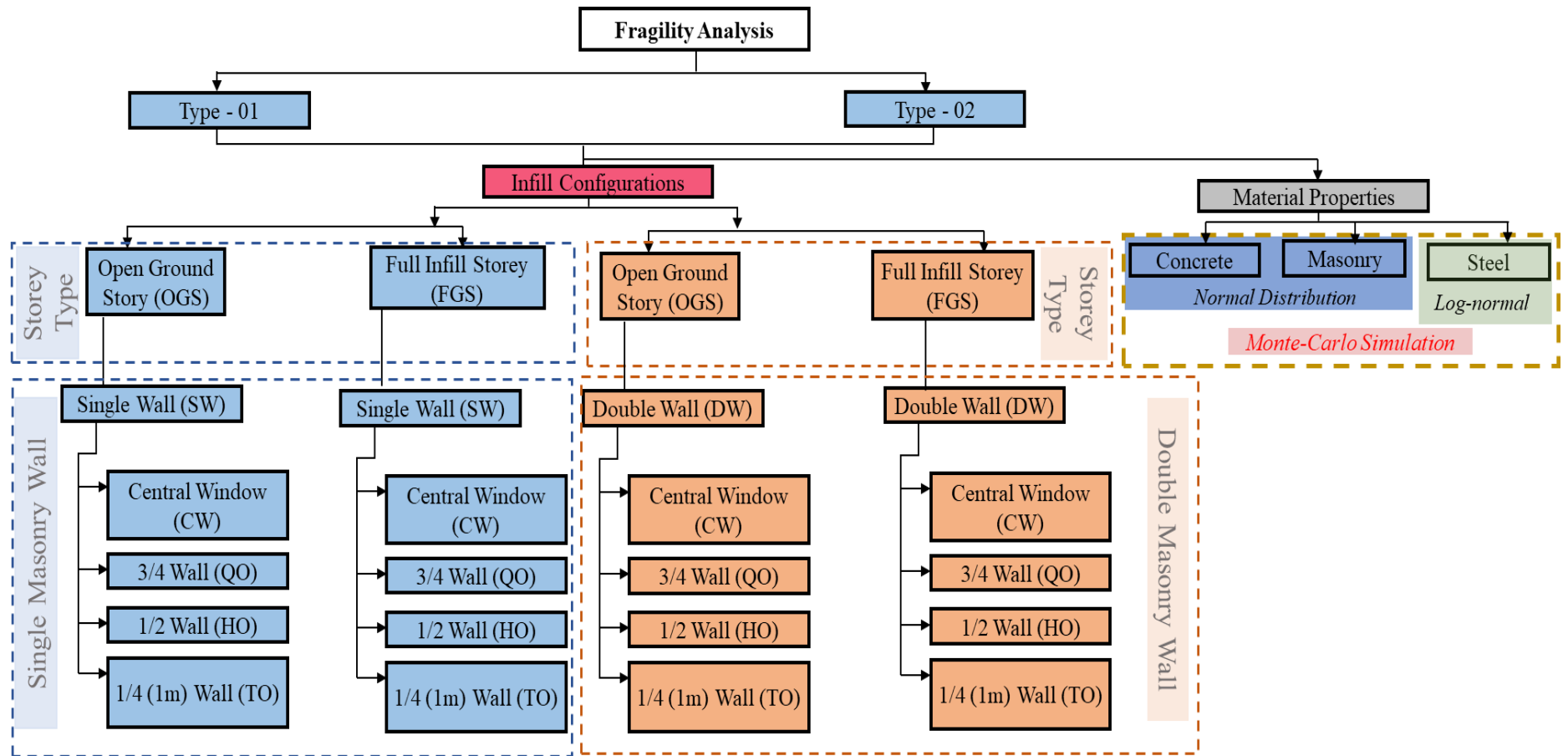


Figure 6-2. Variations in the school buildings considered (ideal cases and material uncertainty)

6.3 Fragility curves

The fragility curves were established by considering the major typologies (T01-OGS, T01-FGS and T02-OGS) obtained from the structural survey (Chapter 4). In addition, four main provinces (Western, Southern, Central and Eastern) have been considered to establish the fragility curves, as they represent the main regional centers of the country to compute the damage matrices. It can be noted that fragility curves are given for all four damage thresholds, and their median curves are drawn in Figures 6-3 and 6-4 with respect to the X and Y directions. However, the variance of each damage thresholds is shaded with their lowest (5th percentile) and highest (95th percentile) limits, which was adapted by combining ideal and material uncertainty cases.

It can be noted from Figures 6-3 and 6-4, the fragilities of three building typologies considerably vary in terms of their probability of exceedance recorded. It is apparent that the buildings with OGS are more vulnerable compared to FGS typology. Consequently, when comparing T02 with T01, the probability of exceeding the CD damage state for T01 buildings (in the X-direction) is approximately 57%, 60%, 50% and 30% greater than for T02 buildings in the western, southern, central and eastern provinces, respectively. Also, when comparing the CD damage states of T01-OGS and T01-FGS building cases, the OGS buildings depicted 28%, 40%, 25%, and 20% higher exceedance than FGS buildings in the western, southern, central and eastern provinces, respectively. Also, similar variations were obtained in the Y direction. As a result, it is possible to conclude that school buildings with OGS are the most vulnerable of the cases examined in this study.

To develop the damage matrices, the response spectra developed by Dananjaya et al. (2020) using 475 years of return period were used. Subsequently, the performance points of the buildings were determined for the cumulative capacity demand spectrum curves using the response spectra of the provinces as stated in Section 2.4 (Figure 2-10). The capacity demand spectrum was cumulated, and their lowest (5th percentile), highest (95th percentile) and mean limits were projected in the response spectrum, and performance points were obtained. Consequently, the performance points are marked as vertical lines in the fragility curves, presented in Figures 6-3 and 6-4.

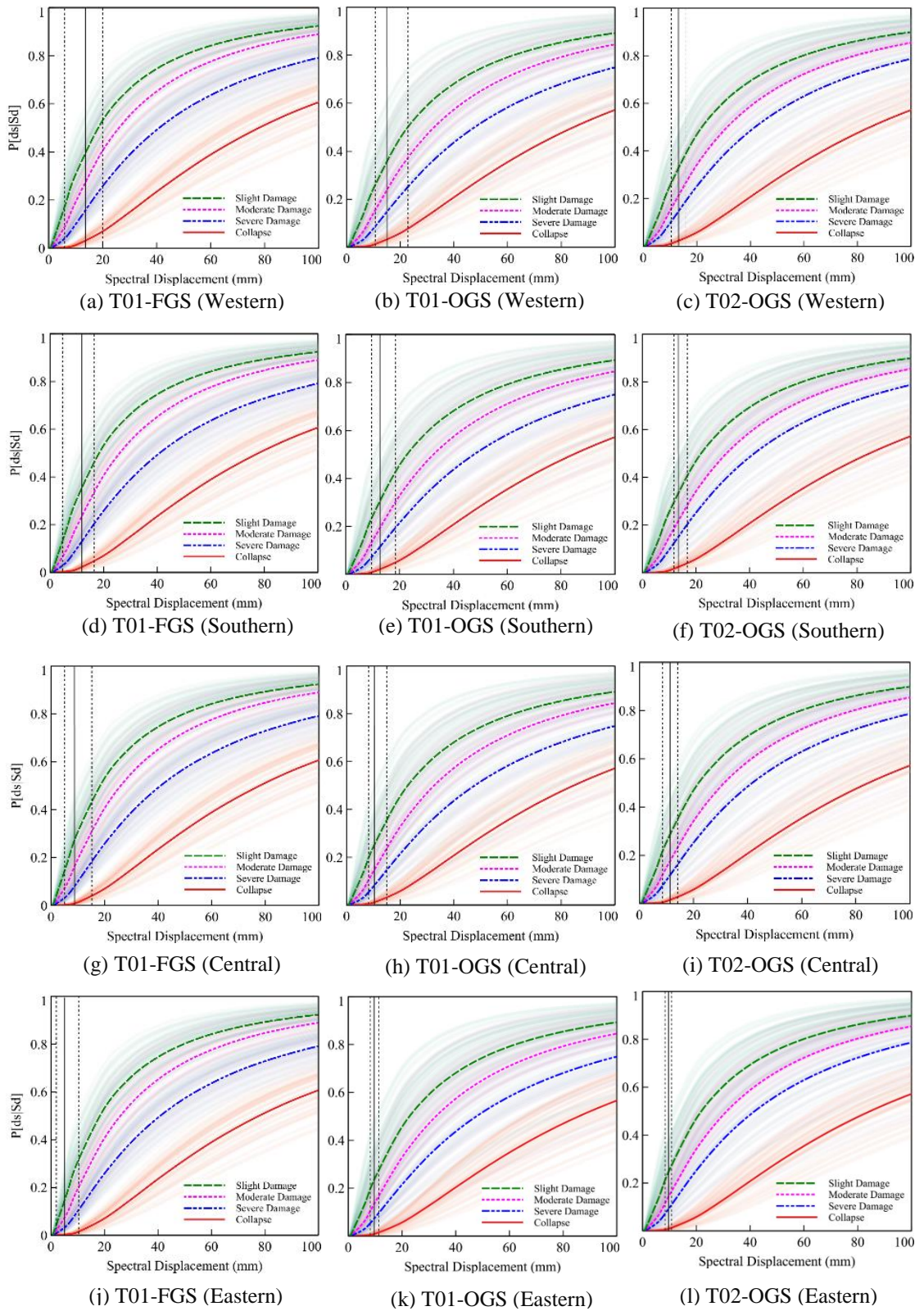


Figure 6-3. Fragility curve of the school buildings with respect to provinces – X direction (Western, South, Central, and Eastern provinces)

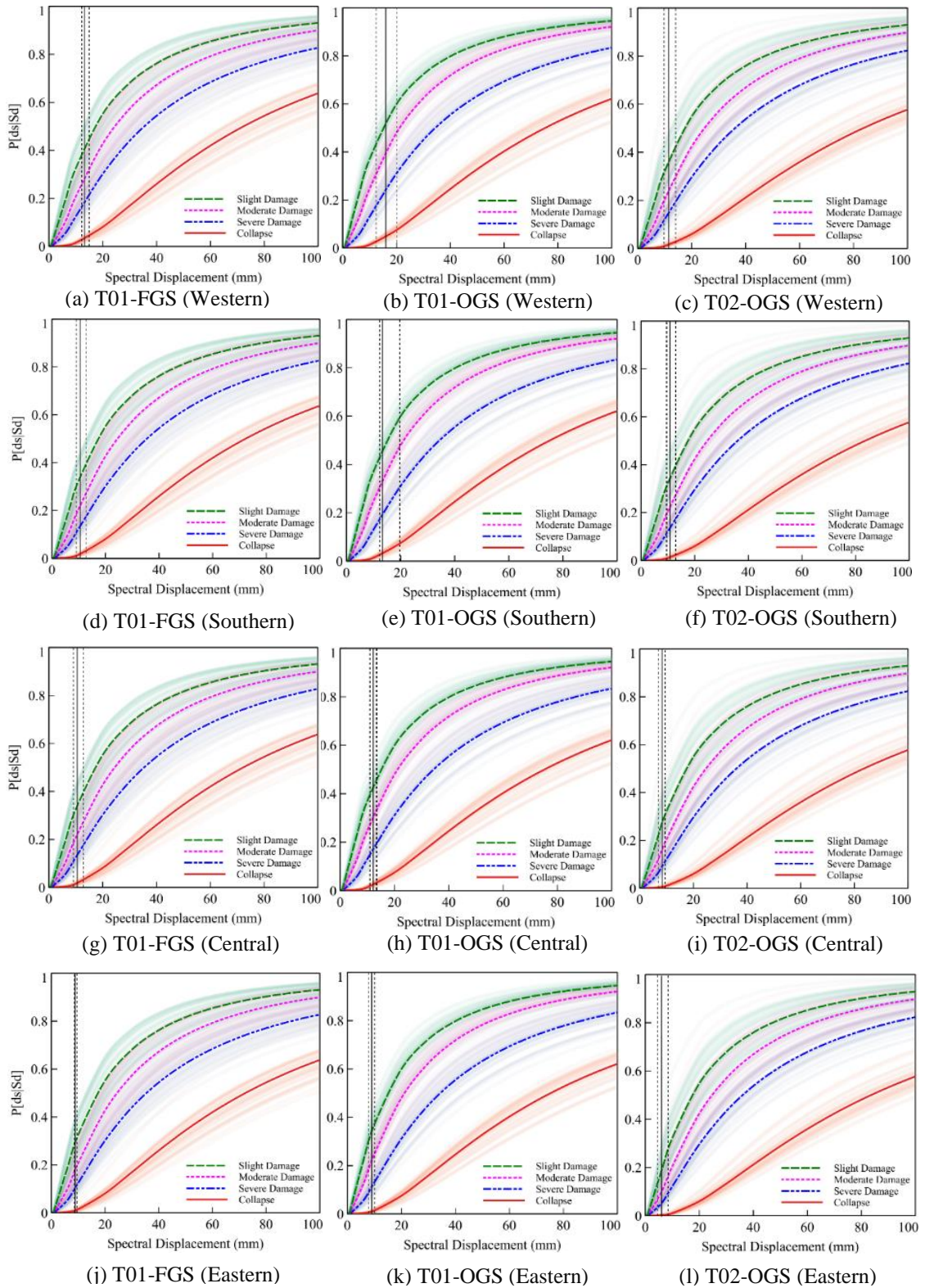


Figure 6-4. Fragility curve of the school buildings with respect to provinces – Y direction (Western, South, Central, and Eastern provinces)

6.4 Damage matrices

The damage matrices of the school building typologies were determined from the fragility curves and performance points marked in the vertical line in Figure 6-3 and 6-4. The damage probability matrices are cumulative probability functions and they can be used to characterise discrete damage possibilities with respect to spectral responses of the building (FEMA, 2013). The damage probability matrices were computed using equations (6-2) to (6-4), where $P_{(0-4)sd}$ states represent the probability of damage states 0-4 (ND-0, SD-1, MD-2, ED-3, and CD-4).

$$P_{0(sd)} = 1 - (P[ds|Sd])_{(1)SD} \quad (6-2)$$

$$P_{i(sd)} = (P[ds|Sd])_{(i)} - (P[ds|Sd])_{(i+1)} \quad (6-3)$$

$$P_{4(sd)} = 1 - (P[ds|Sd])_{(4)CD} \quad (6-4)$$

Figure 6-5 illustrates the damage probability matrices of the school buildings in Sri Lanka by considering the provinces and typology of the buildings. According to Figure 6-5, the T02 building has a lower probability of damage than the other two T01 building types in all provinces, with respective probabilities of 10%, 5%, and 2% for T01-OGS, T01-FGS, and T02-OGS. Also, the building typologies in the province with a lower seismic hazard (i.e. eastern) have shown reduced damage probability matrices than the province with the highest seismic hazard (i.e. western). For example, in the X-direction, T01-OGS cases for SD, MD, ED, and CD cases exhibited 13%, 10%, 11%, and 1% damage levels for the lower seismic region (i.e. eastern) and 18%, 16%, 17%, and 10% for the higher seismic region (i.e. western), respectively. Therefore, the fragility curves and the damage matrices established in this study clearly demonstrate the level of damage probability of the school building typologies constructed in Sri Lanka.

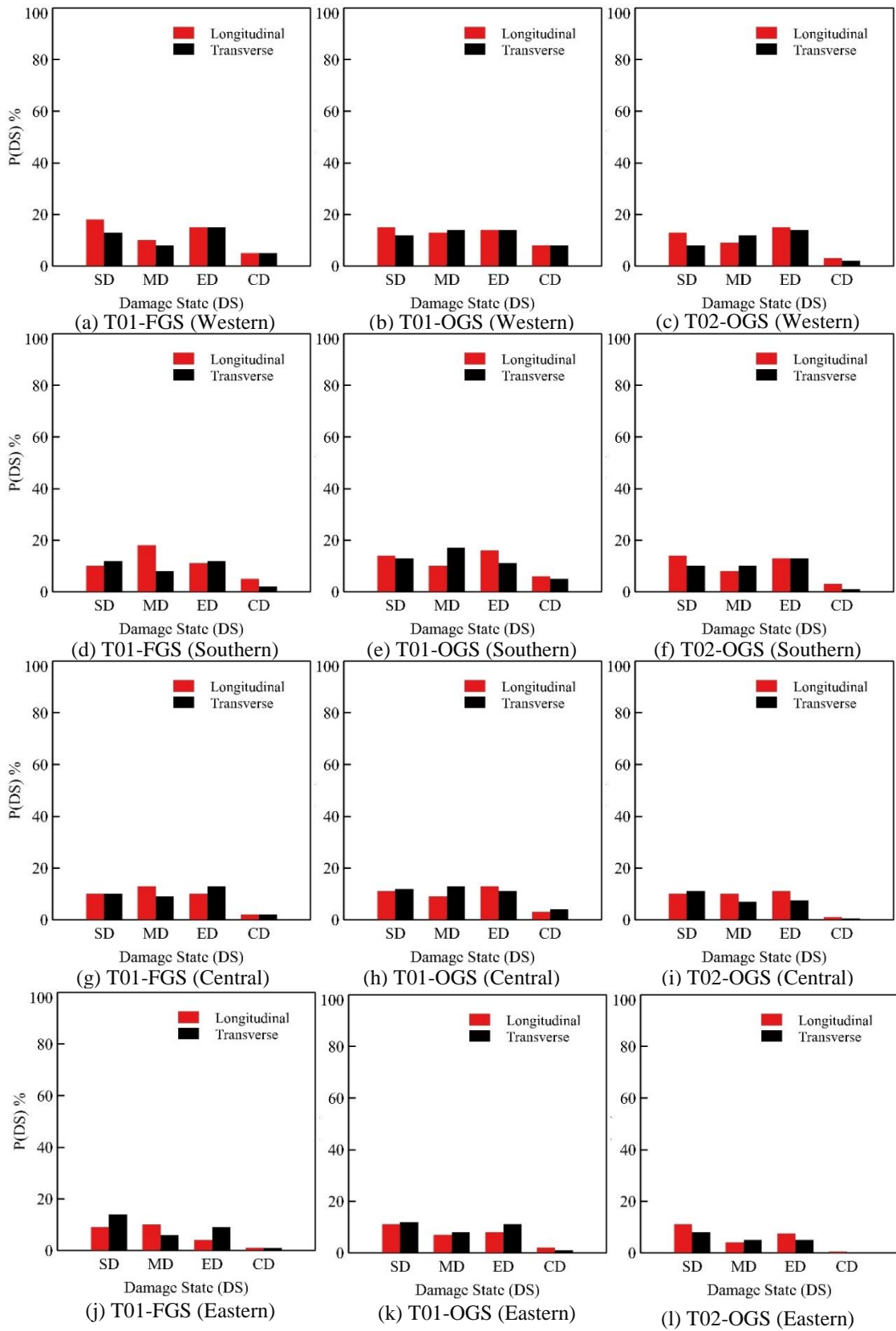


Figure 6-5. Damage probability matrices with respect to provinces

6.5 Summary

The seismic fragility functions were developed in this study as per the ATC-40 (ATC-40, 1996) and HAZUS (FEMA, 2013) guidelines by defining the damage states for Sri Lankan school building typologies that exist. A seismic fragility-based analysis that took into account material uncertainty and the established ideal cases found that school buildings in Sri Lanka are vulnerable to earthquakes. Though the T01-FGS and T02-OGS typologies showed better performance than the T01-OGS, those are still vulnerable to earthquakes. Consequently, it is crucial to assess each building separately to improve its seismic performance. Therefore, the focus of this research is to suggest a quick evaluation approach, which is a RVS method for assessing building seismic scores, thence mitigating measures can be implemented for Sri Lankan school buildings against seismic actions.

7. RAPID VISUAL SCREENING (RVS) OF BUILDINGS FOR POTENTIAL SEISMIC HAZARDS

In order to fulfil the aims of this study, the approach described in Section 2.4 was implemented to develop a seismic RVS method for typological school buildings in Sri Lanka. For that purpose, the basic scores and score modifiers of the typological school buildings by taking into account the different seismic hazard zones in Sri Lanka were developed using the guidelines provided in FEMA P-154 (ATC, 2015a).

7.1 Concept of RVS for school buildings typologies

The school building typologies analysed in preceding chapter revealed variable performance levels subjected to seismic loading. However, performing the detailed seismic analysis for each school building is a challenging task as it cannot be routinely applied. In this regard, a rapid method of screening the buildings to identify vulnerable buildings to earthquakes, may aid in shortlisting buildings for detail analyses. Therefore, the well-established rapid assessment or visual methods around the world as explained in Section 2.4 were taken and applied to the some of the school buildings surveyed in this study. The school buildings used for this purpose and their typologies (T01 and T02) are illustrated in the Figure 7-1 and the results can be seen in Table 7-1.

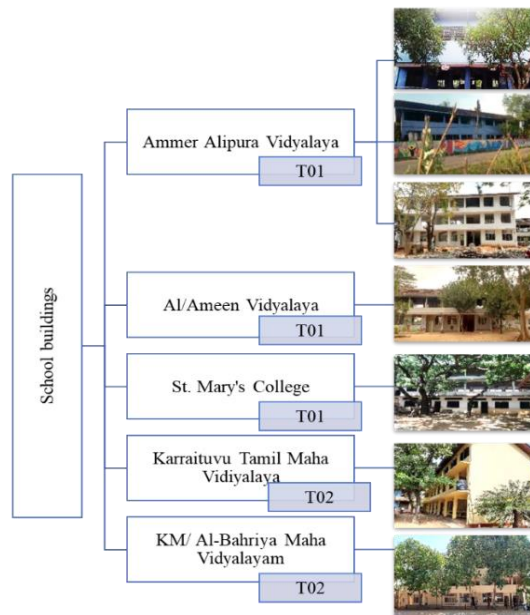


Figure 7-1. Selected schools for rapid assessment methods

As shown in Table 7-1, T01 and T02 buildings with varying storey levels were chosen, and existing RVS methods obtained from the literature were used to assess their applicability to use for those typological RC-MI school buildings in Sri Lanka. To assess the seismic scores or index, FEMA P-154 (ATC, 2015a), NRCC (1992), Arya (2011), NZSEE (2017), Kaplan et al. (2018). and Ningthoujam & Nanda (2018) methods were applied for school buildings in Sri Lanka. It should be noted that the FEMA P-154 (ATC, 2015a) Level 1 and 2 were applied to all the buildings.

Table 7-1. Existing RVS scores/grades of school buildings

No.	School Name	District	Type	Building No	FEM A - P 154	Canada	Arya et al.	NZSEE (IEP)	Turkey (Kaplan et al. (2017))	Ningthoujam & Nanda (2018)
1	Al Ameen Vidyalaya	Ampara	T01	AM-01-01-S2	2.0	5.5	G2	C (33-67%)	Medium Risk (71.14)	Grade 1
2	Ammer Alipura Vidyalaya	Ampara	T01	AM-02-01-S2	2.0	5.5	G2	C (33-67%)	Medium Risk (80.5)	Grade 1
3			T01	AM-02-02-S2	2.0	6	G2	C (33-67%)	Medium Risk (67.54)	Grade 1
4			T01	AM-02-03-S3	2.0	5.5	G2	C (33-67%)	Medium Risk (99.54)	Grade 1
5	St. Mary's College	Trincomalee	T01	TR-01-01-S3	2.6	6	G2	C (33-67%)	High Risk (29.59)	Grade 2
6	KM/KM/Vipulananda Central College - Karaitivu	Ampara	T02	AM-03-01-S3	1.5	6	G2	C (33-67%)	Medium Risk (91.99)	Grade 1
7	KM/ Al-Bahriya Maha Vidyalayam	Ampara	T02	AM-04-01-S3	2.0	6	G2	C (33-67%)	Medium Risk (91.99)	Grade 1

The RVS scores/grading shown in Table 7-1 reveal, that although there are irregularities in Sri Lankan school buildings, the most of them are caused by MI configurations (the opening size effects and the thickness), the RVS scores and grading obtained are similar across the different buildings. Conversely, the majority of RVS, or rapid assessment methods, do not primarily focus on the variability of MI on building seismic performance, therefore the exercise in Table 7-1 lead to similar scores and grading. Meanwhile, Chapter 5 highlighted how MI configuration significantly affects seismic performance. Therefore, the focus of this study was primarily on incorporating structural irregularities in Sri Lankan school buildings, with special

attention on incorporating the variations in MI configurations/arrangements into a RVS method for the typological school buildings in Sri Lanka.

7.2 Establishment RVS method for local context

To propose a RVS to local context, the approach given in FEMA P-154 (ATC, 2015a) was used. The guidance provided in FEMA P-154 (ATC, 2015a) is already explained in Section 2.4. It should be mentioned that FEMA P-154 (ATC, 2015a) is a well-established approach that many countries integrate to their local considerations to develop relevant RVS methods. Therefore, in this study, the proposed RVS method was developed as per FEMA P-154 (ATC, 2015a) method and basic score and score modifiers were proposed as suggested. It is worth noting that the PO curves obtained from numerical analysis (Chapter-05) were transferred as CC curves as per the equations 2-2 to 2-5 denoted in Section 2.4, and response spectra proposed by Dananjaya et al. (2020) was incorporated to assess the performance point of the school buildings. In addition, the basic score, score modifiers and the final scores of the school building were generated based on the seismic hazard map developed by Uduweriya et al. (2020). The proposed seismic hazard map for 475 years of return period can be seen in Figure 7-2.

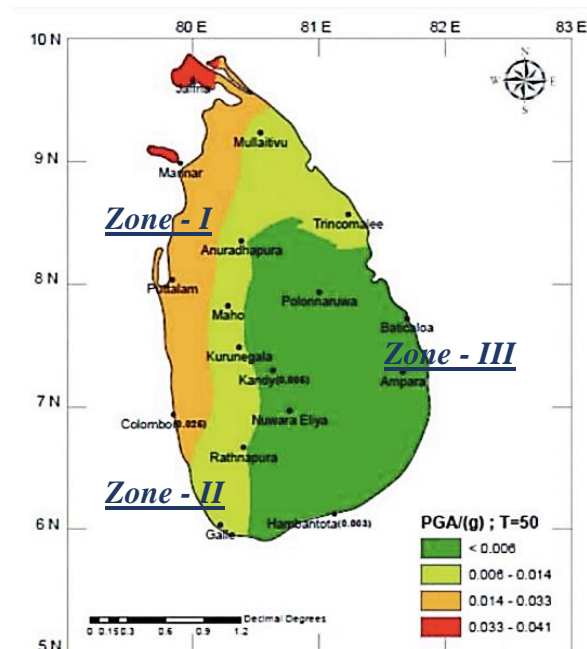


Figure 7-2. Seismic hazard map for 475 years of return periods (Uduweriya et al. (2020))

7.2.1 Development of Basic Score

The response spectra for three zones (see Fig 7-2) were used to develop basic scores of the typological school buildings, whereas the PO curves of those buildings were converted into CC curves by considering the mass of the buildings and the model factors. Based on the equations 2-6 to 2-8 as proposed in FEMA P-154 (ATC, 2015a), the basic scores of the buildings for three zones of T01 and T02 buildings were calculated. It should be noted that the basic scores of the building were calculated by considering complete MI case (no irregularity). The graphical representation of the basic score evaluation followed can be seen in Figure 7-3.

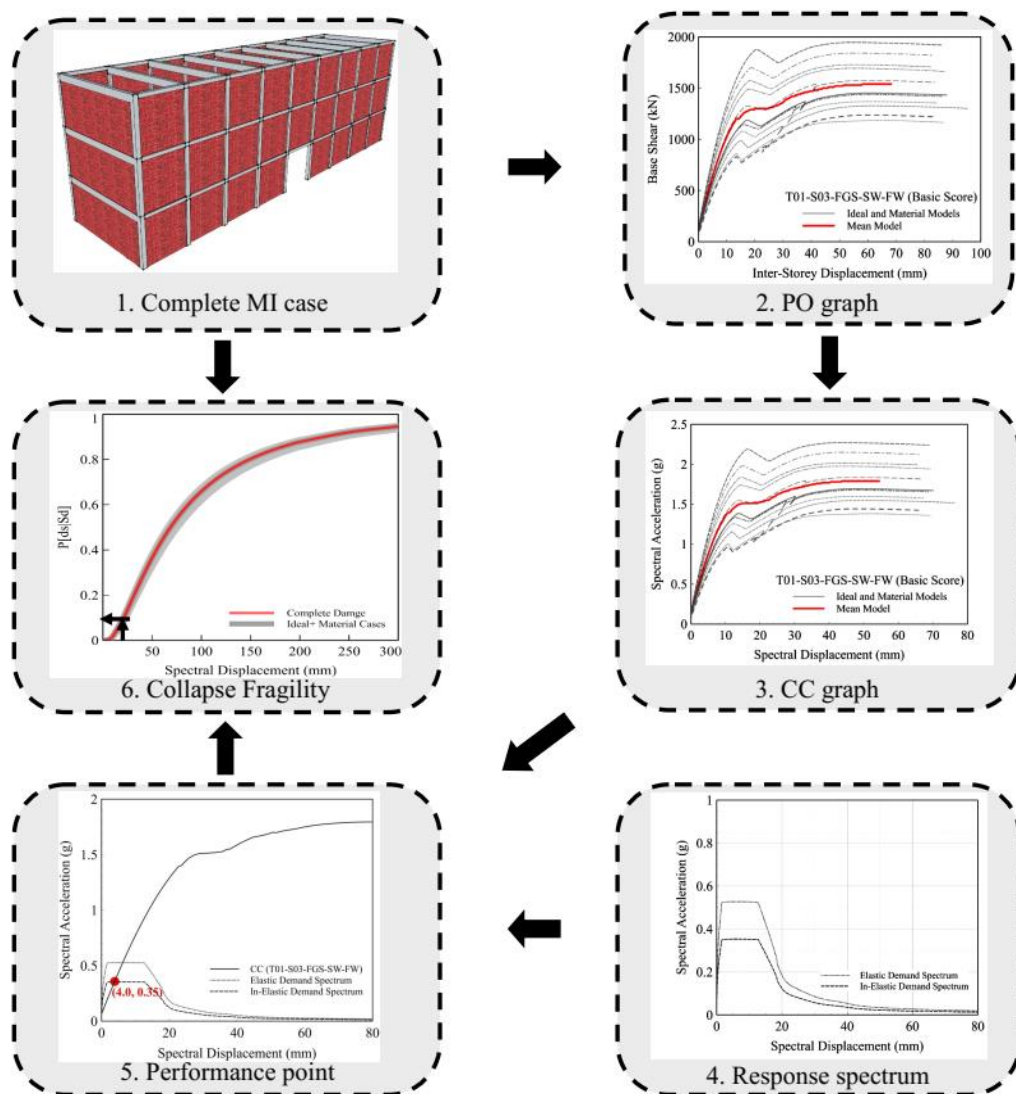


Figure 7-3. Basic score evaluation for Zone- I buildings

As can be seen in Figure 7-3 and detailed illustration given in Section 2-4, the basic scores of the buildings with respect to the zones (as illustrated in Figure 7-2) were evaluated. To compute the basic score to the building located in zone-I, the following equation was used:

$$\text{Basic score} = -\log_{10}(P [\text{collapse}]) \quad (7-1)$$

$$\text{Basic score} = -\log_{10}(P[0.0019]) = 2.7$$

Therefore, the basic score of the building located in Zone- I is 2.7, which is for higher intensity seismic zone. Tables 7-2 shows the basic scores of the typological buildings (T01 and T02) in different seismic zones. It can be seen that the lower the seismic intensity (Zone - I > Zone - II > Zone - III) the higher the score.

Table 7-2. Complete MI case (FW) - Basic score evaluation

Zones	Type	Infilled Frame P[ds]	Basic Score (IF)
Zone-I	T01	0.015	2.7
Zone-II		0.008	3.0
Zone-III		0.004	3.3
Zone-I	T02	0.008	3.0
Zone-II		0.004	3.3
Zone-III		0.0005	4.2

7.2.2 Development of Score Modifiers

The score modifiers were determined by considering the irregularities in the school buildings that had occurred due to the presence of MI configurations. The score modifiers were incorporated for the ideal cases analysed in Chapter 5, and additionally, the major changes in the MI configuration in the T01 and T02 buildings were assigned and analysed to incorporate the vertical and plan irregularities in the buildings. It should be noted that the possible irregularities in the building were adapted from the school buildings surveyed. The methodology as described in Figure 7-3 and Section 2.4.1.2 were followed to generate the score modifiers. The equivalent scores of the particular irregularity were initially calculated, and the score modifier was generated by deducting the equivalent score. Mainly, three potential irregularities were considered: plan irregularity, vertical irregularity, and open ground storey effects, and the cases considered for the analysis can be seen in *Appendix-D*.

7.2.2.1 Open Ground Storey

Many T01 and T02 school buildings contain OGS at the GF as shown in Figure 7-4. When, MIs are not distributed uniformly across adjacent floors, a soft storey mechanism can form, as seen in the GF storey level with MI absences. As a result, the inelastic deformation demand of the GF columns increases, and a soft storey mechanism forms at the GF. Therefore, it should be treated as one of the vulnerability parameters in the buildings, as it also causes mass irregularity as well. The cases considered in the analysis can be seen in *Appendix-D* (Table D-1). Meanwhile, for T02 structures, the middle frame was retained with same MI configuration during the analysis, which was regarded as the CW-SW/ HO-SW configuration common in most Sri Lankan school buildings.



Figure 7-4. Open Ground Storey of T01 and T02 buildings

To evaluate the score modifier for the OGS, the cases analysed from Chapter-5 were directly incorporated with a consideration of opening sizes and thicknesses. Altogether, for T01 and T02, 16 models were considered and performance point of each case were adapted for three zones as shown in Figure 7-2. Table 7-3 shows the score modifiers according to seismic zones incorporating the OGS effects in the typological buildings (detailed score modifiers can be seen in Tables C-2 and C-3 for T01 cases and Table C-4 and C-5 for T02). It should be noted that the IDR was considered, when determining the score modifiers for OGS effects and 95th percentile score of the sample was assigned as the score modifier for the OGS cases. The sample calculation of a score modifier for OGS case is illustrated below:

$$P[\text{collapse}] = CF \times P[\text{complete damage}]$$

$$P[\text{collapse}] = 0.5 \times 0.02 = 0.01$$

$$\text{Equivalent score} = -\log_{10} P[\text{collapse}] = 2.0$$

$$\text{Score Modifier} = \text{Equivalent score} - \text{Basic score} = 2.0 - 2.7 = -0.7$$

Subsequently, a similar approach was used to create the score modifiers for each scenario (as shown in *Appendix-D*), and the 95th percentile of the samples were selected. The MI cases of varying thickness, such as SW and DW, were analysed separately. In addition, it should be emphasised that moderate irregularity collapse factors (see Table 2-3) were applied to the SW cases, while severe irregularity (see Table 2-3) considerations were used for the DW cases. The assumption was made that, though DW cases enhanced the overall stiffness of the building, increasing strut width caused a negative effect on the building.

Table 7-3. Open Ground Storey score modifiers

Specifications	Typologies	Thickness	Zones	Score Modifier
Open Ground Storey effects (OGS)	T01	SW/DW	Zone-I	-0.8
			Zone-II	-0.9
			Zone-III	-1.0
	T02	SW/DW	Zone-I	-1.0
			Zone-II	-1.0
			Zone-III	-1.3

7.2.2.2 Plan Irregularities (Horizontal)

Plan irregularities can occur due to various reasons, such as re-entrant corners and shapes (L, U, and T shapes), diaphragm openings, and large openings due to the irregularity coming from MI on the same floor of the building. The plan irregularities in the typological school buildings mainly comes from the irregularly in MI arrangements. When a floor has some different MI configurations (front and rear) in terms of opening size or thickness, the plan irregularity will occur as the mass of the buildings varies. Figure 7-5 shows some of the plan irregularity conditions in the school buildings, found during the survey, where HO and QO were located on the front and rear sides of the building, respectively.

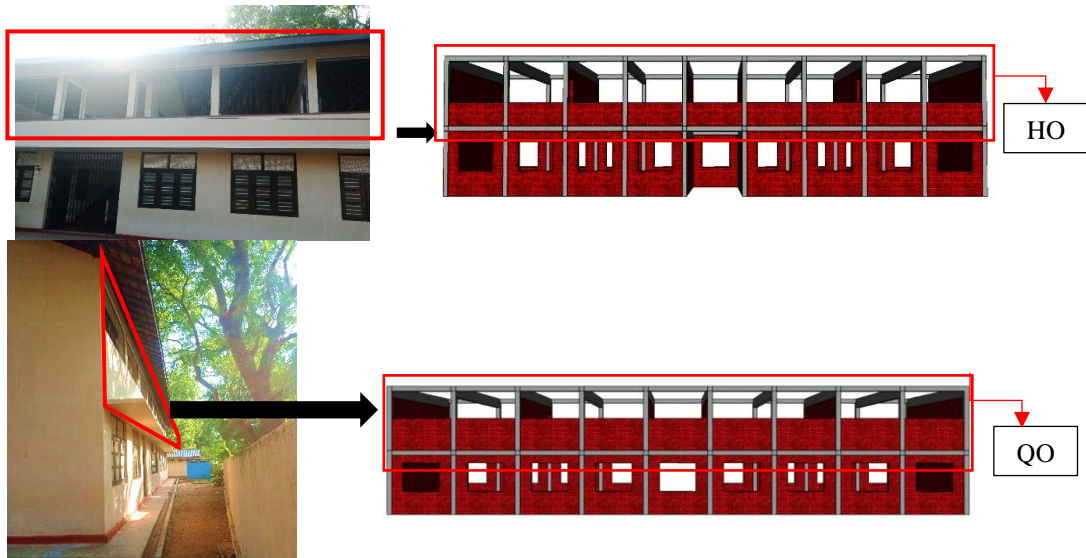


Figure 7-5. Plan irregularity of the school building

As a result, several model cases were developed (as shown in *Appendix-D*) with plan irregularities, and the performances of those buildings were analysed to evaluate the score modifiers for the plan irregularity of the structures. *Appendix-D* contains the scenarios examined for plan irregularities (Table C-6). Table 7-4 displays the 95th percentile of score modifiers for the T01 and T02 school buildings for plan irregularity (see Tables C-7 and C-8 for T01 and C-9 and C-10 for T02).

Table 7-4. Plan irregularities score modifiers

Typologies	Specifications	Thickness	Zones	Score Modifier
Plan Irregularities	T01	SW	Zone-I	-0.9
			Zone-II	-1.0
			Zone-III	-1.1
		DW	Zone-I	-1.1
			Zone-II	-1.1
			Zone-III	-1.2
	T02	SW	Zone-I	-1.0
			Zone-II	-1.1
			Zone-III	-1.7
		DW	Zone-I	-1.2
			Zone-II	-1.3
			Zone-III	-1.8

7.2.2.3 Vertical Irregularities

The significant variation in performance observed during earthquakes is caused by the asymmetric distribution of mass, strength, and stiffness along the vertical direction of the buildings. (Bhosale et al., 2017). The observation from the school structural survey revealed that Sri Lankan school buildings have negligible vertical irregularities that come from the structural system, whereas the presence of MI in the building causes the vertical irregularities to the structure. The vertical irregularity of the school building is shown in Figure 7-6, which depicts the different MI configurations prevail in different storey levels in the building.

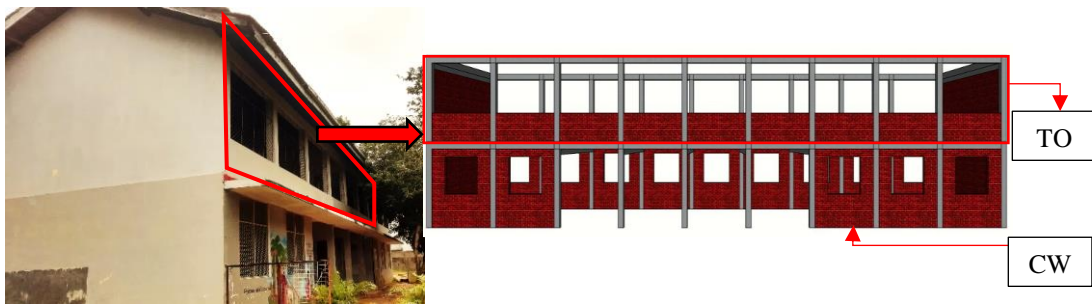


Figure 7-6. Vertical Irregularities in School buildings

Table 7-5. Vertical irregularities score modifiers

Typologies	Specifications	Thickness	Zones	Score Modifier
Vertical Irregularities	T01	SW	Zone-I	-1.0
			Zone-II	-1.0
			Zone-III	-1.1
		DW	Zone-I	-1.3
			Zone-II	-1.5
			Zone-III	-1.5
	T02	SW	Zone-I	-1.1
			Zone-II	-1.2
			Zone-III	-1.7
		DW	Zone-I	-1.6
			Zone-II	-1.8
			Zone-III	-2.5

To incorporate the vertical irregularity that comes from the MI configuration, different cases were analysed integrating different MI configurations in terms of their opening

sizes and the thickness as can be noted in *Appendix-D* (Table C-11). Based on the combinations, the scores were proposed for the SW and DW cases and 95th percentile values obtained from those parameters can be seen in Table 7-5. Also, the all the analysis cases and their points are attached in *Appendix-D* (Table C-12 and Table C-13 for T01 cases and C-14 and C-15 for T02 cases).

7.2.2.4 Short-column effect

Short column effects occur when both tall and small columns (various height of the column in same building) are present in a structure; during an earthquake, short columns incur more damage than tall columns. The short column may develop due to variety of reasons, including the existence of stair case beams, when the buildings located at slope area, and the partial height walls are existing in the buildings. The short column mechanism is explained in Figure 2-3, while Figure 7-7 depicts a probable example of a short column forming in the school buildings. It is important to account for short column effects in the RVS because of the wide variety of MI configurations seen in Sri Lankan school buildings, including QO, HO, and TO combinations with varied thicknesses.



Figure 7-7. Short column effect in school buildings

Therefore, the short column cases were incorporated by considering the cases analysed in Chapter-6, which are the partial MI configuration with different thickness. Table 7-6, shows the 95th percentile values of the cases considered in this study. As short column is an unfavourable attribute in the building, which should be deducted from the basic score of the building.

Table 7-6. Score modifiers for short column effects

Specifications	Typologies	Thickness	Zones	Score Modifier
Short column effect	T01	SW/DW	Zone-I	-1.0
			Zone-II	-1.1
			Zone-III	-1.1
	T02	SW/DW	Zone-I	-1.1
			Zone-II	-1.1
			Zone-III	-1.4

7.2.3 Minimum Score Evaluation

The minimum score was calculated by considering the worst combination of the score modifiers. As instructed in FEMA P-154 (ATC, 2015a), the worst-case scenario (where all the possible deficiencies in the building considered simultaneously) of the buildings were analysed by considering probability of collapse and then it converted as minimum score of the buildings. In addition, the probability of collapse should not be less than zero as maximum possible damage should be 100% of the building. To evaluate the minimum score of the building, the worst-case scenario was assumed as shown in Figure 7-8.

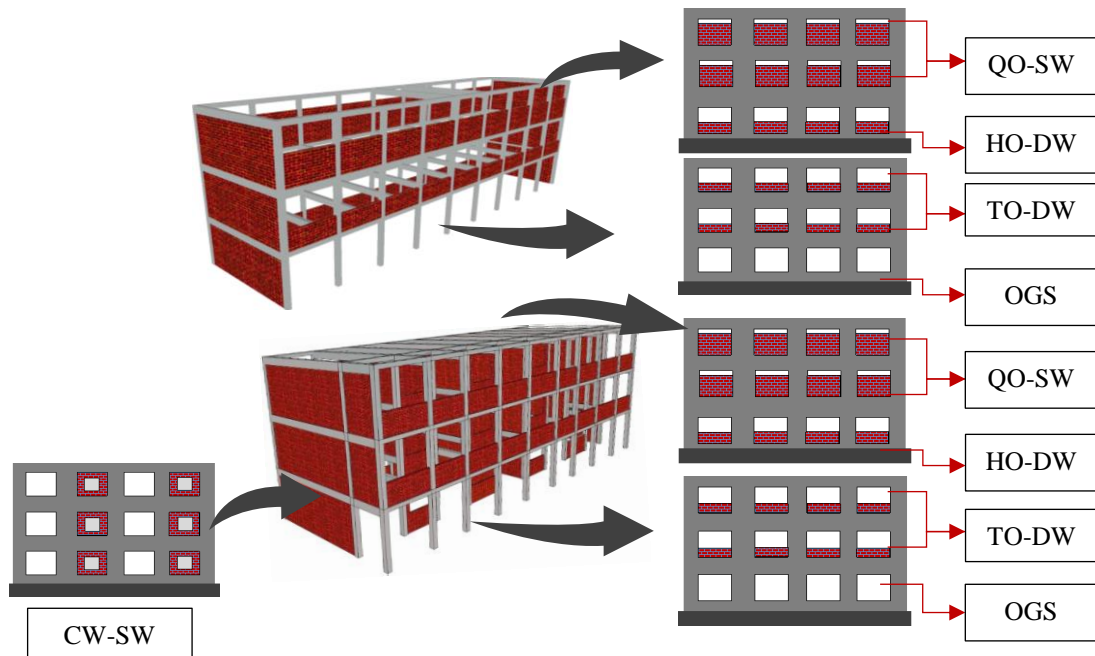


Figure 7-8. Minimum score evaluation (Worst case scenario)

The combination was generated by considering the MI configuration in terms of opening size and the thickness. The vertical irregularity and plan irregularities were assumed and contributed to the final score of the school building. As per the previous score modifiers procedure, the minimum score of the building was computed by considering the seismic zonation and the results are shown in Table 7-7. It should be noted that the building with the lowest score is presumed to be the most vulnerable to earthquakes.

Table 7-7. Minimum score of the T01 and T02 buildings

Specifications	Typologies	Thickness	Zones	Score Modifier
Minimum score	T01	SW/DW	Zone-I	1.0
			Zone-II	1.0
			Zone-III	0.9
	T02	SW/DW	Zone-I	1.2
			Zone-II	1.2
			Zone-III	1.2

7.3 Assessment of proposed RVS method

The proposed RVS method is similar to FEMA-P154 (ATC, 2015a) and general details of the building should be incorporated into the proposed form as similar to FEMA-P154 (ATC, 2015a) during the survey. The screener should have structural/ civil engineering knowledge in order to perform the survey. The suggested RVS approaches are divided into four stages of assessments. These include preliminary data collection (pre-field assessment), building layouts and plans, a detailed survey of the building, and score evaluation.

In the first step, pre-field data will be acquired, such as school basic information, location, and building identification information that can typically be obtained from the outside of the building. Figure 7-9 depicts the preliminary school building data collection parameters.

School Name: _____		Date: _____	
Address: _____		Latitude: _____	
		Longitude: _____	
Purpose of the Building: _____		Year Built: _____	School ID: _____ Building ID: _____
No. Stories: <input type="checkbox"/> Two <input type="checkbox"/> Three	Typology: <input type="checkbox"/> 1 <input type="checkbox"/> 2	Extension/ modification: <input type="checkbox"/> Yes <input type="checkbox"/> No (Highlight in the drawing)	
Foundation: <input type="checkbox"/> Spread Other: _____		Previous Hazard History: _____	

Figure 7-9. Preliminary data collection portion in proposed RVS form

Consequently, as can be seen in Figure 7-10, the building layout/plan should be plotted/attached photographs and the structural attributes such as column and beam dimensions should be stated. Also, the screener should take at least one photograph of each corner of the building, as it will help to process further analysis of the building.

Please Mark the beam and column dimensions		
Side View	Front View	Rear View

Figure 7-10. Photograph/ layout portion in proposed RVS form

In addition, the structural and non-structural details of the MI configuration (an important part in evaluating the scores) will be discussed in this portion as depicted in Figure 7-11. The MI configurations (CW, QO, HO, and TO) with opening sizes presented in the building should be stated clearly by the screener. If there are further concerns, it can be stated in the comment portion.

Story Height: _____	No of Bays: Longitudinal: _____ Transverse: _____	Bay Width: Longitudinal: _____ Transverse: _____
Total Floor Area (Sq.m): _____	Thickness of MI: Exterior _____ Interior _____	Width of MI: Exterior: _____ Interior: _____
Staircase: No: _____ Location: _____	Storey	Front Side
Special Componets: <input type="checkbox"/> Shear Wall <input type="checkbox"/> Taperd (B/C)	GF	<input type="checkbox"/> CW <input type="checkbox"/> QO <input type="checkbox"/> HO <input type="checkbox"/> TO
Roof Truss : <input type="checkbox"/> Wood <input type="checkbox"/> Steel Other: _____	FF	<input type="checkbox"/> CW <input type="checkbox"/> QO <input type="checkbox"/> HO <input type="checkbox"/> TO
Roof Material: _____	SF	<input type="checkbox"/> CW <input type="checkbox"/> QO <input type="checkbox"/> HO <input type="checkbox"/> TO
Opening Window: <input type="checkbox"/> Steel grid <input type="checkbox"/> Wood <input type="checkbox"/> No windows <input type="checkbox"/> Any other: _____		




Figure 7-11. Detailed data survey portion in proposed RVS form

In the final stage, the building score will be assigned for each building typology by considering the irregularity in the buildings. The previous section of this chapter details the irregularities and their impacts on the buildings. In addition, when structures possess vertical and plan irregularities, the short column effect should be neglected. It should be highlighted that though the OGS effect for T02 building adapted, since T02 buildings are OGS categories, the score modifiers are not incorporated in the forms.

Building Risk Scores							
Characteristics		Type - 01			Type - 02		
		Zone-I	Zone-II	Zone-III	Zone-I	Zone - II	Zone - III
Basic Score		2.7	3	3.3	3.0	3.3	4.2
Open Ground Storey (OGS)		-1.0	-0.9	-0.8	-1.0	-1.0	-1.3
Vertical Irregularity (VI)	SW	-1.0	-1.1	-1.0	-1.1	-1.2	-1.7
	DW	-1.5	-1.5	-1.3	-1.6	-1.8	-2.5
Plan Irregularity (PI)	SW	-1.0	-0.9	-1.1	-1.0	-1.1	-1.7
	DW	-1.1	-1.2	-1.1	-1.2	-1.3	-1.8
Short columns (SC)		-1.1	-1.1	-1.0	-1.1	-1.1	-1.4
Minimum score (Smin)		1.0	1.0	0.9	1.2	1.2	1.2
Final Score (Level 1)							

Figure 7-12. Building risk score portion in proposed RVS form

Also, the sample evaluation method to conduct the RVS survey is illustrated in Figure 7-13 (The RVS form and the illustration in detail given in *Appendix-D*). It can be seen that the particular building is vulnerable to earthquakes and further investigation and retrofitting technique should be imposed to the building. As building score is less than the minimum score, it assumed to be seismically vulnerable to earthquake as stated in FEMA P-154 standards (ATC, 2015a).

Rapid Visual Screening of School Buildings - Sri Lanka (Pre-Earthquake Analysis)								
School Name: <u>Al - Ameen Vidyalaya</u>				Date: <u>03.10.2022</u>				
Address: <u>Irakkamam, Ampara</u> <u>Eastern Province</u>				Latitude: <u>7.6823° N</u>		Longitude: <u>81.7345° E</u>		
Purpose of the Building: <u>Class Rooms</u>		Year Built: <u>1998</u>		School ID: <u>EST-AMP_00</u>	Building ID: <u>AM-01-01-S2</u>			
No. Stories: <input checked="" type="checkbox"/> Two <input type="checkbox"/> Three		Typology: <input checked="" type="checkbox"/> 1 <input type="checkbox"/> 2		Extension/ modification: <input checked="" type="checkbox"/> Yes <input type="checkbox"/> No (Highlight in the drawing)				
Foundation: <input checked="" type="checkbox"/> Spread Other: <u>---</u>		Previous Hazard History: <u>---</u>						
Please Mark the beam and column dimensions								
								
Side View		Front View			Rear View			
Story Height: <u>3.0 m</u>		No of Bays: Longitudinal: <u>9</u> Transverse: <u>1</u>		Bay Width: Longitudinal: <u>3.0 m</u> Transverse: <u>7.5 m</u>				
Total Floor Area (Sq.m): <u>100.75 m²</u>		Thickness of MI: Exterior <u>GF:225mm</u> <u>FF: 115 mm</u> Interior <u>115 mm</u>		Width of MI: Exterior: <u>2.6/7.1 m</u> Interior: <u>6.5 m</u>				
Staircase: No: <u>1</u> Location: <u>center</u>		Storey	Front Side	Middle	Rear Side			
Special Components: <input type="checkbox"/> Shear Wall <input type="checkbox"/> Taperd (B/C)		<u>GF</u>	<input checked="" type="checkbox"/> CW <input type="checkbox"/> QO <input type="checkbox"/> HO <input type="checkbox"/> TO	<input type="checkbox"/> CW <input type="checkbox"/> QO <input type="checkbox"/> HO <input type="checkbox"/> TO	<input checked="" type="checkbox"/> CW <input type="checkbox"/> QO <input type="checkbox"/> HO <input type="checkbox"/> TO			
Roof Truss: <input checked="" type="checkbox"/> Wood <input type="checkbox"/> Steel Other: <u>---</u>		<u>FF</u>	<input type="checkbox"/> CW <input type="checkbox"/> QO <input type="checkbox"/> HO <input checked="" type="checkbox"/> TO	<input type="checkbox"/> CW <input type="checkbox"/> QO <input type="checkbox"/> HO <input type="checkbox"/> TO	<input type="checkbox"/> CW <input type="checkbox"/> QO <input type="checkbox"/> HO <input checked="" type="checkbox"/> TO			
Roof Material: <u>Clay tiles</u>		SF	<input type="checkbox"/> CW <input type="checkbox"/> QO <input type="checkbox"/> HO <input type="checkbox"/> TO	<input type="checkbox"/> CW <input type="checkbox"/> QO <input type="checkbox"/> HO <input type="checkbox"/> TO	<input type="checkbox"/> CW <input type="checkbox"/> QO <input type="checkbox"/> HO <input type="checkbox"/> TO			
Opening Window: <input checked="" type="checkbox"/> Steel grid <input type="checkbox"/> Wood <input type="checkbox"/> No windows <input type="checkbox"/> Any other: <u>---</u>								
Building Risk Scores								
Characteristics		Type - 01			Type - 02			
		Zone-I	Zone-II	Zone-III	Zone-I	Zone - II	Zone - III	
Basic Score		2.7	3.0	<u>3.3</u>	3.0	3.3	4.2	
Open Ground Storey (OGS)		-0.8	-0.9	<u>-1.0</u>	-	-	-	
Vertical Irregularity (VI)		SW	-1.0	-1.0	<u>-1.1</u>	-1.1	-1.2	-1.7
		DW	-1.3	-1.5	-1.5	-1.6	-1.8	-2.5
Plan Irregularity (PI)		SW	-0.9	-1.0	-1.1	-1.0	-1.1	-1.7
		DW	-1.1	-1.1	-1.2	-1.2	-1.3	-1.8
Short columns (SC)		-1.0	-1.1	<u>-1.1</u>	-1.1	-1.1	-1.4	
Minimum score (Smin)		1.0	1.1	1.3	0.8	0.9	1.0	
Final Score (Level 1)		0.1						
Comments: <u>Detailed Investigation should be carried out</u> <u>1.3 >> 0.1</u>								

Surveyor Name: Sathurshan

Signature: [Redacted]

Figure 7-13. Example of sample proposed RVS form

7.3.1 Comparison between Proposed RVS and FEMA P-154

To validate the proposed RVS approach, the findings of Table 7-1 were compared to the proposed RVS in Table 7-8. It can be seen that the proposed basic scores for T01 and T02 were closer to the FEMA P-154 (ATC, 2015a) as stated in basic score of low seismicity regional form. However, the vertical irregularity and plan irregularity in the proposed RVS and FEMA P-154 (ATC, 2015a) approaches showed significant variations cause the FEMA P-154 method (ATC, 2015a) is not sensitive to infill configuration as available in the Sri Lankan school buildings. In terms of comparison, it could be seen that the variance in results caused by the irregularities of MI, since it provides more accurate findings in the proposed RVS. The proposed RVS determines the safety classification (safe and not safe) of a building based on its final score, which is higher or lower than the minimum score. Therefore, it can be said that the proposed RVS approach for assessing the seismic risk of school buildings in Sri Lanka is more suitable for Sri Lankan typological RC-MI school buildings.

Table 7-8. The proposed and FEMA P-154 results

No.	School Name	Type	Building ID	Proposed RVS	FEMA P-154 (ATC, 2015a)
1	Al Ameen Vidyalaya	T01	AM-01-01-S2	0.1 (Not safe)	2.0 (Safe)
2	Ammer Alipura Vidyalaya	T01	AM-02-01-S2	0.2 (Not safe)	2.0 (Safe)
3		T01	AM-02-02-S2	1.3 (Safe)	2.0 (Safe)
4		T01	AM-02-03-S3	0.1 (Not safe)	2.0 (Safe)
5	St. Mary's College	T01	TR-01-01-S3	1.1 (Safe)	2.6 (Safe)
6	KM/KM/Vipulananda Central College - Karaitivu	T02	AM-03-01-S3	0.8 (Not safe)	1.5 (Safe)
7	Al-Bahriya Maha Vidyalayam	T02	AM-04-01-S3	1.1 (safe)	2.0 (Safe)

7.4 Summary

A rapid visual survey method for typological school buildings in Sri Lanka is proposed in this chapter. The procedure inspired by FEMA P-154 (ATC, 2015a) was followed, considering the capacity spectrum method, and basic scores, score modifiers and minimum scores were calculated. Consequently, the different seismic zones were considered and their response spectra were obtained from the literature. The basic score and the score modifiers of the building by considering the vertical irregularity, open ground storey effects, short column effects, and plan irregularity were developed. Simultaneously, the minimum score of the building was computed by considering the worst combination of structural vulnerable attributes scenario. The proposed method is applicable and reflects the structural characteristics of the building that are varied by the presence of the MI in the school buildings.

8. SUMMARY AND CONCLUSION

The aim of this study was to propose a rapid visual screening method of school building in Sri Lanka which are seismically vulnerable. Also, the performance of the school buildings and the fragility assessment were developed in this study. The summary and the key findings obtained from the study are given in the following sections.

8.1 Summary of the study

The purpose of this research was to investigate the seismic performance of school buildings in Sri Lanka. The graphical representation of the summary of the work is illustrated in Figure 8-1. Currently, the seismic risk in Sri Lanka is assumed to be low compared to other natural hazard events such as floods, landslides, and tsunamis. However, past earthquake records and studies have shown that Sri Lanka can no longer be considered an aseismic country and an intra-plate earthquake is possible for Sri Lanka. Furthermore, seismic designs are not carried out for critical structures in Sri Lanka, such as hospital and school buildings, which are mainly designed for the gravity load scenario. In this regard, assessing the risk of critical structures being damaged by earthquakes is crucial, and this study attempted to analyse the seismic risk of school buildings in Sri Lanka. Assessing the seismic risk of all school buildings constructed in Sri Lanka is not possible and requires more time and manpower. Therefore, the objectives were defined in order to achieve the aim of proposing a rapid visual screening technique, for the typological RC-MI school buildings in Sri Lanka.

Initially, structural survey on selected school buildings in Sri Lanka. In terms of structural arrangements and MI with opening sizes and thicknesses, the study indicated distinct typologies in school buildings exist in Sri Lanka. T01 and T02 buildings were obtained in structural configuration, where the number of rows of columns varied, with T01 obtaining two rows of columns and T02 obtaining three rows of columns. Consequently, the investigation incorporated OGS (T01 and T02) and FGS (only in T01), where the existence of masonry at GF was influenced, as well as the MI changes regarded as CW, QO, HO, and TO in terms of opening size, and SW and DW as the thickness variations. Secondly, the numerical analysis was carried out using OS

(OpenSees, 2021) and the all the variations adapted from school survey was incorporated and non-linear static pushover analysis method (PO) was employed. In addition, a simplified post-processing method was adopted to account the shear failure of the columns using OS (OpenSees, 2021) output data and Response 2000 (Bentz, 2001) sectional analysis tool was used to assess the shear capacity of the building and based on the results PO graphs were rectified. In order to incorporate the stochastic variations in the material properties, the Monte-Carlo simulation was carried out and integrated into the numerical models analysed. In total, 640 building models were analysed and the seismic fragility curves in terms of building typologies were developed. The analysis results in terms of the IDR showed that T02 buildings showed comparatively better performance than the T01 buildings. Also, the presences of MI in the building enhanced the building performance in terms of increasing the overall stiffness of the building. Nevertheless, strong MI in the building (QO and HO with DW) caused the early shear failure compared to other MI configurations.

In the seismic fragility analysis and damage matrices, four damage threshold limit state based on the Sri Lankan school building condition were selected as (1) slight/cracking of MIs (SD), (2) moderate/failure of MIs (MD) (3) severe/plastic hinges in the columns (SD) and (4) collapse/shear failure of columns (CD). The purpose of fragility was to lead to the aim of the study, which is to generate the RVS method for the Sri Lankan condition. Therefore, the PO curves were converted as the capacity demand spectra using the ATC-40 (FEMA, 2013) method and fragility was generated with respect to probability of damage and the spectral displacement. The analysis revealed that T01-OGS buildings are more vulnerable to earthquake and school buildings located in the western provinces are considerably more damageable than the central and eastern provinces. The proposed RVS method was shown to have comparatively better method of evaluating the seismic risk for the Sri Lankan school buildings compared to FEMA P-154 (ATC, 2015a) as the MI configuration identified in the school buildings were incorporated. Also, presences of MI in the GF for both T01 and T02 would enhance the performance of the building and reduce the damage percentage considerably.

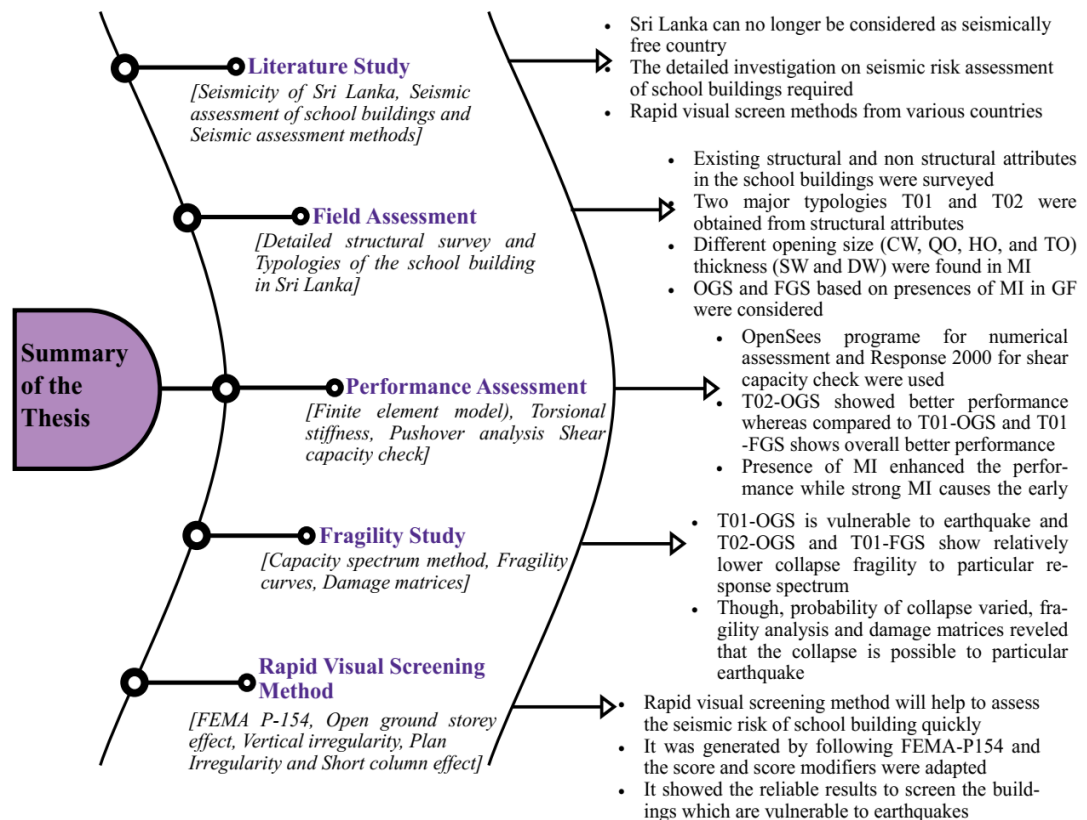


Figure 8-1. Summary of the study methods and findings

8.2 Key findings

The seismic performance assessment of the school buildings in Sri Lanka was studied and the performance in terms of IDR% at GF level which is critical to the failure was considered. Subsequently, the fragility assessment was carried out to leading the RVS score evaluation method as proposed in FEMA P-154 (ATC, 2015a, 2015b) and ATC-40 (FEMA, 2013). Following major conclusions can be drawn from the analyses made and fragility curves produced.

- In accordance with two typologies analysed, the T02 buildings were shown slightly better performance in terms of lateral deformity than the corresponding T01 building cases. Meanwhile, the presences of MI at the GF (T01-FGS) showed significant improvements in the performance of the T01 buildings during the earthquakes. The ultimate shear failure of the columns was noted at the IDRs of 2.8 % - 3.5 % for T02 buildings, whereas the ultimate column shear

failures were noted in the range of 2.4 % to 3.2 % for T01 (OGS and FGS) buildings analysed.

- The simplified method adopted to account for the shear failure of the columns under lateral seismic actions was exhibited to be effective in understanding the seismic performances of the buildings analysed, especially when large numbers of buildings are to be analysed. It should be highlighted that the columns under lower axial load showed earlier shear failure than the columns with larger axial force conditions. Also, the column with strong MI, for instance, QO-DW cases showed short column effects (IDR - 2.5-2.7%) and earliest failure compared to HO and TO cases. Further, the variability of material properties (concrete, steel and masonry) adopted through integrated Monte-Carlo simulations also added to the effectiveness of accounting for inherent variations among the building typologies analysed.
- The seismic fragility curves and damage probability matrices developed for the typological school building in four provinces of Sri Lanka can be used to implement seismic risk mitigation measures in the future. It should be noted from the damage matrices of T01-OGS cases showed more seismic vulnerability in all the provinces considered, especially in western province about 10% of T01-OGS buildings are susceptible to reach the CD state. Then in the same province, the 5% of T01-FGS and 2% of T02-OGS building typologies could reach CD state.
- The proposed RVS approaches to Sri Lankan school building showed comparatively better evaluation of seismic risk than the FEMA P-154 (ATC, 2015a) and therefore it can be used to assess the seismic risk of typological school building with minimal resources.

8.3 Future research

This study was aimed to propose a RVS method for typological Sri Lankan school buildings to assess the seismic vulnerability. As a result, the future work is intrinsic as the further improvement can be made by various aspects. The established numerical modelling procedure in this study, by incorporating stochastic variation of material properties and shear failure phenomenon of the RC columns, can be extended to

analyse other building typologies. Meanwhile, the modelling procedures were shown to be effective in establishing seismic fragility curves for different typological buildings. Additional studies are needed in the future to enhance the understanding of these buildings under seismic action by incorporating aleatory and epistemic uncertainties. In this regard, more detailed studies such as incremental dynamic analyses or advanced techniques in the modelling of buildings such as beam-column connections, different strut models, and MI and structural member connections are required to be performed with realistic seismic aleatory and epistemic data. Also, the fragility and the scores systems were developed for the 475 years of return period and it can be extended for other return periods as well.

REFERENCES

- Abeywardena, K. A. T. M. (2018). Seismic Risk Assessment of Typical Three Storey Reinforced Concrete School Buildings in Sri Lanka. *Master's Thesis, University of Peradeniya, Sri Lanka*, 135.
- Adhikari, R., & Gautam, D. (2019). Component level seismic fragility functions and damage probability matrices for Nepali school buildings. *Soil Dynamics and Earthquake Engineering*, *120*(February), 316–319. <https://doi.org/10.1016/j.soildyn.2019.02.009>
- Aftabur, R., & Shajib, U. (2013). Seismic vulnerability assessment of RC structures: a review. *Asian Transactions on Engineering*, *4*(6), 6.
- Al-Chaar, G., Issa, M., & Sweeney, S. (2002). Behavior of Masonry-Infilled Nonductile Reinforced Concrete Frames. *Journal of Structural Engineering*, *128*(8), 1055–1063. [https://doi.org/10.1061/\(ASCE\)0733-9445\(2002\)128:8\(1055\)](https://doi.org/10.1061/(ASCE)0733-9445(2002)128:8(1055))
- Alam, M. S., & Haque, S. M. (2020). Seismic vulnerability evaluation of educational buildings of Mymensingh city, Bangladesh using rapid visual screening and index based approach. *International Journal of Disaster Resilience in the Built Environment*, *11*(3), 379–402. <https://doi.org/10.1108/IJDRBE-07-2019-0043>
- Aluthapala, U. L. (2016). *Evaluation of Seismic Capacity of Existing Highway Bridges in Sri Lanka*. Master's thesis, University of Moratuwa, Sri Lanka.
- Anelli, A., Santa-Cruz, S., Vona, M., Tarque, N., & Laterza, M. (2019). A proactive and resilient seismic risk mitigation strategy for existing school buildings. *Structure and Infrastructure Engineering*, *15*(2), 137–151. <https://doi.org/10.1080/15732479.2018.1527373>
- Angeletti, P., Bellina, A., Guagenti Grandori, E., Moretti, A., & Petrini, V. (1988). Comparison between vulnerability assessment and damage index, some results. In *Proceedings of 9th World Conference on Earthquake Engineering, Tokyo-Kyoto, Japan* (pp. 181–186). http://www.iitk.ac.in/nicee/wcee/article/9_vol7_181.pdf
- Arya, A. S. (2011). Rapid Structural and Non-structural Assessment of School and Hospital Buildings in SAARC Countries. In *SAARC Disaster Management Centre, New Delhi*. SAARC Disaster Management Centre, New Delhi.
- AS/NZS 1170.4. (2018). Structural Design Actions. Part 4: Earthquake Actions in Australia. In *AS 1170.4-2007 (R2018)*. www.standards.org.au
- ATC-40. (1996). Seismic evaluation and retrofit of concrete buildings: Volume 1. In *Applied Technology Council* (Vol. 1). Applied Technology Council.
- ATC. (1988). *FEMA154: Rapid visual screening of buildings for potential seismic*

- hazard* (1st ed.). Applied Technology Council, Redwood, CA.
- ATC. (2002). *FEMA 154: Rapid Visual Screening of Buildings for Potential Seismic Hazards* (2nd ed., Issue March). www.ATCCouncil.org
- ATC. (2015a). *FEMA P-154: Rapid Visual Screening of Buildings for Potential Seismic Hazards: A Handbook* (3rd ed., Issue August). www.ATCCouncil.org
- ATC. (2015b). *FEMA P-155: Rapid Visual Screening of Buildings for Potential Seismic Hazards: Supporting Documentation* (3rd ed.). www.ATCCouncil.org
- ATC. (2018). *FEMA P-58-2 / Seismic Performance Assessment of Buildings Volume-2* (2nd ed.). Applied Technology Council. www.ATCCouncil.org
- Aydenlou, R. M. (2020). Understanding the basic concepts in seismic rehabilitation. In *Seismic Rehabilitation Methods for Existing Buildings* (pp. 1–63). Butterworth-Heinemann. <https://doi.org/10.1016/b978-0-12-819959-6.00001-4>
- Bektaş, N., & Keyes-Brassai, O. (2022). Conventional RVS Methods for Seismic Risk Assessment for Estimating the Current Situation of Existing Buildings: A State-of-the-Art Review. *Sustainability*, *14*(5), 1–40. <https://doi.org/10.3390/su14052583>
- Bentz. (2000). Sectional analysis of reinforced concrete members- Appendix A: program manuals. *University of Toronto, Ph.D Thesis, November*, 87.
- Bentz. (2001). *Response-2000 Shell-2000 Triax-2000 Membrane-2000 User Manual* (pp. 1–85). Department of Civil Engineering, University of Toronto. <http://www.ecf.utoronto.ca/~bentz/t2k.htm>
- Bentz, E. C., Vecchio, F. J., & Collins, M. P. (2006). Simplified modified compression field theory for calculating shear strength of reinforced concrete elements. *ACI Structural Journal*, *103*(4), 614–624. <https://doi.org/10.14359/16438>
- Bhalkikar, A., & Pradeep Kumar, R. (2021). A comparative study of different rapid visual survey methods used for seismic assessment of existing buildings. *Structures*, *29*, 1847–1860. <https://doi.org/10.1016/j.istruc.2020.12.026>
- Bhosale, A. S., Davis, R., & Sarkar, P. (2017). Vertical Irregularity of Buildings: Regularity Index versus Seismic Risk. *ASCE-ASME Journal of Risk and Uncertainty in Engineering Systems, Part A: Civil Engineering*, *3*(3), 04017001. <https://doi.org/10.1061/ajrua6.0000900>
- CAC. (2010). *Seismic Evaluation Procedures for Hospital Buildings*. California Administrative Code, California Code of Regulations. <https://up.codes/viewer/california/ca-administrative-code-2016/chapter/6/seismic-evaluation-procedures-for-hospital-buildings#6>
- Cavaleri, L., Di Trapani, F., Asteris, P. G., & Sarhosis, V. (2017). Influence of column

shear failure on pushover based assessment of masonry infilled reinforced concrete framed structures: A case study. *Soil Dynamics and Earthquake Engineering*, 100, 98–112. <https://doi.org/10.1016/j.soildyn.2017.05.032>

Celarec, D., & Dolšek, M. (2013). Practice-oriented probabilistic seismic performance assessment of infilled frames with consideration of shear failure of columns. *Earthquake Engineering and Structural Dynamics*, 42(9), 1339–1360. <https://doi.org/10.1002/eqe.2275>

CEN. (2004). EN 1998-5. Eurocode 8 - Design of structures for earthquake resistance - Part 5: Foundations, retaining structures and geotechnical aspects. *European Committee for Standardization*.

Chopra, A., & Goel, R. (1999). Capacity-Demand-Diagram Methods for Estimating Seismic Deformation of Inelastic Structures: SDF Systems. In *Pacific Earthquake Engineering Research Center*. https://digitalcommons.calpoly.edu/cenv_fac/53

Curry, J. R. (1989). The Sunda Arc: A model for oblique plate convergence. *Netherlands Journal of Sea Research*, 24(2–3), 131–140. [https://doi.org/10.1016/0077-7579\(89\)90144-0](https://doi.org/10.1016/0077-7579(89)90144-0)

Dananjaya, R. M. S., Wijesundara, K. K., Seneviratne, H. N., & Dissanayake, P. B. R. (2020). Determination of Response Spectra for Sri Lankan Cities using Finite Difference Method. *Engineer: Journal of the Institution of Engineers, Sri Lanka*, 53(3), 45. <https://doi.org/10.4038/engineer.v53i3.7419>

Data Management Center. (2022). <https://ds.iris.edu/ds/nodes/dmc/>

Demartinis, K., & Dritsos, S. (2006). First-level pre-earthquake assessment of buildings using fuzzy logic. *Earthquake Spectra*, 22(4), 865–885. <https://doi.org/10.1193/1.2358176>

DeMasi, T. (2006). *Assessing the Vulnerability of Post-Disaster Housing Expansion: A Case Study in Tsunami-Affected Thailand*. Bachelor's Thesis, Worcester Polytechnic Institute (WPI).

Dhungel, R., Guragain, R., Joshi, N., Pradhan, D., & Acharya, S. P. (2012). Seismic vulnerability assessment of public school buildings in nawalparasi and lamjung district of nepal. *15th World Conference on Earthquake Engineering 2012*, 10.

Dissanayake, C. B. (2005). A new plate boundary near Sri Lanka: Implications for future geohazards. *Journal of the National Science Foundation of Sri Lanka*, 33(1), 5–8. <https://doi.org/10.4038/jnsfsr.v33i1.2361>

Domaneschi, M., Zamani Noori, A., Pietropinto, M. V., & Cimellaro, G. P. (2021). Seismic vulnerability assessment of existing school buildings. *Computers and Structures*, 248, 106522. <https://doi.org/10.1016/j.compstruc.2021.106522>

- Dongwon, K., Insub, C., Junhee, K., & HakJong, C. (2022). Assessment on Economic Effect of Seismic Retrofit to RC School Building Considering Expected Damage. *12th National Conference on Earthquake Engineering*.
- Elwood, K. J., & Moehle, J. P. (2008). Dynamic Shear and Axial-Load Failure of Reinforced Concrete Columns. *Journal of Structural Engineering*, *134*(7), 1189–1198. [https://doi.org/10.1061/\(asce\)0733-9445\(2008\)134:7\(1189\)](https://doi.org/10.1061/(asce)0733-9445(2008)134:7(1189))
- EN:1992-1-1:2004-(E). (2004). *Eurocode 2: Design of concrete structures - Part 1-1: General rules and rules for buildings*.
- ESRI. (2018). *ArcGIS: Mapping & Analytics Software and Services*. <https://www.esri.com/en-us/arcgis/about-arcgis/overview>
- FEMA-273. (1997). NEHRP guidelines for the seismic rehabilitation of buildings. In *Federal Emergency Management Agency* (Issue October). Federal Emergency Management Agency.
- FEMA-356. (2000). *Prestandard and Commentary for Seismic Rehabilitation of Buildings*.
- FEMA. (2002). *HAZUS ®MH M R4 User Manual*. Federal Emergency Management Agency (FEMA). www.fema.gov/plan/prevent/hazus.
- FEMA. (2013). *Multi-hazard Loss Estimation Methodology, HAZUS-MH 2.1 Earthquake Model Technical Manual*. 718. www.msc.fema.gov
- FEMA. (2020). Hazus Earthquake Model Technical Manual. *Federal Emergency Management Agency, October*, 1–436.
- Fernando, M. J., & Kulasinghe, A. N. S. (1986). Seismicity of Sri Lanka. *Physics of the Earth and Planetary Interiors*, *44*(2), 99–106. [https://doi.org/10.1016/0031-9201\(86\)90036-1](https://doi.org/10.1016/0031-9201(86)90036-1)
- Furtado, A., Rodrigues, H., Varum, H., & Costa, A. (2017). Evaluation of different strengthening techniques' efficiency for a soft storey building. *European Journal of Environmental and Civil Engineering*, *21*(4), 371–388. <https://doi.org/10.1080/19648189.2015.1119064>
- Gamage. (2015). Earthquake Ground Motion Models for Sri Lanka. *Ph.D Dissertation, Victoria University, Australia*, 252.
- Gamage, P., & Venkatesan, S. (2020). Seismicity and seismotectonics in and around Sri Lanka: a synoptic review. In *Bulletin of Engineering Geology and the Environment* (Vol. 79, Issue 2, pp. 571–586). Springer. <https://doi.org/10.1007/s10064-019-01576-1>
- Gautam, D., Adhikari, R., Rupakhety, R., & Koirala, P. (2020). An empirical method for seismic vulnerability assessment of Nepali school buildings. *Bulletin of*

Earthquake Engineering, 18(13), 5965–5982. <https://doi.org/10.1007/s10518-020-00922-z>

- Ghafar, M., Ramly, N., Alel, M., Adnan, A., Mohamad, E. T., & Yunus, M. Z. M. (2015). A simplified method for preliminary seismic vulnerability assessment of existing building in Kundasang, Sabah, Malaysia. *Jurnal Teknologi*, 72(3), 1–7. <https://doi.org/10.11113/jt.v72.4003>
- Haldar, P., Singh, Y., & Paul, D. K. (2013). Identification of seismic failure modes of URM infilled RC frame buildings. *Engineering Failure Analysis*, 33, 97–118. <https://doi.org/10.1016/j.engfailanal.2013.04.017>
- Harirchian, E., Jadhav, K., Mohammad, K., Hosseini, S. E. A., & Lahmer, T. (2020). A comparative study of MCDM methods integrated with rapid visual seismic vulnerability assessment of existing RC structures. *Applied Sciences (Switzerland)*, 10(18), 6411. <https://doi.org/10.3390/APP10186411>
- Hasan, R., Xu, L., & Grierson, D. E. (2002). Push-over analysis for performance-based seismic design. *Computers and Structures*, 80(31), 2483–2493. [https://doi.org/10.1016/S0045-7949\(02\)00212-2](https://doi.org/10.1016/S0045-7949(02)00212-2)
- Idham, N. C. (2011). *Seismic Vulnerability Assessment In Vernacular Houses: The Rapid Visual Screening Procedure for Non Engineered Building with Application to Java Indonesia*. Doctoral dissertation, Eastern Mediterranean University (EMU).
- International Seismological Centre*. (2022). <http://www.isc.ac.uk/>
- Jain, S. K., Mitra, K., Kumar, M., & Shah, M. (2010). A proposed rapid visual screening procedure for seismic evaluation of RC-frame buildings in India. *Earthquake Spectra*, 26(3), 709–729. <https://doi.org/10.1193/1.3456711>
- Jainih, V., & Harith, N. S. H. (2020). Seismic vulnerability assessment in Kota Kinabalu, Sabah. *IOP Conference Series: Earth and Environmental Science*, 476(1), 012053. <https://doi.org/10.1088/1755-1315/476/1/012053>
- Jayasinghe, M. T. R., Kulatilake, S. A. S., Alwis, K., Angamma, R. B., & Perera, G. (1997). Earthquake design techniques for Sri Lanka. *Research for Industry*, January, 13.
- JBDPA. (2001). Standard for seismic capacity evaluation of existing reinforced concrete buildings. In *The Japan Building Disaster Prevention Association*.
- Kaplan, O., Guney, Y., Topcu, A., & Ozelikors, Y. (2018). A rapid seismic safety assessment method for mid-rise reinforced concrete buildings. *Bulletin of Earthquake Engineering*, 16(2), 889–915. <https://doi.org/10.1007/s10518-017-0229-0>
- Karsan, I. D., & Jirsa, J. O. (1969). Behavior of Concrete Under Compressive

- Loadings. *Journal of the Structural Division*, 95(12), 2543–2564. <https://doi.org/10.1061/jsdeag.0002424>
- Kassem, M. M., Beddu, S., Ooi, J. H., Tan, C. G., El-Maissi, A. M., & Nazri, F. M. (2021). Assessment of seismic building vulnerability using rapid visual screening method through web-based application for Malaysia. *Buildings*, 11(10), 485. <https://doi.org/10.3390/buildings11100485>
- Kularatne, C. (2010). Development of Disaster Resistant School Buildings. *University of Moratuwa, Master's Thesis*.
- Lewangamage, C. S., & Kularathna, H. G. S. R. (2015). An approach to seismic analysis of (engineered) buildings in Sri Lanka. *Engineer*, 48(1), 39. <https://doi.org/10.4038/engineer.v48i1.6847>
- Leyton, F., Ruiz, J., Campos, J., & Kausel, E. (2009). Intraplate and interplate earthquakes in Chilean subduction zone: A theoretical and observational comparison. *Physics of the Earth and Planetary Interiors*, 175(1–2), 37–46. <https://doi.org/10.1016/j.pepi.2008.03.017>
- López, O. A., Hernández, J. J., Del Re, G., Puig, J., & Espinosa, L. (2007). Reducing seismic risk of school buildings in Venezuela. *Earthquake Spectra*, 23(4), 771–790. <https://doi.org/10.1193/1.2791000>
- Mander, J. B., Priestley, M. J. N., & Park, R. (1989). Theoretical Stress-Strain Model for Confined Concrete. *J. Struct. Eng*, 114(8), 1804–1826.
- Marasingha, J. K. (2013). Seismic Assessment of School Building in Sri Lanka. *Master's Thesis, University of Peradeniya, Sri Lanka*, 114.
- MATLAB. (2017). *The MathWorks, Inc. (2017a)*. <https://www.mathworks.com/>
- Maziligüney, L. (2020). Seismic Vulnerability Assessment Of Reinforced Concrete School Buildings in Turkey [Middle East Technical University]. In *Ph.D dissertation, Middle East Technical University*. <https://doi.org/10.1007/s42107-020-00311-6>
- Mazzoni, S., McKenna, F., Scott, M. H., Fenves, G. L., & Iii, A. (2006). *Open System for Earthquake Engineering Simulation (OpenSees) OpenSees Command Language Manual*.
- McKenna, F., Fenves, G. L., Scott, M. H., & Jeremic, B. (2000). Open System for Earthquake Engineering Simulation (OpenSees). Pacific Earthquake Engineering Research Center. *University of California, Berkeley, CA*, Article OpenSees3.3.0. <https://opensees.berkeley.edu/>
- METU. (2003). *Earthquake Master Plan For Istanbul*. Metropolitan Municipality of Istanbul Planning and Construction Directorate Geotechnical and Earthquake Investigation Department.

- Ministry of Education. (2020). *Annual School Census of Sri Lanka Final Report - 2020*. 151.
- Mohamad, I. I., Mohd Yunus, M. Z., & Harith, N. S. H. (2019). Assessment of building vulnerability by integrating rapid visual screening and geographic information system: A case study of Ranau township. *IOP Conference Series: Materials Science and Engineering*, 527(1), 012042. <https://doi.org/10.1088/1757-899X/527/1/012042>
- Nanda, R. P., Paul, N. K., & Chanu, N. M. (2019). Seismic loss estimation tool as rapid survey for prioritizing buildings for disaster preparedness: case study to hospital buildings. *Natural Hazards*, 95(3), 769–781. <https://doi.org/10.1007/s11069-018-3518-2>
- NBRO. (2015). Hazard Resilient Housing Construction Manual - Resilient Construction Series No. 1. In *National Building Research Organisation (NBRO), Sri Lanka* (Issue 1). www.nbro.gov.lk
- NDMA. (2020). *A Primer on Rapid Visual Screening (RVS) Consolidating Earthquake Safety Assessment Efforts in India*. National Disaster Management Authority.
- Ningthoujam, M. C., & Nanda, R. P. (2018). Rapid visual screening procedure of existing building based on statistical analysis. *International Journal of Disaster Risk Reduction*, 28, 720–730. <https://doi.org/10.1016/j.ijdr.2018.01.033>
- NRCC. (1992). Manual for screening of buildings for seismic investigation. In *National Research Council Canada*.
- NSET. (2000). *Seismic vulnerability of the public school buildings of Kathmandu valley and methods for reducing it. August 2000*, 116. <https://s3.us-east-1.amazonaws.com/media.archnet.org/system/publications/contents/8876/original/DTP101375.pdf?1391607850>
- NZSEE. (1996). *Research Report 058 Seismic assessment of New Zealand highway bridges: development and testing of preliminary screening procedures*. <https://www.nzta.govt.nz/resources/research/reports/58>
- NZSEE. (2006). *Assessment and improvement of the structural performance of buildings in earthquakes*. New Zealand Society for Earthquake Engineering, Wellington, New Zealand.
- NZSEE. (2014). *Assessment and Improvement of the Structural Performance of Buildings in Earthquakes (Section 3, Initial Seismic Assessment)* (Vol. 3, Issue September). New Zealand Society For Earthquake Engineering.
- NZSEE. (2017). *The Seismic Assessment of Existing Buildings - Initial Seismic Assessment: Part B*.

- O'Reilly, G. J., Perrone, D., Fox, M., Monteiro, R., & Filiatrault, A. (2018). Seismic assessment and loss estimation of existing school buildings in Italy. *Engineering Structures*, *168*, 142–162. <https://doi.org/10.1016/j.engstruct.2018.04.056>
- O'Reilly, G. J., & Sullivan, T. J. (2017). Probabilistic seismic assessment and retrofit considerations for Italian RC frame buildings. *Bulletin of Earthquake Engineering*, *16*(3), 1447–1485. <https://doi.org/10.1007/s10518-017-0257-9>
- OASP. (2000). *Provisions for PreEarthquake Vulnerability Assessment of Public Buildings (Part A)*. Greek Earthquake Planning and Protection Organization.
- OpenSees. (2021). *Open System for Earthquake Engineering Simulation (3.3.0)*. Pacific Earthquake Engineering Research Center (PEER). <https://opensees.berkeley.edu/>
- Palagala, V. Y., & Singhal, V. (2021). Structural score to quantify the vulnerability for quick seismic assessment of RC framed buildings in India. *Engineering Structures*, *243*(May), 112659. <https://doi.org/10.1016/j.engstruct.2021.112659>
- Perrone, D., Aiello, M. A., Pecce, M., & Rossi, F. (2015). Rapid visual screening for seismic evaluation of RC hospital buildings. *Structures*, *3*, 57–70. <https://doi.org/10.1016/j.istruc.2015.03.002>
- Popovics, S. (1973). A numerical approach to the complete stress-strain curve of concrete. *Cement and Concrete Research*, *3*(5), 583–599. [https://doi.org/10.1016/0008-8846\(73\)90096-3](https://doi.org/10.1016/0008-8846(73)90096-3)
- Porter, K. (2021). A Beginner's Guide to Fragility, Vulnerability, and Risk. In *Encyclopedia of Earthquake Engineering* (pp. 1–29). Springer, Berlin, Heidelberg. https://doi.org/10.1007/978-3-642-36197-5_256-1
- Prasanna, K. P. N. (2016). *Comparative Study on Seismic Analysis of Buildings for Different Code of Practices Commonly Used in Sri Lanka*. Master's thesis, University of Moratuwa, Sri Lanka.
- Rai, D. C. (2005). Review of Documents on Seismic Strengthening of Existing Buildings. In *Document no-IITK-GSDMA-EQ03* (Vol. 7, pp. 0–11). <http://www.iitk.ac.in/nicee/IITK-GSDMA/EQ07.pdf>
- Rajkumari, S., Thakkar, K., & Goyal, H. (2022). Fragility analysis of structures subjected to seismic excitation: A state-of-the-art review. In *Structures* (Vol. 40, pp. 303–316). Elsevier. <https://doi.org/10.1016/j.istruc.2022.04.023>
- Rautela, P., Joshi, G. C., & Ghildiyal, S. (2020). Economics of seismic resilience of educational infrastructure in high earthquake hazard prone Himalayan province of Uttarakhand in India. *International Journal of Disaster Risk Reduction*, *43*, 101363. <https://doi.org/10.1016/j.ijdr.2019.101363>
- Rodgers, J. E. (2012). Why Schools are Vulnerable to Earthquakes. *Proceedings of*

the 15th World Conference on Earthquake Engineering, 24–28.

- Ruggieri, S., Perrone, D., Leone, M., Uva, G., & Aiello, M. A. (2020). A prioritization RVS methodology for the seismic risk assessment of RC school buildings. *International Journal of Disaster Risk Reduction*, 51(June), 101807. <https://doi.org/10.1016/j.ijdr.2020.101807>
- Rupakheti, D., & Apichayakul, P. (2019). Development of rapid visual screening form for Nepal based on the data collected from-its 2015 earthquake. *IOP Conference Series: Earth and Environmental Science*, 365(1), 012027. <https://doi.org/10.1088/1755-1315/365/1/012027>
- Saiidi, M., & Sozen, M. A. (1981). Simple nonlinear seismic analysis of R/C structures. *ASCE J Struct Div*, 107(5), 937–952. <https://doi.org/10.1061/jsdeag.0005714>
- Sangiorgio, V., Uva, G., & Aiello, M. A. (2020). A multi-criteria-based procedure for the robust definition of algorithms aimed at fast seismic risk assessment of existing RC buildings. *Structures*, 24, 766–782. <https://doi.org/10.1016/j.istruc.2020.01.048>
- Sarmah, T., & Das, S. (2018). Earthquake Vulnerability Assessment for RCC Buildings of Guwahati City using Rapid Visual Screening. *Procedia Engineering*, 212, 214–221. <https://doi.org/10.1016/j.proeng.2018.01.028>
- Seneviratne, H. N., Perera, L. R. K., Wijesundara, K. K., Dananjaya, R. M. S., & De S. Jayawardena, U. (2020). Seismicity around Sri Lanka from Historical Records and its Engineering Implications. *Engineer: Journal of the Institution of Engineers, Sri Lanka*, 53(2), 47. <https://doi.org/10.4038/engineer.v53i2.7412>
- Seneviratne, H. N., Wijesundara, K. K., Perera, L. R. K., & Dissanayake, P. B. R. (2020). A Macro Seismic Hazard Zonation for Sri Lanka. *Engineer: Journal of the Institution of Engineers, Sri Lanka*, 53(3), 37. <https://doi.org/10.4038/engineer.v53i3.7418>
- SERC. (2002). *Formulation of Guidelines for Assessment of Strength and Performance of Existing Buildings and Recommendations on Retrofitting Schemes to Ensure Resistance to Earthquakes*.
- Shanthika, K., Jayasinghe, J. A. S. C., & Bandara, C. S. (2022). Influence of Slab System in Transfer of Lateral Loads to Reinforced Concrete Shear Wall. *Engineer: Journal of the Institution of Engineers, Sri Lanka*, 55(2), 111. <https://doi.org/10.4038/engineer.v55i2.7513>
- Siddharth, & Sinha, A. K. (2022). Seismic vulnerability assessment of buildings of Patna by rapid visual screening. *International Journal of Advanced Technology and Engineering Exploration*, 9(86), 61–71. <https://doi.org/10.19101/IJATEE.2021.874745>

- Sinha, R., & Goyal, A. (2004). A National Policy for Seismic Vulnerability Assessment of Buildings and Procedure for Rapid Visual Screening of Buildings for Potential Seismic Vulnerability. *Indian Institute of Technology Kanpur (IITK)*, 120. <https://www.ncbi.nlm.nih.gov>
- SSESL. (2006). Reinforcement detailing to mitigate seismic effects. *Society of Structural Engineers Sri Lanka*, 41.
- Sucuoğlu, H., Yazgan, U., & Yakut, A. (2007). A screening procedure for seismic risk assessment in urban building stocks. *Earthquake Spectra*, 23(2), 441–458. <https://doi.org/10.1193/1.2720931>
- Suribabu, D., Dumka, R. K., Paikray, J., Kothiyari, G. C., Thakkar, M., Swamy, K. V., Taloor, A. K., & Prajapati, S. (2022). Geodetic characterization of active Katrol Hill Fault (KHF) of Central Mainland Kachchh, western India. *Geodesy and Geodynamics*, 13(3), 247–253. <https://doi.org/10.1016/j.geog.2021.05.003>
- Thamboo, J. A., & Dhanasekar, M. (2019a). Correlation between the performance of solid masonry prisms and wallettes under compression. *Journal of Building Engineering*, 22, 429–438. <https://doi.org/10.1016/j.job.2019.01.007>
- Thamboo, J. A., & Dhanasekar, M. (2019b). Correlation between the performance of solid masonry prisms and wallettes under compression. *Journal of Building Engineering*, 22, 429–438. <https://doi.org/10.1016/j.job.2019.01.007>
- Tischer, H. (2012). *Rapid seismic vulnerability assessment of school buildings in Québec*. Doctoral Dissertation, McGill, Canada.
- Tiwari, P., Maurya, D. M., Shaikh, M., Patidar, A. K., Vanik, N., Padmalal, A., Vasaikar, S., & Chamyal, L. S. (2021). Surface trace of the active Katrol Hill Fault and estimation of paleo-earthquake magnitude for seismic hazard, Western India. *Engineering Geology*, 295, 106416. <https://doi.org/10.1016/j.enggeo.2021.106416>
- Tu, Y. H., Liu, T. W., Ao, L. C., & Yeh, P. L. (2010). Nonlinear Static Seismic Analysis and Its Validation Using. *9th U.S. National and 10th Canadian Conference on Earthquake Engineering*, 848, 10.
- UBC. (1997). Uniform Building Code: Volume-1. In *International Conference of Building Officials* (6th ed.).
- Uduweriya, S. B., Wijesundara, K. K., Dissanayake, P. B. R., Susantha, K. A. S., & Seneviratne, H. N. (2020). Seismic Response of Sri Lanka using PSHA Technique. *Engineer: Journal of the Institution of Engineers, Sri Lanka*, 53(2), 39. <https://doi.org/10.4038/engineer.v53i2.7411>
- USGS-NEIC. (2020). *Earthquake Catalog*. U.S. Geological Survey-National Earthquake Information Center. <https://earthquake.usgs.gov/earthquakes/search/>

- Van Orman, J., Cochran, J. R., Weissel, J. K., & Jestin, F. (1995). Distribution of shortening between the Indian and Australian plates in the central Indian Ocean. *Earth and Planetary Science Letters*, 133(1–2), 35–46. [https://doi.org/10.1016/0012-821X\(95\)00061-G](https://doi.org/10.1016/0012-821X(95)00061-G)
- Vatteri, A. P., D’Ayala, D., & Gehl, P. (2022). Bayesian networks for assessment of disruption to school systems under combined hazards. *International Journal of Disaster Risk Reduction*, 74. <https://doi.org/10.1016/j.ijdr.2022.102924>
- Young, W. C., Budynas, R. G., & Sadegh, A. M. (2012). *Roark’s Formulas for Stress and Strain Eighth Edition* (8th editio). McGraw-Hill.
- Zain, M., Usman, M., Farooq, S. H., & Mehmood, T. (2019). Seismic Vulnerability Assessment of School Buildings in Seismic Zone 4 of Pakistan. *Advances in Civil Engineering*, 2019. <https://doi.org/10.1155/2019/5808256>

APPENDIX A: SELECTED SURVEYED SCHOOL BUILDINGS DETAILS

Appendix A-1: School survey form

1. School building details			
School ID : BD/01/01/S02	Building ID : 01	Date 10.02.2021	Surveyor Names M. Sathurshan
Location Mallthe central college, Pattiyagedara, Bandarawela			
2. Building Plan		3. Survey Photos	
<p>Upper Flow</p> <p>Ground Flow</p>		X Front	YES
		X Back	YES
		Y Front	YES
		Y Back	YES
		Building corner	YES
		Staircase	YES
		Roof void	Not applicable
		Deterioration	Not applicable
		Others (specify)	
		Note: X is the longest dimension. Add details of dimensions if not rectangular. Mark on sketch front and back. Highlight external infills	
4. Building Elevation			
Elevation Sketch. Include openings			

5. Building Characteristics				
5.1 Year of Construction				
Year construction	1986	Age	36 years	
5.2 Storeys and bays				
Storeys	2	Avg storey H	3 m	
#Bays X*	9	Avg bay width X**	3.1 m	
#Bays Y*	1	Avg bay width Y**	7.5 m	
* = include bays with staircase		** = do not include width of bays with staircase		
5.3 Staircases				
#Staircases	1	Staircase bay width in X	2.8 m	
Staircase location (indicate bay #)	Middel Bay	Staircase bay width in Y	7 m	
6. Structural Information				
6.1 Structural System				
Typical column dimensions (width*height in cm)	Ground floor	25X25	Upper floors (width*height in cm)	25X25
Typical X beam dimensions (width*height in cm)	Ground floor	25X25	Upper floors (width*height in cm)	25X25
Typical Y beam dimensions (width*height in cm)	Ground floor	25X45	Upper floors (width*height in cm)	25X45
Floor typology	RC Slab		Floor average thickness (in cm)	15
Staircase typology	Cantliver		Condition of structure	Fair
Foundations	Plinth		Apron	Yes
6.2 Walls & Openings				
X direction				
Infills connection to structure	On 4 sides			
Typical wall thickness (width in cm)	External (width in cm)	11.5	Internal (width in cm)	0
Openings	# Windows/bay (front)	1	# Doors/bay (front)	1
	# Windows/bay (back)	1	# Doors/bay (back)	1
	Average window (width*height in m)	1.8X1.2	Average door (width*height in m)	0.8X2.1
Grills	#Grills/bay (Front)	1	#Grills/bay (Back)	0
Y direction				
Infills connection to structure	On 4 sides			
Typical wall thickness (width in cm)	External (width in cm)	22.5	Internal (width in cm)	22.5
Openings	# Windows/bay (front)	0	# Doors/bay (front)	0
	# Windows/bay (back)	0	# Doors/bay (back)	0
	Average window (width*height in m)	0	Average door (width*height in m)	0
Grills	#Grills/bay (Front)	0	#Grills/bay (Back)	0
6.3 Roof				

General Information

Structural attributes

Non-structural attributes

Appendix A-2: Selected surveyed school buildings details

Table A-1. Selected surveyed school buildings details

Ref.	Building ID	School Name	District	Address	GPS
NU01	NU/01/01/S03	CP/KOT/Jayahela National School	Nuwara Eliya	CP/KOT/Jayahela National School, Nuwara Eliya	7°01'00.6"N 80°40'06.7"E
NU02	NU/02/01/S02	CP/KOT/Punduloya National School	Nuwara Eliya	CP/KOT/Punduloya National School , Punduloya	7°00'53.8"N
	NU/02/02/S02				80°40'08.1"E
NU03	NU/03/01/S02	N/Pallebowala Secondary School	Nuwara Eliya	N/Pallebowala Secondary School,Pallebowala	7°09'20.5"N 80°44'10.0"E
KU01	KU/01/01/S03	Ma Eliya Maha Vidyalaya	Kurunegala	Wa/Ma/Po/Pi/Ma Eliya Maha Vidyalaya, Ma eliya	7°44'44.4"N 80°25'07.9"E
BD01	BD/01/01/S02	Maliththa central college	Badulla	BD/Maliththa central college, Pattiyagedara, Bandarawela	6°49'58.9"N 80°59'34.2"E
BD02	BD/02/01/S02	Vapassawela Navodya Maha vidyalaya	Badulla	BD/Vapassawela Navodya Maha Vidyalaya, UVA-Maligathenna	6°54'07.8"N
	BD/02/02/S02				80°59'01.9"E
BD03	BD/03/01/S02	St.Joseph's College	Badulla	BD/ St. Joseph's College, Bandarawela	6°49'44.5"N
	BD/03/02/S03				80°59'42.2"E
	BD/03/03/S02				
BD04	BD/04/01/S03	Haliela Central college	Badulla	B/ Haliela Central College, Haliela	6°57'39.8"N
	BD/04/02/S03				81°02'06.2"E
MO02	MO/01/01/S02	Pelwatta Navodya Vidyalaya	Monaragala	Mo/Pelwatta Navodya Vidyalaya, Buttala	6°44'56.4"N 81°11'42.7"E
AM01	AM/01/01/S02	KM/STR/Al Ameen Vidyalaya	Ampara	KM/STR/Al Ameen Vidyalaya, Varipathanchenai	7°15'10.9"N
	AM/01/02/S02				81°42'35.0"E
	AM/01/02/S02				
AM02	AM/02/01/S02	KM/STR/Ameer Alipura Vidyalaya	Ampara	KM/STR/Ameer Alipura Vidyalaya, Irakkamam	7°14'28.1"N
	AM/02/02/S03				81°42'57.8"E
AM03	AM/03/01/S02	Panama Maha Vidyalaya	Ampara	Am/Panama Maha Vidyalaya, Ampara	6°45'24.2"N
	AM/03/02/S02				81°48'17.8"E
	AM/03/03/S02				

AM04	AM/04/01/S02	Sinhapura Sinhala Vidyalaya	Ampara	Am/Sinhapura Sihala Vidyalaya, Potuvil	6°50'16.1"N 81°49'58.9"E
TR01	TR/01/01/S03	St Mary's College (National School)	Trincomalee	St Mary's College (National School), Trincomalee	8°34'15.9"N
	TR/01/02/S03				81°14'09.7"E
TR02	TR/02/01/S03	Sri Koneshwara Hindu College	Trincomalee	T/R.K.M. Sri Koneshawara Hindu College, Trincomalee	8°34'28.4"N
	TR/02/02/S03				81°14'06.0"E
	TR/02/03/S03				
TR03	TR/03/01/S03	T /Zahira College (National School)	Trincomalee	T /Zahira College (National School), Trincomalee	8°34'21.3"N
	TR/03/02/S02				81°13'57.9"E
JF01	JF/01/01/S03	J/Nelliady Central college	Jaffna	J/Nelliady Central college, Karaveddy, Jaffna	9°48'00.3"N
	JF/01/02/S02				80°12'03.2"E
JF02	JF/02/01/S02	J/Vathiry Sacred Heart College	Jaffna	J/ Vathiri Secret Heart College, Jaffna	9°48'00.0"N 80°12'00.0"E
KD01	KD/01/01/S02	Gangasiripura College	Kandy	Gangasiripura college, Ambagamuwa Road	7°09'48.2"N
	KD/01/02/S02				80°34'06.0"E
KD02	KD/02/01/S02	Senarathgama Junior School	Kandy	Senarathgama Junior School, Katugastota	7°19'19.7"N 80°36'22.1"E
KD03	KD/03/01/S02	Jinaraja Maha Vidyalaya	Kandy	CP/GP/Jinaraja Maha Vidyalaya, Sinhapitiya, Gampola	7°09'40.3"N
	KD/03/02/S02				80°33'25.0"E
	KD/04/01/S02				
KD04	KD/04/02/S03	Wickramabahu Central College	Kandy	Wickramabahu Central College, Gampola	7°09'48.9"N 80°33'47.2"E

NU-01-01-S02/03: NU – District; 01- 1st School; 01 - First buildings; S02/03- Storey

Appendix A-3: Selected school building structural details

Table A-2. School building structural details

ID	Year of Construction	# Storeys	Storey Height (m)	# Bays X	Av. Bay Width x (m)	No. Bays Y	Av. Bay Width Y (m)	# Staircases	Material of load resisting system	Staircase (Cantilevered/Ramp)	Staircase Location	Column mm	Beam (X) (mm)	Beam (Y) (mm)	Floor Type	Floor Thickness (mm)	Structure condition	Foundations
NU/01/01/S03	2018	3	3.50	9	3.25	1	7.75 +2.4	1	RC	Cantilever step	Middle	300X 300	300X 225	300X 450	RC Slab	150	Fair	Plinth
NU/02/01/S02	1995	2	3.50	9	3.00	1	7.50	1	RC	Cantilever step	Corner	400X 400	300X 225	300X 450	RC Slab	125	Fair	Pad
NU/02/02/S02	1996	2	3.10	9	3.00	1	7.50	1	RC	Cantilever step	Middle	400X 400	300X 225	300X 450	RC Slab	150	Fair	Pad
NU/03/01/S02	NA	2	3.00	9	3.25	1	7.75	1	RC	Ramp	Corner	225X 225	225X 225	225X 450	RC Slab	150	Fair	Plinth
KU/01/01/S03	1998	3	3.00	9	3.00	1	6.00	1	RC	Cantilever step	Middle	250X 250	250X 250	250X 400	RC Slab	150	Fair	Plinth
BD/01/01/S02	2019	2	3.00	9	3.10	1	7.50	1	RC	Cantilever step	Corner	250X 250	250X 250	250X 450	RC Slab	150	Fair	Plinth
BD/02/01/S02	1986	2	3.00	9	3.10	1	7.50	1	RC	Cantilever step	Corner	250X 250	250X 250	250X 450	RC Slab	150	Fair	Plinth
BD/02/02/S02	2015	2	3.00	9	3.10	1	7.50	1	RC	Cantilever step	Middle	300X 225	225X 225	225X 400	RC Slab	150	Fair	Plinth
BD/03/01/S02	2001	2	3.10	9	3.10	1	7.70	1	RC	Cantilever step	Middle	225X 225	225X 225	225X 450	RC Slab	150	Fair	Plinth
BD/03/02/S03	2005	3	3.00	9	2.80	1	7.70	1	RC	Cantilever step	Middle	225X 300	225X 225	225X 450	RC Slab	150	Fair	Plinth
BD/03/03/S02	NA	2	4.00/3.00	7	2.80	1	7.50	2	RC	Ramp	Corner	300X 300	150X 150	150X 225	RC Slab	125	Fair	Plinth
BD/04/01/S03	NA	3	3.00	9	3.00	2	7.75 +2.4	1	RC	Cantilever step	Middle	225X 225	225X 225	225X 400	RC Slab	150	Fair	Plinth

BD/04/02/S03	NA	3	3.00	9	3.00	2	7.75 +2.4	1	RC	Cantilever step	Middle	225X 225	225X 225	225X 400	RC Slab	150	Fair	Plinth
MO/01/01/S02	2018	2	3.20	9	3.10	1	7.50	1	RC	Cantilever step	Middle	225X 225	225X 225	225X 500	RC Slab	125	Fair	Plinth
AM/01/01/S02	2004	2	3.00	9	3.00	1	7.90	1	RC	Cantilever step	Middle	225X 225	225X 225	225X 400	RC Slab	150	Fair	Plinth
AM/01/02/S02	2008	2	3.00	5	3.00	1	9.40	1	RC	Cantilever step	Corner	300X 300	300X 300	300X 450	RC Slab	150	Fair	N/A
AM/01/02/S02	2018	2	3.00	7	3.00	1	7.90	1	RC	Cantilever step	Middle	250X 250	250X 250	250X 400	RC Slab	150	Fair	N/A
AM/02/01/S02	1998	2	3.00	9	3.00	1	7.90	1	RC	Cantilever step	Middle	250X 250	250X 250	250X 450	RC Slab	150	Fair	Pad
AM/02/02/S03	2021	3	3.00	7	3.00	1	7.50	1	RC	Cantilever step	5th Bay	225X 225	225X 300	225X 500	RC Slab	200	Excel lent	Pad
AM/03/01/S02	2003	2	3.00	9	3.00	1	7.90	1	RC	Cantilever step	Middle	225X 225	225X 225	225X 500	RC Slab	125	Fair	N/A
AM/03/02/S02	2011	2	3.00	8	3.10	1	6.50	1	RC	Cantilever step	Corner	225X 225	225X 225	225X 450	RC Slab	125	Fair	N/A
AM/03/03/S02	2009	2	4.00	9	2.85	1	7.70	1	RC	Cantilever step	9th Bay	225X 225	225X 225	225X 500	RC Slab	125	Fair	N/A
AM/04/01/S02	2008	2	3.20	1 6	3.50	1	6.50	2	RC	Cantilever step	Corners (1/13)	225X 225	225X 225	225X 350	RC Slab	125	Fair	N/A
TR/01/01/S03	NA	3	3.00	9	3.00	1	7.90	1	RC	Cantilever step	Corner	225X 225	225X 300	225X 450	RC Slab	150	Fair	N/A
TR/01/02/S03	2018	3	3.6/3 .2	9	3.00	1	10.0 0	1	RC	Cantilever step	Corner	300X 300	225X 300	300X 600	RC Slab	150	Excel lent	N/A
TR/02/01/S03	NA	3	2.80	1 4	3.00	1	7.00	1	RC	Cantilever step	Middle, Corner (5/14)	225X 225	225X 225	225X 450	RC Slab	150	Fair	N/A
TR/02/02/S03	NA	3	2.80	1 4	3.00	1	7.70	1	RC	Cantilever step	Corners (1/14)	225X 225	225X 225	225X 450	RC Slab	150	Fair	N/A
TR/02/03/S03	NA	3	2.80	1 1	3.00	1	8.00	1	RC	Cantilever step	Corner	225X 450	225X 225	225X 450	RC Slab	150	Fair	N/A

TR/03/01/S03	NA	3	2.90	1 1	3.10	1	7.40	1	RC	Cantilever step	Middle (7)	225X 225	225X 225	225X 450	RC Slab	150	Fair	N/A
TR/03/02/S02	NA	2	2.80	9	3.00	1	7.00	1	RC	Cantilever step	Corner	225X 225	225X 225	225X 450	RC Slab	150	Fair	N/A
JF/01/01/S03	2007	3	3.00	9	3.00	1	8.00	1	RC	Cantilever step	Middle	225X 225	225X 225	225X 500	RC Slab	150	Fair	N/A
JF/01/02/S02	2004	3	3.00	1 3	3.00	1	7.50	1	RC	Cantilever step	Middle	225X 225	225X 225	225X 450	RC Slab	150	Fair	N/A
JF/02/01/S02	20014	2	3.00	9	3.00	1	7.50	1	RC	Cantilever step	Corner	225X 225	225X 225	225X 450	RC Slab	150	Fair	N/A
KD/01/01/S02	2007	2	3.00	9	3.00	1	7.70	1	RC	Cantilever step	Corner	225X 225	225X 225	225X 450	RC Slab	150	Fair	Plinth
KD/01/02/S02	1985	2	3.00	1 4	3.00	1	7.85	1	RC	Cantilever step	Middle	225X 225	225X 225	225X 400	RC Slab	150	Fair	Plinth
KD/02/01/S02	NA	2	3.00	7	3.60	1	7.75 +2.4	1	RC	Cantilever step	Corner	300X 300	225X 225	225X 450	RC Slab	150	Fair	Plinth
KD/03/01/S02	2019	2	3.50	9	3.00	1	7.5+ 2.4	1	RC	Cantilever step	Corner	225X 225	225X 225	225X 400	RC Slab	152	Fair	N/A
KD/03/02/S02	NA	2	3.00	9	3.00	1	7.5+ 2.4	1	RC	Cantilever step	Middle	225X 225	225X 300	225X 500	RC Slab	150	Fair	Plinth
KD/04/01/S02	NA	2	3.00	1 0	3.00	1	7.50	1	RC	Cantilever step	Corner	225X 225	225X 225	225X 500	RC Slab	150	Fair	Plinth
KD/04/02/S03	NA	3	3.00	1 0	3.00	1	7.75	1	RC	Cantilever step	Corner	300X 300	225X 225	225X 500	RC Slab	150	Fair	Plinth

Appendix A-4: Selected school building non-structural details

Table A-3. School building non-structural details

ID	Material of external walls	Typical wall thickness (X) (mm) (Internal)	Typical wall thickness (X) (mm) (External)	Opening type (Front)	Windows X direction (m) (Front)	Opening Type (Rear)	Windows X direction (m) (Rear)	Door X direction	Typical wall thickness Y direction (mm)	Typical wall thickness Y direction (mm)	Windows/external doors material	Roof Structural System (RC / Timber / Steel)	Roof Covering (Tiles/Metal Sheets/Bitumen)	Roof Pitch (Flat/Mono/Multi)	Roof Condition (Excellent/Fair/Poor)	Modifications (No/Extensions Storeys)
NU/01/01/S03	MI	115	115	CW	1.3X1.8	CW	1.3X1.8	1.0X2.7	115	115	Aluminium	Steel	Metal Sheets	Multi	Fair	No
NU/02/01/S02	MI	225	225	CW	1.0X1.6	CW	1.0X1.6	1.0X2.5	225	115	Aluminium	Steel	Asbastors Sheet	Multi	Fair	No
NU/02/02/S02	MI	225	225	CW	1.3X1.6	CW	1.3X1.6	1.0X2.5	225	115	Aluminium	Steel	Metal Sheets	Multi	Fair	Extension
NU/03/01/S02	MI	115	115	CW	1.8X1.25	CW	1.8X1.25	0.9X2.1	115	115	Timber	Steel	Asbastors Sheet	Multi	Fair	No
KU/01/01/S03	MI	115	115	HO	1.8X1.2	HO	1.8X1.2	0.9X2.0	225	225	Timber	Steel	Asbastors Sheet	Multi	Fair	No
BD/01/01/S02	MI	115	115	CW	1.8X1.2	CW	1.8X1.2	0.8X2.1	225	115	Timber	Timber	Tiles	Multi	Fair	No
BD/02/01/S02	MI	225	225	CW	1.8X1.2	CW	1.8X1.2	0.8X2.1	225	225	Timber	Timber	Tiles	Multi	Poor	No
BD/02/02/S02	MI	115	115	CW	1.8X1.2	CW	1.8X1.2	0.85X2.1	115	115	Aluminium	RC	RC	Flat	Fair	No
BD/03/01/S02	MI	115	115	CW	1.2X1.2	CW	1.2X1.2	0.85X2.1	115	115	Aluminium	Steel	Asbastors Sheet	Multi	Fair	No
BD/03/02/S03	MI	115	115	CW	2.2X1.2	CW	2.2X1.2	0.8X2.1	225	115	Aluminium	Steel	Metal Sheet	Multi	Fair	No

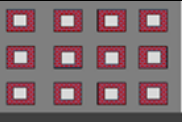
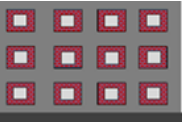
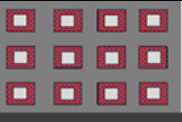
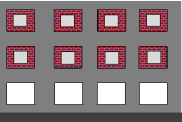
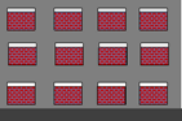
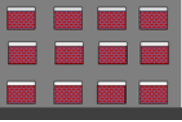
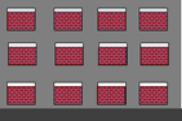
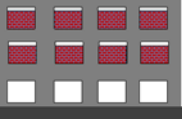
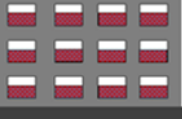
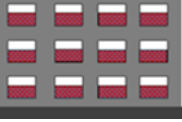
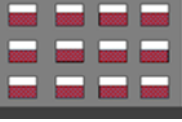
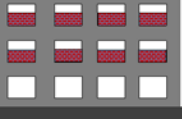
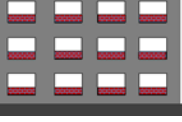
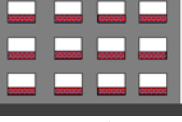
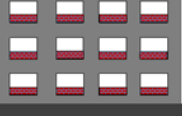
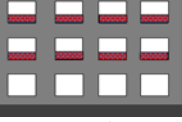
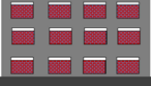
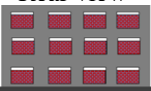
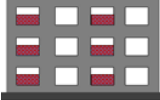
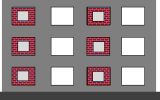
BD/03/03/S02	MI	225	225	HO	1.5X1.8	HO	1.5X1.8	0.95X2.4	225	225	Timber	Steel	Metal Sheet	Multi	Fair	No
BD/04/01/S03	MI	115	115	CW	1.25X1.8	CW	1.25X1.8	0.9X2.1	115	115	Timber	Steel	Asbastors Sheet	Multi	Excellent	No
BD/04/02/S03	MI	115	115	TO	2.25X2.0	TO	2.25X1.8	0.9X2.1	115	115	Steel	Steel	Asbastors Sheet	Multi	Excellent	No
MO/01/01/S02	MI	115	115	HO	2.7X1.3	HO	2.7X1.3	0.9X2.1	225	225	Aluminium	Steel	Asbastors Sheet	Multi	Excellent	No
AM/01/01/S02	MI	115	225	TO (FF)	2.7X2.0	HO	2.7X1.2	0.9X2.1	225	225	Timber	Steel	Tiles	Multi	Fair	No
AM/01/02/S02	MI	115	225	CW	2.7X1.3	CW	1.1X1.3	1.2X2.1	225	115	Aluminium	Steel	Tiles	Single	Excellent	No
AM/01/02/S02	MI	115	225	CW	1.8X2.1	CW	1.8X2.1	1.0X2.1	225	115	Aluminium	Steel	Asbastors Sheet	Multi	Excellent	No
AM/02/01/S02	MI	115	225	TO (FF)/CW(GF)	2.7X2.0	TO(FF), CW(GF)	2.5X1.8	1.0X2.1	225	115	Aluminium	Steel	Tiles	Multi	Fair	No
AM/02/02/S03	MI	115	225	TO (FF/SF)/CW(GF)	2.7X2.0 1.8X1.8	QO	1.8X0.8	0.85X2.0	225	115		Steel	Asbastors Sheet	Multi	Excellent	No
AM/03/01/S02	MI	225	225	CW	1.4X1.8	CW	1.4X1.8	1.0X2.5	225	225	Timber	Steel	Asbastors Sheet	Multi	Fair	No
AM/03/02/S02	MI	225	225	CW	1.5X1.8	CW	1.5X1.8	1.1X2.0	225	225		Timber	Tiles	Multi	Fair	No
AM/03/03/S02	MI	225	225	CW	1.5X1.8	CW	1.5X1.8	1.1X2.1	225	225	Aluminium	Steel	Tiles	Multi	Fair	No
AM/04/01/S02	MI	115	225	TO	3.0X2.3	HO	1.1X1.8	0.8X2.0	225	225	Aluminium	Steel	Metal Sheet	Multi	Fair	No
TR/01/01/S03	MI	115	115	HO	2.7X1.8	QO	2.7X0.8	1.0X2.1	115	115	Steel	Steel	Asbastors Sheet	Multi	Fair	No
TR/01/02/S03	MI	115	115	TO	2.7X2.3	CW	2.7X1.8	1.0X2.1	115	115	Steel	Steel	Asbastors Sheet	Multi	Excellent	No
TR/02/01/S03	MI	115	115	CW	1.8X1.2	CW	1.8X1.2	0.8X2.1	225	225	Timber	Timber	Asbastors Sheet	Multi	Fair	No

TR/02/02/S03	MI	115	115	TO	2.7X1.8	QO	2.7X0.8	0.8X2.1	225	225	Steel/Timber	Steel	Asbastors Sheet	Multi	Fair	No
TR/02/03/S03	MI	115	225	TO	2.7X1.8	QO	2.7X0.8	0.8X2.1	225	115	Steell	Steel	Asbastors Sheet	Multi	Fair	No
TR/03/01/S03	MI	115	225	CW	1.5X1.8	CW	1.5X1.8	1.0X2.1	225	225	Timber	Steel	Asbastors Sheet	Multi	Fair	No
TR/03/02/S02	MI	225	225	CW	1.5X1.8	CW	1.5X1.8	0.8X2.1	225	225	Aluminium	Timber	Tiles	Multi	Fair	No
JF/01/01/S03	MI	115	115	QO	2.7X1.2	QO	2.7X1.2	0.8X2.0	115	115	Steel	Timber	Asbastors Sheet	Multi	Fair	No
JF/01/02/S02	MI	115	115	CW	2.7X1.2	QO	2.7X1.2	0.8X2.0	115	115	Timber	Timber	Asbastors Sheet	Multi	Fair	No
JF/02/01/S02	MI	115	115	CW	1.5X1.2	CW	1.5X1.2	0.9X2.0	115	115	Timber	Timber	Tiles	Multi	Fair	No
KD/01/01/S02	MI	115	115	CW	1.8X1.2	CW	1.8X1.2	0.9X2.0	225	225	Aluminium	Steel	Asbastors Sheet	Multi	Fair	No
KD/01/02/S02	MI	115	115	CW	1.8X1.2	CW/ HO (GF)	1.8X1.2	0.9X2.1	115	115	Timber	Steel	Asbastors Sheet	Multi	Fair	No
KD/02/01/S02	MI	115	115	HO	2.4X1.5	CW	2.4X1.2	0.8X2.1	115	115	Timber	Steel	Asbastors Sheet	Multi	Fair	No
KD/03/01/S02	MI	115	115	CW	1.2X1.0	CW	1.2X1.0	0.9X2.1	115	115	Aluminium	Steel	Asbastors Sheet	Multi	Fair	No
KD/03/02/S02	MI	115	115	CW	1.2X1.0	CW	1.2X1.0	1.0X2.1	115	115	Aluminium	Steel	Asbastors Sheet	Multi	Fair	No
KD/04/01/S02	MI	115	115	CW	1.3X1.0	CW	1.3X1.0	0.9X2.4	115	115	Aluminium	Steel	Asbastors Sheet	Multi	Fair	No
KD/04/02/S03	MI	115	115	CW	1.3X1.1	CW	1.3X1.1	0.9X2.5	115	115	Aluminium	Steel	Asbastors Sheet	Multi	Fair	No

CW- Central window, HO- Half opening, QO- Quarter opening and TO- Three quarter opening (1m wall)

APPENDIX B: IDEAL CASES

Table B-1. T01 building with MI configurations

No	Case Name	Case Description	Symmetric Illustration	
			FGS	OGS
1	T01-S03- FGS(OGS)-SW (DW)-CW	T01 building with the CW presented cases in the adjacent storeys and SW/DW cases. (for OGS the GF has no MI)	 Front view  Rear view	 Front view  Rear view
2	T01-S03- FGS(OGS)-SW (DW)-QO	T01 building with the QO presented cases in the adjacent storeys and SW/DW cases. (for OGS the GF has no MI)	 Front view  Rear view	 Front view  Rear view
3	T01-S03- FGS(OGS)-SW (DW)-HO	T01 building with the HO presented cases in the adjacent storeys and SW/DW cases. (for OGS the GF has no MI)	 Front view  Rear view	 Front view  Rear view
4	T01-S03- FGS(OGS)-SW (DW)-TO	T01 building with the TO presented cases in the adjacent storeys and SW/DW cases. (for OGS the GF has no MI)	 Front view  Rear view	 Front view  Rear view
5	Similarly for T02 the similar MI configurations with the variation in middle frame where half opening cases (MHO) and central window cases (MCW) were considered			
	T02-S03- MHO(MCW)-SW (DW)-QO	 Rear view  Front view	 MHO	OR  MCW

APPENDIX C: OPENSEES AND MONTE CARLO SIMULATION CODING

B.1 OpenSees Coding

The OpenSees codes are shown for the T01-S03-FGS-DW-CW cases and similar criterial was followed and additional nodes were added whenever required to generate the models.

```
# -----
# Three story 3D building
# -----
wipe
set time_start [clock milliseconds]

puts "=====
puts "OpenSees Navigator: Version 2.5.8"
puts "File sourced: D:/Master's - UOM/OS - Model/OSN/Analysis/1.tcl"
puts "=====

puts "\n#####"
puts "# Analysis-Sequence 1 #"
puts "#####"
set tStart [clock clicks -milliseconds]

# -----
# A.1 Type of Model
# 3D Basic model
model BasicBuilder -ndm 3 -ndf 6
# -----
# Units mm, kN, ton
# Source files
source LibUnits.tcl
# -----
# Frame Section
set NStory 3; # number of stories above ground level
set NBayX 2; # number of bays in X direction
set NBayZ 2; # number of bays in Z direction
puts "Number of Stories in Y: $NStory; Number of bays in X: $NBayX; Number of bays in Z: $NBayZ"
# -----
# A.2 Nodes
# node nodeTag (ndm coords) <-mass (ndf massValues)>
#GF-Nodes
node 1 0.00 0.00 0.00 -ndf 6
node 2 3.00 0.00 0.00 -ndf 6
node 3 6.00 0.00 0.00 -ndf 6
node 4 9.00 0.00 0.00 -ndf 6
node 5 12.00 0.00 0.00 -ndf 6
node 6 15.00 0.00 0.00 -ndf 6
node 7 18.00 0.00 0.00 -ndf 6
node 8 21.00 0.00 0.00 -ndf 6
node 9 24.00 0.00 0.00 -ndf 6
node 10 27.00 0.00 0.00 -ndf 6

node 11 0.00 7.50 0.00 -ndf 6
node 12 3.00 7.50 0.00 -ndf 6
node 13 6.00 7.50 0.00 -ndf 6
node 14 9.00 7.50 0.00 -ndf 6
node 15 12.00 7.50 0.00 -ndf 6
node 16 15.00 7.50 0.00 -ndf 6
node 17 18.00 7.50 0.00 -ndf 6
node 18 21.00 7.50 0.00 -ndf 6
node 19 24.00 7.50 0.00 -ndf 6
node 20 27.00 7.50 0.00 -ndf 6

#FF-Nodes
node 21 0.00 0.00 3.00 -ndf 6
node 22 3.00 0.00 3.00 -ndf 6
node 23 6.00 0.00 3.00 -ndf 6
node 24 9.00 0.00 3.00 -ndf 6
node 25 12.00 0.00 3.00 -ndf 6
node 26 15.00 0.00 3.00 -ndf 6
```

```

node 27 18.00 0.00 3.00 -ndf 6
node 28 21.00 0.00 3.00 -ndf 6
node 29 24.00 0.00 3.00 -ndf 6
node 30 27.00 0.00 3.00 -ndf 6

node 31 0.00 7.50 3.00 -ndf 6
node 32 3.00 7.50 3.00 -ndf 6
node 33 6.00 7.50 3.00 -ndf 6
node 34 9.00 7.50 3.00 -ndf 6
node 35 12.00 7.50 3.00 -ndf 6
node 36 15.00 7.50 3.00 -ndf 6
node 37 18.00 7.50 3.00 -ndf 6
node 38 21.00 7.50 3.00 -ndf 6
node 39 24.00 7.50 3.00 -ndf 6
node 40 27.00 7.50 3.00 -ndf 6

#SF-Nodes
node 41 0.00 0.00 6.00 -ndf 6
node 42 3.00 0.00 6.00 -ndf 6
node 43 6.00 0.00 6.00 -ndf 6
node 44 9.00 0.00 6.00 -ndf 6
node 45 12.00 0.00 6.00 -ndf 6
node 46 15.00 0.00 6.00 -ndf 6
node 47 18.00 0.00 6.00 -ndf 6
node 48 21.00 0.00 6.00 -ndf 6
node 49 24.00 0.00 6.00 -ndf 6
node 50 27.00 0.00 6.00 -ndf 6

node 51 0.00 7.50 6.00 -ndf 6
node 52 3.00 7.50 6.00 -ndf 6
node 53 6.00 7.50 6.00 -ndf 6
node 54 9.00 7.50 6.00 -ndf 6
node 55 12.00 7.50 6.00 -ndf 6
node 56 15.00 7.50 6.00 -ndf 6
node 57 18.00 7.50 6.00 -ndf 6
node 58 21.00 7.50 6.00 -ndf 6
node 59 24.00 7.50 6.00 -ndf 6
node 60 27.00 7.50 6.00 -ndf 6

#Roof-Nodes
node 61 0.00 0.00 9.00 -ndf 6
node 62 3.00 0.00 9.00 -ndf 6
node 63 6.00 0.00 9.00 -ndf 6
node 64 9.00 0.00 9.00 -ndf 6
node 65 12.00 0.00 9.00 -ndf 6
node 66 15.00 0.00 9.00 -ndf 6
node 67 18.00 0.00 9.00 -ndf 6
node 68 21.00 0.00 9.00 -ndf 6
node 69 24.00 0.00 9.00 -ndf 6
node 70 27.00 0.00 9.00 -ndf 6

node 71 0.00 7.50 9.00 -ndf 6
node 72 3.00 7.50 9.00 -ndf 6
node 73 6.00 7.50 9.00 -ndf 6
node 74 9.00 7.50 9.00 -ndf 6
node 75 12.00 7.50 9.00 -ndf 6
node 76 15.00 7.50 9.00 -ndf 6
node 77 18.00 7.50 9.00 -ndf 6
node 78 21.00 7.50 9.00 -ndf 6
node 79 24.00 7.50 9.00 -ndf 6
node 80 27.00 7.50 9.00 -ndf 6

# Master Nodes
node 100 13.50 3.75 3.00 -ndf 6; # Master Node - GF
node 200 13.50 3.75 6.00 -ndf 6; # Master Node - FF
node 300 13.50 3.75 9.00 -ndf 6; # Master Node - SF

```

puts "Coordnates have been created"

```

#-----
# A.3 Restraints
## Single point constraints - SPC
# fix $nodeTag (ndf $constrValues)
# SPC tag Dx Dy Dz Rx Ry Rz
# Frame - 1
fix 1 1 1 1 1 1 1
fix 2 1 1 1 1 1 1
fix 3 1 1 1 1 1 1
fix 4 1 1 1 1 1 1
fix 5 1 1 1 1 1 1
fix 6 1 1 1 1 1 1

```

```

fix 7 1 1 1 1 1 1
fix 8 1 1 1 1 1 1
fix 9 1 1 1 1 1 1
fix 10 1 1 1 1 1 1

#Frame - 2
fix 11 1 1 1 1 1 1
fix 12 1 1 1 1 1 1
fix 13 1 1 1 1 1 1
fix 14 1 1 1 1 1 1
fix 15 1 1 1 1 1 1
fix 16 1 1 1 1 1 1
fix 17 1 1 1 1 1 1
fix 18 1 1 1 1 1 1
fix 19 1 1 1 1 1 1
fix 20 1 1 1 1 1 1

# MPCConstraint.tcl
# Master Nodes
fix 100 0 0 1 1 1 0
fix 200 0 0 1 1 1 0
fix 300 0 0 1 1 1 0

## Multi point constraints - MPC
# Rigid Diaphragm: MPCConstraint01: perpDir mNodeTag sNodeTags
rigidDiaphragm 3 100 21 22 23 24 25 26 27 28 29 30 31 32 33 34 35 36 37 38 39 40
rigidDiaphragm 3 200 41 42 43 44 45 46 47 48 49 50 51 52 53 54 55 56 57 58 59 60
rigidDiaphragm 3 300 61 62 63 64 65 66 67 68 69 70 71 72 73 74 75 76 77 78 79 80

## NodeMass.tcl
# Node tag mx my mz mlx mly mlz
mass 100 481.00 481.00 0.00 0.00 0.00 0.00
mass 200 481.00 481.00 0.00 0.00 0.00 0.00
mass 300 197.00 197.00 0.00 0.00 0.00 0.00

puts "Restraints have been created"

#-----
# Materials.tcl

#uniaxialMaterial Concrete01 matTag fpc epsc0 fpcu epsU
#Concrete
uniaxialMaterial Concrete01 11 -22000 -0.003 -1500 -0.0132; #Core
uniaxialMaterial Concrete01 10 -20000 -0.0025 -1500 -0.0062; #Cover

#R/F
#uniaxialMaterial Steel01 matTag Fy E0 b <a1 a2 a3 a4>
uniaxialMaterial Steel01 21 460000 200000000 0.005 0.0 1.0 0.0 1.0

# Wall
uniaxialMaterial Concrete01 31 -1500 -0.003 -1200 -0.0038

puts "Materials have been created"

#-----
# A.5 Section
# Fiber Section

#the geometry of the patch is defined by four vertices: I J K L. The coordinates of each of the four vertices is specified in COUNTER CLOCKWISE
sequence https://opensees.berkeley.edu/wiki/index.php/File:QuadPatch.gif

set Asc16 [expr 3.14*16*$mm*16*$mm/4]; # dia 16 mm Column
set Asc20 [expr 3.14*20*$mm*20*$mm/4]; # dia 20 mm Column
set Asc25 [expr 3.14*25*$mm*25*$mm/4]; # dia 25 mm Column

# Section 6 - (225*225) - 4Y16 - Column
#Torsional constant calculation for torsional stiffness GJ ( Reference: https://en.wikipedia.org/wiki/Torsion\_constant )
set a1 [expr max(225*$mm, 225*$mm)]
set b1 [expr min(225*$mm, 225*$mm)]
set J1 [expr $a1*pow($b1,3)*(16/3-3.36*($b1/$a1)*(1-pow($b1,4)/(12*pow($a1,4)))]
set Gc1 21000000;

# Column (225X225) - 4Y20
section Fiber 100 -GJ [expr $Gc1*$J1] {
#patch quad matTag numSubdivIJ numSubdivJK yI zI yJ zJ yK zK yL zL
patch quad 11 10 10 -8.750000E-02 +8.750000E-02 -8.750000E-02 -8.750000E-02 +8.750000E-02 -8.750000E-02 +8.750000E-02
+8.750000E-02; #Patch 01
patch quad 10 3 10 -1.130000E-01 +1.130000E-01 -8.750000E-02 +8.750000E-02 +8.750000E-02 +8.750000E-02 +1.130000E-01
+1.130000E-01; #Patch 02
patch quad 10 3 10 -8.750000E-02 -8.750000E-02 -1.130000E-01 -1.130000E-01 +1.130000E-01 -1.130000E-01 +8.750000E-02
-8.750000E-02; #Patch 03

```

```

    patch quad 10 10 3 -1.130000E-01 +1.130000E-01 -1.130000E-01 -1.130000E-01 -8.750000E-02 -8.750000E-02 -8.750000E-02
+8.750000E-02 ; #Patch 04
    patch quad 10 10 3 +8.750000E-02 +8.750000E-02 +8.750000E-02 -8.750000E-02 +1.130000E-01 -1.130000E-01 +1.130000E-
01 +1.130000E-01 ; #Patch 05

    # Layer Straight matTag numBar areaBar yStart zStart yEnd zEnd
    layer straight 21 2 [expr $Ascol20] -8.750000E-02 +8.750000E-02 -8.750000E-02 -8.750000E-02 ; #Bottom Layer
    layer straight 21 2 [expr $Ascol20] +8.750000E-02 +8.750000E-02 +8.750000E-02 -8.750000E-02 ; #Top Layer
}

#Torsional constant calculation for torsional stiffness GJ ( Reference: https://en.wikipedia.org/wiki/Torsion_constant )
set a2 [expr max(225*$mm, 300*$mm)]
set b2 [expr min(225*$mm, 300*$mm)]
set J2 [expr $a2*pow($b2,3)*(16/3-3.36*($b2/$a2)*(1-pow($b2,4)/(12*pow($a2,4))))]
set Gc2 11165735.8;

#Beam_X (300X225) - 4Y16
section Fiber 200 -GJ [expr $Gc2*$J2] {
    #patch quad matTag numSubdivIJ numSubdivJK yI zI yJ zJ yK zK yL zL
    patch quad 11 10 10 -1.250000E-01 +8.750000E-02 -1.250000E-01 -8.750000E-02 +1.250000E-01 -8.750000E-02 +1.250000E-01
+8.750000E-02 ; #Patch 01
    patch quad 10 3 10 -1.500000E-01 +1.130000E-01 -1.250000E-01 +8.750000E-02 +1.250000E-01 +8.750000E-02 +1.500000E-
01 +1.130000E-01 ; #Patch 02
    patch quad 10 3 10 -1.250000E-01 -8.750000E-02 -1.500000E-01 -1.130000E-01 +1.500000E-01 -1.130000E-01 +1.250000E-01
-8.750000E-02 ; #Patch 03
    patch quad 10 10 3 -1.500000E-01 +1.130000E-01 -1.500000E-01 -1.130000E-01 -1.250000E-01 -8.750000E-02 -1.250000E-01
+8.750000E-02 ; #Patch 04
    patch quad 10 10 3 +1.250000E-01 +8.750000E-02 +1.250000E-01 -8.750000E-02 +1.500000E-01 -1.130000E-01 +1.500000E-
01 +1.130000E-01 ; #Patch 05

    # Layer Straight matTag numBar areaBar yStart zStart yEnd zEnd
    layer straight 21 2 [expr $Ascol16] -1.250000E-01 +8.750000E-02 -1.250000E-01 -8.750000E-02 ; #Bottom Layer
    layer straight 21 2 [expr $Ascol16] +1.250000E-01 +8.750000E-02 +1.250000E-01 -8.750000E-02 ; #Top Layer
}

#Beam_Y (525*225) 2Y16 3Y25:
#Torsional constant calculation for torsional stiffness GJ ( Reference: https://en.wikipedia.org/wiki/Torsion_constant )
set a4 [expr max(525*$mm, 225*$mm)]
set b4 [expr min(525*$mm, 225*$mm)]
set J4 [expr $a4*pow($b4,3)*(16/3-3.36*($b4/$a4)*(1-pow($b4,4)/(12*pow($a4,4))))]
set Gc4 11165735.8;

section Fiber 300 -GJ [expr $Gc4*$J4] {
    #patch quad matTag numSubdivIJ numSubdivJK yI zI yJ zJ yK zK yL zL
    patch quad 11 10 10 -2.500000E-01 +8.750000E-02 -2.500000E-01 -8.750000E-02 +2.500000E-01 -8.750000E-02 +2.500000E-01
+8.750000E-02 ; #Patch 01
    patch quad 10 3 10 -2.750000E-01 +1.130000E-01 -2.500000E-01 +8.750000E-02 +2.500000E-01 +8.750000E-02 +2.750000E-
01 +1.130000E-01 ; #Patch 02
    patch quad 10 3 10 -2.500000E-01 -8.750000E-02 -2.750000E-01 -1.130000E-01 +2.750000E-01 -1.130000E-01 +2.500000E-01
-8.750000E-02 ; #Patch 03
    patch quad 10 10 3 -2.750000E-01 +1.130000E-01 -2.750000E-01 -1.130000E-01 -2.500000E-01 -8.750000E-02 -2.500000E-01
+8.750000E-02 ; #Patch 04
    patch quad 10 10 3 +2.500000E-01 +8.750000E-02 +2.500000E-01 -8.750000E-02 +2.750000E-01 -1.130000E-01 +2.750000E-
01 +1.130000E-01 ; #Patch 05

    # Layer Straight matTag numBar areaBar yStart zStart yEnd zEnd
    layer straight 21 3 [expr $Ascol25] -2.500000E-01 +8.750000E-02 -2.500000E-01 -8.750000E-02 ; #Bottom Layer
    layer straight 21 2 [expr $Ascol16] +2.500000E-01 +8.750000E-02 +2.500000E-01 -8.750000E-02 ; #Top Layer
}

puts "Fiber sections have been created"

#-----
# A6. Elements
set IDColTransf1
set IDBeamXTransf 2
set IDBeamYTransf 3
# geomTransf Corotational transfTag vecxzX vecxzY vecxzZ
geomTransf Corotational $IDColTransf 0 1 0;
geomTransf Corotational $IDBeamXTransf 0 -1 0;
geomTransf Corotational $IDBeamYTransf -1 0 0;

#Define Beam-Column Elements
set np 5; # number of Gauss integration points for nonlinear curvature distribution-- np=2 for linear distribution ok

#GColumns
# Element : eleTag NodeI NodeJ NIP secTag geoTranTag <-mass massDens> <-iter maxIters tol>
element forceBeamColumn 1 1 21 np 100 $IDColTransf -mass 0.00 -iter 10 +1.00E-12 -integration Lobatto
element forceBeamColumn 2 2 22 np 100 $IDColTransf -mass 0.00 -iter 10 +1.00E-12 -integration Lobatto

```


element	corotTruss	157	61	42	0.0585	31	-rho	0.00	-cMass	0.00	-doRayleigh	0.00
element	corotTruss	158	62	43	0.0585	31	-rho	0.00	-cMass	0.00	-doRayleigh	0.00
element	corotTruss	159	63	44	0.0585	31	-rho	0.00	-cMass	0.00	-doRayleigh	0.00
element	corotTruss	160	64	45	0.0585	31	-rho	0.00	-cMass	0.00	-doRayleigh	0.00
element	corotTruss	161	65	46	0.0585	31	-rho	0.00	-cMass	0.00	-doRayleigh	0.00
element	corotTruss	162	66	47	0.0585	31	-rho	0.00	-cMass	0.00	-doRayleigh	0.00
element	corotTruss	163	67	48	0.0585	31	-rho	0.00	-cMass	0.00	-doRayleigh	0.00
element	corotTruss	164	68	49	0.0585	31	-rho	0.00	-cMass	0.00	-doRayleigh	0.00
element	corotTruss	165	69	50	0.0585	31	-rho	0.00	-cMass	0.00	-doRayleigh	0.00
element	corotTruss	166	71	52	0.0585	31	-rho	0.00	-cMass	0.00	-doRayleigh	0.00
element	corotTruss	167	72	53	0.0585	31	-rho	0.00	-cMass	0.00	-doRayleigh	0.00
element	corotTruss	168	73	54	0.0585	31	-rho	0.00	-cMass	0.00	-doRayleigh	0.00
element	corotTruss	169	74	55	0.0585	31	-rho	0.00	-cMass	0.00	-doRayleigh	0.00
element	corotTruss	170	75	56	0.0585	31	-rho	0.00	-cMass	0.00	-doRayleigh	0.00
element	corotTruss	171	76	57	0.0585	31	-rho	0.00	-cMass	0.00	-doRayleigh	0.00
element	corotTruss	172	77	58	0.0585	31	-rho	0.00	-cMass	0.00	-doRayleigh	0.00
element	corotTruss	173	78	59	0.0585	31	-rho	0.00	-cMass	0.00	-doRayleigh	0.00
element	corotTruss	174	79	60	0.0585	31	-rho	0.00	-cMass	0.00	-doRayleigh	0.00
element	corotTruss	179	31	12	0.0585	31	-rho	0.00	-cMass	0.00	-doRayleigh	0.00
element	corotTruss	180	32	13	0.0585	31	-rho	0.00	-cMass	0.00	-doRayleigh	0.00
element	corotTruss	181	33	14	0.0585	31	-rho	0.00	-cMass	0.00	-doRayleigh	0.00
element	corotTruss	182	34	15	0.0585	31	-rho	0.00	-cMass	0.00	-doRayleigh	0.00
element	corotTruss	183	35	16	0.0585	31	-rho	0.00	-cMass	0.00	-doRayleigh	0.00
element	corotTruss	184	36	17	0.0585	31	-rho	0.00	-cMass	0.00	-doRayleigh	0.00
element	corotTruss	185	37	18	0.0585	31	-rho	0.00	-cMass	0.00	-doRayleigh	0.00
element	corotTruss	186	38	19	0.0585	31	-rho	0.00	-cMass	0.00	-doRayleigh	0.00
element	corotTruss	187	39	20	0.0585	31	-rho	0.00	-cMass	0.00	-doRayleigh	0.00
element	corotTruss	188	20	30	0.0585	31	-rho	0.00	-cMass	0.00	-doRayleigh	0.00
element	corotTruss	190	21	2	0.0585	31	-rho	0.00	-cMass	0.00	-doRayleigh	0.00
element	corotTruss	191	22	3	0.0585	31	-rho	0.00	-cMass	0.00	-doRayleigh	0.00
element	corotTruss	192	23	4	0.0585	31	-rho	0.00	-cMass	0.00	-doRayleigh	0.00
element	corotTruss	193	24	5	0.0585	31	-rho	0.00	-cMass	0.00	-doRayleigh	0.00
element	corotTruss	194	26	7	0.0585	31	-rho	0.00	-cMass	0.00	-doRayleigh	0.00
element	corotTruss	195	27	8	0.0585	31	-rho	0.00	-cMass	0.00	-doRayleigh	0.00
element	corotTruss	196	28	9	0.0585	31	-rho	0.00	-cMass	0.00	-doRayleigh	0.00
element	corotTruss	197	29	10	0.0585	31	-rho	0.00	-cMass	0.00	-doRayleigh	0.00

#Full Wall corotatinal truss (Y-Direction) - 225 mm

# element	eleTag	NodeI	NodeJ	A	matTag	<-rho rho>	<-cMass flag>	<-doRayleigh flag>				
element	corotTruss	175	31	41	0.169	31	-rho	0.00	-cMass	0.00	-doRayleigh	0.00
element	corotTruss	176	51	61	0.169	31	-rho	0.00	-cMass	0.00	-doRayleigh	0.00
element	corotTruss	177	40	50	0.169	31	-rho	0.00	-cMass	0.00	-doRayleigh	0.00
element	corotTruss	178	60	70	0.169	31	-rho	0.00	-cMass	0.00	-doRayleigh	0.00
element	corotTruss	188	11	21	0.169	31	-rho	0.00	-cMass	0.00	-doRayleigh	0.00
element	corotTruss	189	20	30	0.169	31	-rho	0.00	-cMass	0.00	-doRayleigh	0.00

puts "Elements have been created"

#-----

A.7 LoadPattern

LoadPattern "LoadPatterngravity": patternTag tsTag factor

Element

pattern Plain 1 Linear -fact +1.00 {

# eleLoad	eleTags	beamUniform	Wy	Wz	<Wx>				
eleLoad	-ele		61	-type	-beamUniform	-23.10	0.00	0.00	
eleLoad	-ele		62	-type	-beamUniform	-23.10	0.00	0.00	
eleLoad	-ele		63	-type	-beamUniform	-31.20	0.00	0.00	
eleLoad	-ele		64	-type	-beamUniform	-23.10	0.00	0.00	
eleLoad	-ele		65	-type	-beamUniform	-31.20	0.00	0.00	
eleLoad	-ele		66	-type	-beamUniform	-31.20	0.00	0.00	
eleLoad	-ele		67	-type	-beamUniform	-23.10	0.00	0.00	
eleLoad	-ele		68	-type	-beamUniform	-31.20	0.00	0.00	
eleLoad	-ele		69	-type	-beamUniform	-23.10	0.00	0.00	
eleLoad	-ele		70	-type	-beamUniform	-23.10	0.00	0.00	
eleLoad	-ele		71	-type	-beamUniform	-23.10	0.00	0.00	
eleLoad	-ele		72	-type	-beamUniform	-23.10	0.00	0.00	
eleLoad	-ele		73	-type	-beamUniform	-31.20	0.00	0.00	
eleLoad	-ele		74	-type	-beamUniform	-23.10	0.00	0.00	
eleLoad	-ele		75	-type	-beamUniform	-31.20	0.00	0.00	
eleLoad	-ele		76	-type	-beamUniform	-31.20	0.00	0.00	
eleLoad	-ele		77	-type	-beamUniform	-23.10	0.00	0.00	
eleLoad	-ele		78	-type	-beamUniform	-31.20	0.00	0.00	
eleLoad	-ele		79	-type	-beamUniform	-23.10	0.00	0.00	
eleLoad	-ele		80	-type	-beamUniform	-23.10	0.00	0.00	
eleLoad	-ele		91	-type	-beamUniform	-9.60	0.00	0.00	
eleLoad	-ele		92	-type	-beamUniform	-9.60	0.00	0.00	
eleLoad	-ele		93	-type	-beamUniform	-9.60	0.00	0.00	
eleLoad	-ele		94	-type	-beamUniform	-9.60	0.00	0.00	
eleLoad	-ele		95	-type	-beamUniform	-9.60	0.00	0.00	
eleLoad	-ele		96	-type	-beamUniform	-9.60	0.00	0.00	
eleLoad	-ele		97	-type	-beamUniform	-9.60	0.00	0.00	

```

eleLoad -ele      98      -type      -beamUniform      -9.60      0.00      0.00
eleLoad -ele      99      -type      -beamUniform      -9.60      0.00      0.00
eleLoad -ele     100      -type      -beamUniform      -9.60      0.00      0.00
eleLoad -ele     101      -type      -beamUniform      -9.60      0.00      0.00
eleLoad -ele     102      -type      -beamUniform      -9.60      0.00      0.00
eleLoad -ele     103      -type      -beamUniform      -9.60      0.00      0.00
eleLoad -ele     104      -type      -beamUniform      -9.60      0.00      0.00
eleLoad -ele     105      -type      -beamUniform      -9.60      0.00      0.00
eleLoad -ele     106      -type      -beamUniform      -9.60      0.00      0.00
eleLoad -ele     107      -type      -beamUniform      -9.60      0.00      0.00
eleLoad -ele     108      -type      -beamUniform      -9.60      0.00      0.00
eleLoad -ele     109      -type      -beamUniform      -9.60      0.00      0.00
eleLoad -ele     110      -type      -beamUniform      -9.60      0.00      0.00
eleLoad -ele     111      -type      -beamUniform      -9.60      0.00      0.00
eleLoad -ele     112      -type      -beamUniform      -9.60      0.00      0.00
eleLoad -ele     113      -type      -beamUniform      -9.60      0.00      0.00
eleLoad -ele     114      -type      -beamUniform      -9.60      0.00      0.00
eleLoad -ele     115      -type      -beamUniform      -9.60      0.00      0.00
eleLoad -ele     116      -type      -beamUniform      -9.60      0.00      0.00
eleLoad -ele     117      -type      -beamUniform      -9.60      0.00      0.00
eleLoad -ele     118      -type      -beamUniform      -9.60      0.00      0.00
eleLoad -ele     119      -type      -beamUniform      -9.60      0.00      0.00
eleLoad -ele     120      -type      -beamUniform      -9.60      0.00      0.00
eleLoad -ele     121      -type      -beamUniform      -9.60      0.00      0.00
eleLoad -ele     122      -type      -beamUniform      -9.60      0.00      0.00
eleLoad -ele     123      -type      -beamUniform      -9.60      0.00      0.00
eleLoad -ele     124      -type      -beamUniform      -9.60      0.00      0.00
eleLoad -ele     125      -type      -beamUniform      -9.60      0.00      0.00
eleLoad -ele     126      -type      -beamUniform      -9.60      0.00      0.00
eleLoad -ele     127      -type      -beamUniform      -3.60      0.00      0.00
eleLoad -ele     128      -type      -beamUniform      -3.60      0.00      0.00
eleLoad -ele     129      -type      -beamUniform      -3.60      0.00      0.00
eleLoad -ele     130      -type      -beamUniform      -3.60      0.00      0.00
eleLoad -ele     131      -type      -beamUniform      -3.60      0.00      0.00
eleLoad -ele     132      -type      -beamUniform      -3.60      0.00      0.00
eleLoad -ele     133      -type      -beamUniform      -3.60      0.00      0.00
eleLoad -ele     134      -type      -beamUniform      -3.60      0.00      0.00
eleLoad -ele     135      -type      -beamUniform      -3.60      0.00      0.00
eleLoad -ele     136      -type      -beamUniform      -3.60      0.00      0.00
eleLoad -ele     137      -type      -beamUniform      -3.60      0.00      0.00
eleLoad -ele     138      -type      -beamUniform      -3.60      0.00      0.00
eleLoad -ele     139      -type      -beamUniform      -3.60      0.00      0.00
eleLoad -ele     140      -type      -beamUniform      -3.60      0.00      0.00
eleLoad -ele     141      -type      -beamUniform      -3.60      0.00      0.00
eleLoad -ele     142      -type      -beamUniform      -3.60      0.00      0.00
eleLoad -ele     143      -type      -beamUniform      -3.60      0.00      0.00
eleLoad -ele     144      -type      -beamUniform      -3.60      0.00      0.00
eleLoad -ele      81      -type      -beamUniform      -3.60      0.00      0.00
eleLoad -ele      82      -type      -beamUniform      -3.60      0.00      0.00
eleLoad -ele      83      -type      -beamUniform      -3.60      0.00      0.00
eleLoad -ele      84      -type      -beamUniform      -3.60      0.00      0.00
}

# LoadPattern "PushoverX": patternTag tsTag factor
pattern Plain 2 3 -fact+1.000000E+00 {
  # Load nodeTag LoadValues
  load 100 +0.50 0.00 0.00 0.00 0.00
  load 200 +0.87 0.00 0.00 0.00 0.00
  load 300 +1.00 0.00 0.00 0.00 0.00
}

puts "Load Patterns have been created"
#-----
# A.8 Time Series
# TimeSeries "Gravity": tsTag cFactor
timeSeries Constant 2 -factor +1.00
# TimeSeries "Pushover": tsTag cFactor
timeSeries Linear 4 -factor +1.00

#-----
# B1. Recorders - Model Analysis
# BeamColumn Recorder: fileName <eleTag> arguments
recorder Node -file EigenDefaultCase_Node_EigenVectors_EigenVec_1.out -time -node 100 200 300 -dof 1 2 eigen1
recorder Node -file EigenDefaultCase_Node_EigenVectors_EigenVec_2.out -time -node 100 200 300 -dof 1 2 eigen2
recorder Node -file EigenDefaultCase_Node_EigenVectors_EigenVec_3.out -time -node 100 200 300 -dof 1 2 eigen3

#-----
#C1. Modal Analysis
constraints Transformation ; # Constraint Handler

```

```

numberer Plain ;           # DOF Numberer
system UmfPack -lvalueFact 10 ; # System of Equations
test NormDispIncr +1.00E-12 25 ; # Convergence Test
algorithm Newton ;        # Solution Algorithm
integrator Newmark +0.5 +0.25 ; # Integrator
analysis Transient ;      # Analysis Type

set pi [expr acos(-1.0)]
set eigFID [open EigenDefaultCase_Node_EigenVectors_EigenVal.out w]
set lambda [eigen -fullGenLapack 3]
puts $eigFID " lambda      omega      period      frequency"
foreach lambda $lambda {
    set omega [expr sqrt($lambda)]
    set period [expr 2.0*$pi/$omega]
    set frequ [expr 1.0/$period]
    puts $eigFID [format "%+1.6e %+1.6e %+1.6e %+1.6e" $lambda $omega $period $frequ]
}
close $eigFID
set tStop [clock clicks -milliseconds]
puts "o Time taken: [expr ($tStop-$tStart)/1000.0] sec"

wipe
set time_end [clock milliseconds]
set elapsed [expr ($time_end - $time_start)/1000.0]
puts "Elapsed time: $elapsed sec."
exit

#-----
#B.2 Gravity and Pushover recorders
recorder Node -file PushoverX_Node_BaseShearX_RFrc.out -time -node 1 2 3 4 5 6 7 8 9 10 11 12 13 14 15 16 17 18 19 20 -
-dof 1 reaction
recorder Node -file PushoverX_Node_DisplacementX_Dsp.out -time -node 89 100 101 -dof 1 disp

#-----
# D.1 Analysis Parameters
# Gravity Analysis -- load-controlled static analysis
puts "Gravity Analysis"
set Tol 1.0e-6;           # convergence tolerance for test
variable constraintsTypeGravity Transformation; # default;
constraints $constraintsTypeGravity ; # how it handles boundary conditions
numberer RCM;            # renumber dof's to minimize band-width (optimization), if you want to
system BandGeneral ;     # how to store and solve the system of equations in the analysis (large model: try UmfPack)
test NormDispIncr $Tol 30 ; # determine if convergence has been achieved at the end of an iteration step
algorithm Newton;        # use Newton's solution algorithm: updates tangent stiffness at every iteration
set NstepGravity 10;     # apply gravity in 100 steps
set DGravity [expr 1./$NstepGravity]; # first load increment;
integrator LoadControl $DGravity; # determine the next time step for an analysis
analysis Static;         # define type of analysis static or transient
analyze $NstepGravity;   # apply gravity
#----- maintain constant gravity loads and reset time to zero
loadConst -time 0.0;     # hold gravity constant and restart time

puts "Model Built"

wipeAnalysis

#-----
# D.1 Analysis Parameters
# Gravity Analysis -- load-controlled static analysis
constraints Transformation
numberer RCM
system BandGeneral
test EnergyIncr +1.00E-03 2500
algorithm KrylovNewton
integrator DisplacementControl 300 1 +0.0001
analysis Static

puts "Analysis Completed"
#-----

B.2 Monte- Carlo Simulation (MATLAB)
%%Monte Carlo Simulation – Material Uncertainty
%% Data Analysis
%Clear the work Space
clc;
clear;

%-----

```

```

Define Concrete, Steel and Masonry Variables
Concrete - mu= 20 MPa, COV = 15% sigma = 3
Steel - mu= 460 MPa, COV = 5% sigma = 23
Masonry - mu= 1.5 MPa, COV = 30% sigma = 0.45
concrete = normrnd(20,3,100,1);

% -----
%rng('default') % For reproducibility
m = 460;
v = 10;
mu = log((m^2)/sqrt(v+m^2));
sigma = sqrt(log(v/(m^2)+1));
steel = lognrnd(mu,sigma,[100,1]);

% -----
masonry = normrnd(1.5,0.45,100,1);

%% Distribution Graph
figure
subplot (1,3,1)
histfit(concrete)
subplot (1,3,2)
histfit(steel)
subplot (1,3,3)
histfit(masonry)

```

APPENDIX D: ADAPTATION OF SCORE MODIFIERS

Table D-1. Open Ground Storey effects

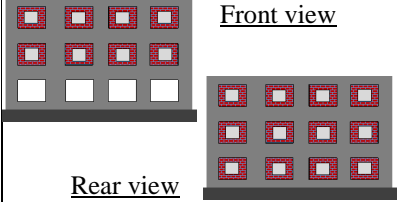
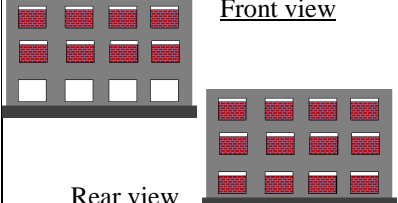
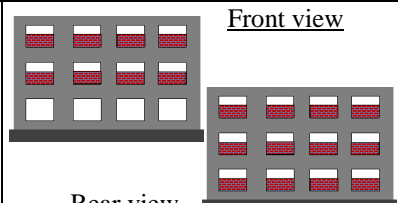
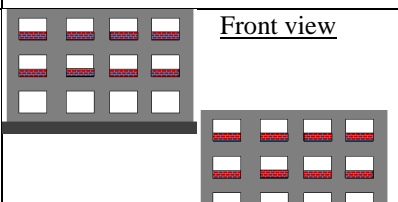
No	Case Name	Case Description	Symmetric Illustration
1	T01/T02-DW/SW-OGS-CW	T01/T02 building with the CW presented cases in the adjacent storeys and SW/DW cases	
2	T01/T02-DW/SW-OGS-QO	T01/T02 building with the QO presented cases in the adjacent storeys and SW/DW cases	
3	T01/T02-DW/SW-OGS-HO	T01/T02 building with the HO presented cases in the adjacent storeys and SW/DW cases	
4	T01/T02-DW/SW-OGS-TO	T01/T02 building with the TO presented cases in the adjacent storeys and SW/DW cases	

Table D-2. T01 Score modifiers for Open Ground Storey DW cases

Typologies	Specifications	District	Median	P[ds]	Equivalent Score	Basic Score	Score Modifier
T01	DW-CW	Zone-I	68	0.02	2.00	2.7	-0.7
		Zone-II	68	0.01	2.30	3.0	-0.7
		Zone-III	68	0.006	2.52	3.3	-0.8
	DW-QO	Zone-I	66	0.01	2.30	2.7	-0.4
		Zone-II	66	0.006	2.52	3.0	-0.5
		Zone-III	66	0.003	2.82	3.3	-0.5
	DW-HO	Zone-I	67	0.02	2.00	2.7	-0.7
		Zone-II	67	0.01	2.30	3.0	-0.7
		Zone-III	67	0.003	2.82	3.3	-0.5
	DW-TO	Zone-I	63	0.03	1.82	2.7	-0.9
		Zone-II	63	0.015	2.12	3.0	-0.9
		Zone-III	63	0.004	2.70	3.3	-0.6

Table D-3. T01 Score modifiers for Open Ground Storey SW cases

Typologies	Specifications	District	Median	P[ds]	Equivalent Score	Basic Score	Score Modifier
T01	SW-CW	Zone-I	68	0.04	2.00	2.7	-0.7
		Zone-II	68	0.02	2.30	3.0	-0.7
		Zone-III	68	0.008	2.70	3.3	-0.6
	SW-QO	Zone-I	66	0.02	2.30	2.7	-0.4
		Zone-II	66	0.008	2.70	3.0	-0.3
		Zone-III	66	0.004	3.00	3.3	-0.3
	SW-HO	Zone-I	67	0.035	2.06	2.7	-0.7
		Zone-II	67	0.02	2.30	3.0	-0.7
		Zone-III	67	0.01	2.60	3.3	-0.7
	SW-TO	Zone-I	63	0.05	1.90	2.7	-0.8
		Zone-II	63	0.02	2.30	3.0	-0.7
		Zone-III	63	0.009	2.65	3.3	-0.6

Table D-4. T02 Score modifiers for Open Ground Storey DW cases

Typologies	Specifications	District	Median	P[ds]	Equivalent Score	Basic Score	Score Modifier
T02	DW-CW	Zone-I	75	0.01	2.30	3.0	-0.7
		Zone-II	75	0.005	2.60	3.3	-0.7
		Zone-III	75	0.0008	3.40	4.2	-0.8
	DW-QO	Zone-I	67	0.008	2.40	3.0	-0.6
		Zone-II	67	0.004	2.70	3.3	-0.6
		Zone-III	67	0.0005	3.60	4.2	-0.6
	DW-HO	Zone-I	70	0.018	2.05	3.0	-0.9
		Zone-II	70	0.009	2.35	3.3	-0.9
		Zone-III	70	0.002	3.00	4.2	-1.2
	DW-TO	Zone-I	62	0.02	2.00	3.0	-1.0
		Zone-II	62	0.009	2.35	3.3	-0.9
		Zone-III	62	0.002	3.00	4.2	-1.2

Table D-5. T02 Score modifiers for Open Ground Storey DW cases

Typologies	Specifications	District	Median	P[ds]	Equivalent Score	Basic Score	Score Modifier
T02	SW-CW	Zone-I	79	0.01	2.60	3.0	-0.7
		Zone-II	79	0.006	2.82	3.3	-0.7
		Zone-III	79	0.0009	3.65	4.2	-0.8
	SW-QO	Zone-I	78	0.01	2.60	3.0	-0.6
		Zone-II	78	0.004	3.00	3.3	-0.6
		Zone-III	78	0.0007	3.76	4.2	-0.6
	SW-HO	Zone-I	70	0.013	2.49	3.0	-0.9
		Zone-II	70	0.007	2.76	3.3	-0.9
		Zone-III	70	0.001	3.60	4.2	-1.2
	SW-TO	Zone-I	62	0.024	2.22	3.0	-1.0
		Zone-II	62	0.014	2.46	3.3	-0.9
		Zone-III	62	0.002	3.30	4.2	-1.2

Table D-6. Plan Irregularity cases

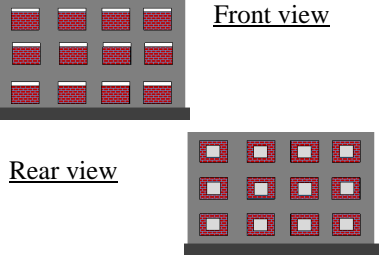
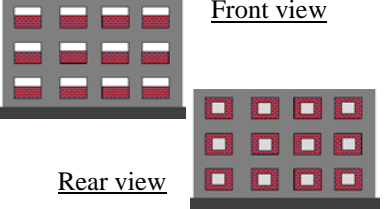
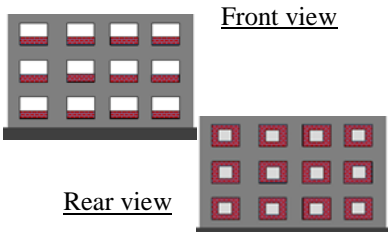
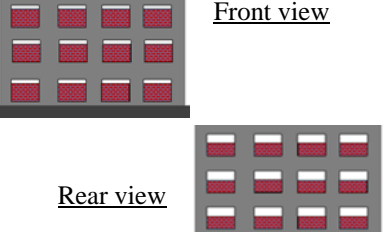
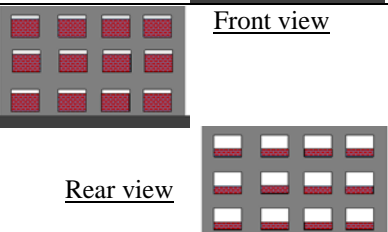
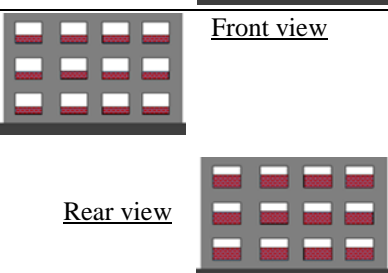
No	Case Name	Case Description	Symmetric Illustration
1	T01/T02-SW/DW-(RCW-FQO)	T01/T02 building with the CW located in rear side and QO presented in front side presented cases in the same storeys and SW/DW cases	 <p>Front view</p> <p>Rear view</p>
2	T01/T02-SW/DW-(RCW-FHO)	T01/T02 building with the CW located in rear side and HO presented in front side presented cases in the same storeys and SW/DW cases	 <p>Front view</p> <p>Rear view</p>
3	T01/T02-SW/DW-(RCW-FTO)	T01/T02 building with the CW located in rear side and TO presented in front side presented cases in the same storeys and SW/DW cases	 <p>Front view</p> <p>Rear view</p>
4	T01/T02-SW/DW-(RQO-FHO)	T01/T02 building with the QO located in rear side and HO presented in front side presented cases in the same storeys and SW/DW cases	 <p>Front view</p> <p>Rear view</p>
5	T01/T02-SW/DW-(RQO-FTO)	T01/T02 building with the QO located in rear side and TO presented in front side presented cases in the same storeys and SW/DW cases	 <p>Front view</p> <p>Rear view</p>
6	T01/T02-SW/DW-(RHO-FTO)	T01/T02 building with the HO located in rear side and TO presented in front side presented cases in the same storeys and SW/DW cases	 <p>Front view</p> <p>Rear view</p>

Table D-7. T01 Score modifiers for plan irregularities DW cases

Typologies	Specifications	District	Median	P[ds]	Equivalent Score	Basic Score	Score Modifier
T01	RCW-FHO (DW)	Zone-I	69	0.03	1.8	2.7	-0.9
		Zone-II	69	0.015	2.1	3.0	-0.9
		Zone-III	69	0.005	2.6	3.3	-0.7
	RCW-FQO (DW)	Zone-I	66	0.028	1.9	2.7	-0.9
		Zone-II	66	0.015	2.1	3.0	-0.9
		Zone-III	66	0.009	2.3	3.3	-0.9
	RCW-FTO (DW)	Zone-I	61	0.03	1.8	2.7	-0.9
		Zone-II	61	0.009	2.3	3.0	-0.6
		Zone-III	61	0.004	2.7	3.3	-0.6
	RHO-FTO (DW)	Zone-I	74	0.05	1.6	2.7	-1.1
		Zone-II	74	0.025	1.9	3.0	-1.1
		Zone-III	74	0.005	2.6	3.3	-0.7
	RQO-FHO (DW)	Zone-I	70	0.035	1.8	2.7	-1.0
		Zone-II	70	0.015	2.1	3.0	-0.9
		Zone-III	70	0.005	2.6	3.3	-0.7
	RQO-FTO (DW)	Zone-I	67	0.04	1.7	2.7	-1.0
		Zone-II	67	0.02	2.0	3.0	-1.0
		Zone-III	67	0.01	2.3	3.3	-1.0

Table D-8. T01 Score modifiers for plan irregularities SW cases

Typologies	Specifications	District	Median	P[ds]	Equivalent Score	Basic Score	Score Modifier
T01	RCW-FHO (SW)	Zone-I	92	0.03	2.0	2.7	-0.7
		Zone-II	92	0.015	2.3	3.0	-0.7
		Zone-III	92	0.005	2.6	3.3	-0.7
	RCW-FQO (SW)	Zone-I	72	0.028	2.1	2.7	-0.6
		Zone-II	72	0.015	2.4	3.0	-0.6
		Zone-III	72	0.009	3.2	3.3	-0.1
	RCW-FTO (SW)	Zone-I	78	0.03	2.2	2.7	-0.5
		Zone-II	78	0.009	2.5	3.0	-0.5
		Zone-III	78	0.004	3.2	3.3	-0.1
	RHO-FTO (SW)	Zone-I	74	0.05	1.8	2.7	-0.9
		Zone-II	74	0.025	2.2	3.0	-0.8
		Zone-III	74	0.005	2.8	3.3	-0.5
	RQO-FHO (SW)	Zone-I	76	0.035	2.0	2.7	-0.7
		Zone-II	76	0.015	2.3	3.0	-0.7
		Zone-III	76	0.005	2.4	3.3	-0.9
	RQO-FTO (SW)	Zone-I	70	0.04	1.8	2.7	-0.9
		Zone-II	70	0.02	2.1	3.0	-0.9
		Zone-III	70	0.01	2.3	3.3	-1.0

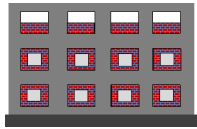
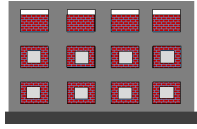
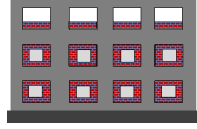
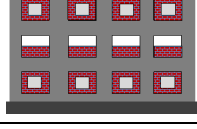

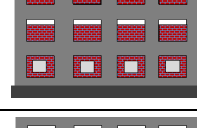

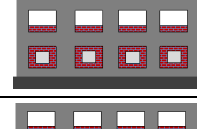
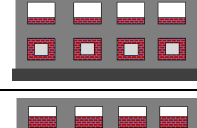
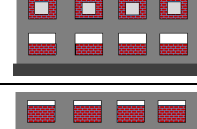

Table D-9. T02 Score modifiers for plan irregularities DW cases

Typologies	Specifications	District	Median	P[ds]	Equivalent Score	Basic Score	Score Modifier
T02	RCW-FHO (DW)	Zone-I	75	0.018	2.0	3.0	-0.9
		Zone-II	75	0.008	2.4	3.3	-0.9
		Zone-III	75	0.0016	3.1	4.2	-1.1
	RCW-FQO (DW)	Zone-I	74	0.02	2.0	3.0	-1.0
		Zone-II	74	0.008	2.4	3.3	-0.9
		Zone-III	74	0.0018	3.0	4.2	-1.1
	RCW-FTO (DW)	Zone-I	74	0.018	2.0	3.0	-0.9
		Zone-II	74	0.006	2.5	3.3	-0.8
		Zone-III	74	0.0018	3.0	4.2	-1.1
	RHO-FTO (DW)	Zone-I	67	0.03	1.8	3.0	-1.2
		Zone-II	67	0.018	2.0	3.3	-1.2
		Zone-III	67	0.008	2.4	4.2	-1.8
	RQO-FHO (DW)	Zone-I	72	0.01	2.3	3.0	-0.7
		Zone-II	72	0.0016	3.1	3.3	-0.2
		Zone-III	72	0.0008	3.4	4.2	-0.8
	RQO-FTO (DW)	Zone-I	66	0.018	2.0	3.0	-0.9
		Zone-II	66	0.004	2.7	3.3	-0.6
		Zone-III	66	0.0008	3.4	4.2	-0.8

Table D-10. T02 Score modifiers for plan irregularities SW cases

Typologies	Specifications	District	Median	P[ds]	Equivalent Score	Basic Score	Score Modifier
T02	RCW-FHO (SW)	Zone-I	74	0.012	2.2	3.0	-0.8
		Zone-II	74	0.006	2.5	3.3	-0.8
		Zone-III	74	0.001	3.3	4.2	-0.9
	RCW-FQO (SW)	Zone-I	70	0.01	2.3	3.0	-0.7
		Zone-II	70	0.004	2.7	3.3	-0.6
		Zone-III	70	0.0006	3.5	4.2	-0.7
	RCW-FTO (SW)	Zone-I	73	0.01	2.3	3.0	-0.7
		Zone-II	73	0.005	2.6	3.3	-0.7
		Zone-III	73	0.0009	3.3	4.2	-0.8
	RHO-FTO (SW)	Zone-I	66	0.018	2.0	3.0	-0.9
		Zone-II	66	0.011	2.3	3.3	-1.0
		Zone-III	66	0.004	2.7	4.2	-1.5
	RQO-FHO (SW)	Zone-I	79	0.009	2.3	3.0	-0.6
		Zone-II	79	0.006	2.5	3.3	-0.8
		Zone-III	79	0.001	3.3	4.2	-0.9
	RQO-FTO (SW)	Zone-I	69	0.016	2.1	3.0	-0.9
		Zone-II	69	0.01	2.3	3.3	-1.0
		Zone-III	69	0.003	2.8	4.2	-1.4

Table D-11. Vertical Irregularity cases

No	Case Name	Case Description	Symmetric Illustration (similar configuration in front and rear)
1	T01/T02- SW/DW- {GF(CW)- FF(CW)-SF(HO)}	T01/T02 building with the CW located at GF, CW located at FF and HO located at SF with SW/DW cases	
2	T01/T02- SW/DW- {GF(CW)- FF(CW)-SF(QO)}	T01/T02 building with the CW located at GF, CW located at FF and QO located at SF with SW/DW cases	
3	T01/T02- SW/DW- {GF(CW)- FF(CW)-SF(TO)}	T01/T02 building with the CW located at GF, CW located at FF and TO located at SF with SW/DW cases	
4	T01/T02- SW/DW- {GF(CW)- FF(HO)-SF(CW)}	T01/T02 building with the CW located at GF, HO located at FF and CW located at SF with SW/DW cases	
5	T01/T02- SW/DW- {GF(CW)- FF(HO)-SF(HO)}	T01/T02 building with the CW located at GF, HO located at FF and HO located at SF with SW/DW cases	
6	T01/T02- SW/DW- {GF(CW)- FF(QO)-SF(CW)}	T01/T02 building with the CW located at GF, QO located at FF and CW located at SF with SW/DW cases	
7	T01/T02- SW/DW- {GF(CW)- FF(QO)-SF(QO)}	T01/T02 building with the CW located at GF, QO located at FF and QO located at SF with SW/DW cases	
8	T01/T02- SW/DW- {GF(CW)-FF(TO)- SF(CW)}	T01/T02 building with the CW located at GF, TO located at FF and CW located at SF with SW/DW cases	
9	T01/T02- SW/DW- {GF(CW)-FF(TO)- SF(TO)}	T01/T02 building with the CW located at GF, TO located at FF and TO located at SF with SW/DW cases	
10	T01/T02- SW/DW- {GF(HO)- FF(CW)-SF(HO)}	T01/T02 building with the HO located at GF, CW located at FF and HO located at SF with SW/DW cases	
11	T01/T02- SW/DW- {GF(HO)- FF(CW)-SF(QO)}	T01/T02 building with the HO located at GF, CW located at FF and QO located at SF with SW/DW cases	

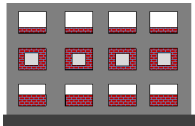
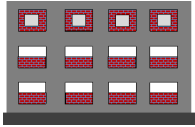
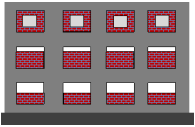
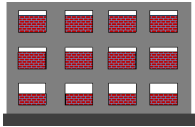
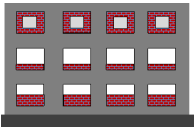

12	T01/T02- SW/DW- {GF(HO)- FF(CW)-SF(TO)}	T01/T02 building with the HO located at GF, CW located at FF and TO located at SF with SW/DW cases	
13	T01/T02- SW/DW- {GF(HO)-FF(HO)- SF(CW)}	T01/T02 building with the HO located at GF, HO located at FF and CW located at SF with SW/DW cases	
14	T01/T02- SW/DW- {GF(HO)-FF(QO)- SF(CW)}	T01/T02 building with the HO located at GF, QO located at FF and CW located at SF with SW/DW cases	
15	T01/T02- SW/DW- {GF(HO)-FF(QO)- SF(QO)}	T01/T02 building with the HO located at GF, QO located at FF and QO located at SF with SW/DW cases	
16	T01/T02- SW/DW- {GF(HO)-FF(TO)- SF(CW)}	T01/T02 building with the HO located at GF, TO located at FF and CW located at SF with SW/DW cases	
17	T01/T02- SW/DW- {GF(HO)-FF(TO)- SF(TO)}	T01/T02 building with the HO located at GF, TO located at FF and TO located at SF with SW/DW cases	

Table D-12. T01 Score modifiers for Vertical irregularities DW cases

Typologies	Specifications	District	Median	P[ds]	Equivalent Score	Basic Score	Score Modifier
T01	GF(CW)- FF(CW)- SF(HO) (DW)	Zone-I	64	0.0044	2.7	2.7	-0.1
		Zone-II	64	0.003	2.8	3.0	-0.2
		Zone-III	64	0.0016	3.1	3.3	-0.2
	GF(CW)- FF(CW)- SF(QO) (DW)	Zone-I	69	0.0038	2.7	2.7	0.0
		Zone-II	69	0.003	2.8	3.0	-0.2
		Zone-III	69	0.002	3.0	3.3	-0.3
	GF(CW)- FF(CW)- SF(TO) (DW)	Zone-I	58	0.008	2.4	2.7	-0.3
		Zone-II	58	0.004	2.7	3.0	-0.3
		Zone-III	58	0.0024	2.9	3.3	-0.4
	GF(CW)- FF(HO)- SF(CW) (DW)	Zone-I	66	0.04	1.7	2.7	-1.0
		Zone-II	66	0.018	2.0	3.0	-0.9
		Zone-III	66	0.008	2.4	3.3	-0.9
	GF(CW)- FF(HO)- SF(HO) (DW)	Zone-I	67	0.05	1.6	2.7	-1.1
		Zone-II	67	0.024	1.9	3.0	-1.1
		Zone-III	67	0.01	2.3	3.3	-1.0
	GF(CW)- FF(QO)- SF(CW) (DW)	Zone-I	69	0.005	2.6	2.7	-0.1
		Zone-II	69	0.003	2.8	3.0	-0.2
		Zone-III	69	0.002	3.0	3.3	-0.3
	GF(CW)- FF(QO)- SF(QO) (DW)	Zone-I	68	0.006	2.5	2.7	-0.2
		Zone-II	68	0.004	2.7	3.0	-0.3
		Zone-III	68	0.0018	3.0	3.3	-0.2
	Zone-I	72	0.06	1.5	2.7	-1.2	
	Zone-II	72	0.048	1.6	3.0	-1.4	

	GF(CW)- FF(TO)- SF(CW) (DW)	Zone-III	72	0.02	2.0	3.3	-1.3
	GF(CW)- FF(TO)- SF(TO) (DW)	Zone-I	66	0.08	1.4	2.7	-1.3
		Zone-II	66	0.044	1.7	3.0	-1.3
		Zone-III	66	0.02	2.0	3.3	-1.3
	GF(HO)- FF(CW)- SF(HO) (DW)	Zone-I	73	0.036	1.7	2.7	-1.0
		Zone-II	73	0.02	2.0	3.0	-1.0
		Zone-III	73	0.01	2.3	3.3	-1.0
	GF(HO)- FF(CW)- SF(QO) (DW)	Zone-I	76	0.036	1.7	2.7	-1.0
		Zone-II	76	0.02	2.0	3.0	-1.0
		Zone-III	76	0.006	2.5	3.3	-0.8
	GF(HO)- FF(CW)- SF(TO) (DW)	Zone-I	69	0.024	1.9	2.7	-0.8
		Zone-II	69	0.01	2.3	3.0	-0.7
		Zone-III	69	0.002	3.0	3.3	-0.3
	GF(HO)- FF(HO)- SF(CW) (DW)	Zone-I	73	0.03	1.8	2.7	-0.9
		Zone-II	73	0.02	2.0	3.0	-1.0
		Zone-III	73	0.01	2.3	3.3	-1.0
	GF(HO)- FF(QO)- SF(CW) (DW)	Zone-I	71	0.036	1.7	2.7	-1.0
		Zone-II	71	0.02	2.0	3.0	-1.0
		Zone-III	71	0.008	2.4	3.3	-0.9
	GF(HO)- FF(QO)- SF(QO) (DW)	Zone-I	71	0.038	1.7	2.7	-1.0
		Zone-II	71	0.022	2.0	3.0	-1.0
Zone-III		71	0.01	2.3	3.3	-1.0	
GF(HO)- FF(TO)- SF(CW) (DW)	Zone-I	73	0.06	1.5	2.7	-1.2	
	Zone-II	73	0.03	1.8	3.0	-1.2	
	Zone-III	73	0.008	2.4	3.3	-0.9	
GF(HO)- FF(TO)- SF(TO) (DW)	Zone-I	67	0.07	1.5	2.7	-1.3	
	Zone-II	67	0.036	1.7	3.0	-1.2	
	Zone-III	67	0.01	2.3	3.3	-1.0	

Table D-13. T01 Score modifiers for Vertical irregularities SW cases

Typologies	Specifications	District	Median	P[ds]	Equivalent Score	Basic Score	Score Modifier	
T01	GF(CW)- FF(CW)- SF(HO) (DW)	Zone-I	66	0.01	2.6	2.7	-0.1	
		Zone-II	66	0.003	3.1	3.0	0.1	
		Zone-III	66	0.0018	3.3	3.3	0.1	
	GF(CW)- FF(CW)- SF(QO) (DW)	Zone-I	70	0.012	2.5	2.7	-0.2	
		Zone-II	70	0.004	3.0	3.0	0.0	
		Zone-III	70	0.0014	3.5	3.3	0.2	
	GF(CW)- FF(CW)- SF(TO) (DW)	Zone-I	62	0.016	2.4	2.7	-0.3	
		Zone-II	62	0.004	3.0	3.0	0.0	
		Zone-III	62	0.0012	3.5	3.3	0.2	
	GF(CW)- FF(HO)- SF(CW) (DW)	Zone-I	68	0.018	2.3	2.7	-0.4	
		Zone-II	68	0.01	2.6	3.0	-0.4	
		Zone-III	68	0.0016	3.4	3.3	0.1	
	GF(CW)- FF(HO)- SF(HO) (DW)	Zone-I	65	0.04	2.0	2.7	-0.7	
		Zone-II	65	0.02	2.3	3.0	-0.7	
		Zone-III	65	0.012	2.5	3.3	-0.8	
	GF(CW)- FF(QO)- SF(CW) (DW)	Zone-I	69	0.018	2.3	2.7	-0.4	
		Zone-II	69	0.004	3.0	3.0	0.0	
		Zone-III	69	0.0012	3.5	3.3	0.2	
			Zone-I	69	0.018	2.3	2.7	-0.4

GF(CW)- FF(QO)- SF(QO) (DW)	Zone-II	69	0.004	3.0	3.0	0.0
	Zone-III	69	0.0012	3.5	3.3	0.2
GF(CW)- FF(TO)- SF(CW) (DW)	Zone-I	73	0.038	2.0	2.7	-0.7
	Zone-II	73	0.02	2.3	3.0	-0.7
	Zone-III	73	0.012	2.5	3.3	-0.8
GF(CW)- FF(TO)- SF(TO) (DW)	Zone-I	66	0.072	1.7	2.7	-1.0
	Zone-II	66	0.04	2.0	3.0	-1.0
	Zone-III	66	0.02	2.3	3.3	-1.0
GF(HO)- FF(CW)- SF(HO) (DW)	Zone-I	71	0.046	1.9	2.7	-0.8
	Zone-II	71	0.024	2.2	3.0	-0.8
	Zone-III	71	0.01	2.6	3.3	-0.7
GF(HO)- FF(CW)- SF(QO) (DW)	Zone-I	69	0.04	2.0	2.7	-0.7
	Zone-II	69	0.02	2.3	3.0	-0.7
	Zone-III	69	0.008	2.7	3.3	-0.6
GF(HO)- FF(CW)- SF(TO) (DW)	Zone-I	64	0.036	2.0	2.7	-0.7
	Zone-II	64	0.016	2.4	3.0	-0.6
	Zone-III	64	0.004	3.0	3.3	-0.3
GF(HO)- FF(HO)- SF(CW) (DW)	Zone-I	67	0.048	1.9	2.7	-0.8
	Zone-II	67	0.03	2.1	3.0	-0.9
	Zone-III	67	0.008	2.7	3.3	-0.6
GF(HO)- FF(QO)- SF(CW) (DW)	Zone-I	89	0.04	2.0	2.7	-0.7
	Zone-II	89	0.02	2.3	3.0	-0.7
	Zone-III	89	0.007	2.8	3.3	-0.5
GF(HO)- FF(QO)- SF(QO) (DW)	Zone-I	70	0.04	2.0	2.7	-0.7
	Zone-II	70	0.016	2.4	3.0	-0.6
	Zone-III	70	0.004	3.0	3.3	-0.3
GF(HO)- FF(TO)- SF(CW) (DW)	Zone-I	67	0.038	2.0	2.7	-0.7
	Zone-II	67	0.02	2.3	3.0	-0.7
	Zone-III	67	0.008	2.7	3.3	-0.6
GF(HO)- FF(TO)- SF(TO) (DW)	Zone-I	67	0.036	2.0	2.7	-0.7
	Zone-II	67	0.016	2.4	3.0	-0.6
	Zone-III	67	0.003	3.1	3.3	-0.2

Table D-14. T02 Score modifiers for Vertical irregularities DW cases

Typologies	Specifications	District	Median	P[ds]	Equivalent Score	Basic Score	Score Modifier
T01	GF(CW)- FF(CW)- SF(HO) (DW)	Zone-I	72	0.024	1.9	3.0	-1.1
		Zone-II	72	0.014	2.2	3.3	-1.1
		Zone-III	72	0.004	2.7	4.2	-1.5
	GF(CW)- FF(CW)- SF(QO) (DW)	Zone-I	72	0.024	1.9	3.0	-1.1
		Zone-II	72	0.016	2.1	3.3	-1.2
		Zone-III	72	0.006	2.5	4.2	-1.7
	GF(CW)- FF(CW)- SF(TO) (DW)	Zone-I	67	0.02	2.0	3.0	-1.0
		Zone-II	67	0.01	2.3	3.3	-1.0
		Zone-III	67	0.0018	3.0	4.2	-1.1
	GF(CW)- FF(HO)- SF(CW) (DW)	Zone-I	70	0.018	2.0	3.0	-0.9
		Zone-II	70	0.006	2.5	3.3	-0.8
		Zone-III	70	0.0016	3.1	4.2	-1.1
	GF(CW)- FF(HO)- SF(HO) (DW)	Zone-I	71	0.02	2.0	3.0	-1.0
		Zone-II	71	0.01	2.3	3.3	-1.0
		Zone-III	71	0.0014	3.2	4.2	-1.0

GF(CW)- FF(QO)- SF(CW) (DW)	Zone-I	75	0.026	1.9	3.0	-1.1
	Zone-II	75	0.014	2.2	3.3	-1.1
	Zone-III	75	0.002	3.0	4.2	-1.2
GF(CW)- FF(QO)- SF(QO) (DW)	Zone-I	76	0.02	2.0	3.0	-1.0
	Zone-II	76	0.01	2.3	3.3	-1.0
	Zone-III	76	0.001	3.3	4.2	-0.9
GF(CW)- FF(TO)- SF(CW) (DW)	Zone-I	82	0.044	1.7	3.0	-1.3
	Zone-II	82	0.032	1.8	3.3	-1.5
	Zone-III	82	0.014	2.2	4.2	-2.0
GF(CW)- FF(TO)- SF(TO) (DW)	Zone-I	64	0.08	1.4	3.0	-1.6
	Zone-II	64	0.06	1.5	3.3	-1.8
	Zone-III	64	0.02	2.0	4.2	-2.2
GF(HO)- FF(CW)- SF(HO) (DW)	Zone-I	75	0.042	1.7	3.0	-1.3
	Zone-II	75	0.032	1.8	3.3	-1.5
	Zone-III	75	0.01	2.3	4.2	-1.9
GF(HO)- FF(CW)- SF(QO) (DW)	Zone-I	80	0.046	1.6	3.0	-1.3
	Zone-II	80	0.026	1.9	3.3	-1.4
	Zone-III	80	0.016	2.1	4.2	-2.1
GF(HO)- FF(CW)- SF(TO) (DW)	Zone-I	71	0.042	1.7	3.0	-1.3
	Zone-II	71	0.02	2.0	3.3	-1.3
	Zone-III	71	0.008	2.4	4.2	-1.8
GF(HO)- FF(HO)- SF(CW) (DW)	Zone-I	75	0.036	1.7	3.0	-1.2
	Zone-II	75	0.02	2.0	3.3	-1.3
	Zone-III	75	0.01	2.3	4.2	-1.9
GF(HO)- FF(QO)- SF(CW) (DW)	Zone-I	78	0.038	1.7	3.0	-1.3
	Zone-II	78	0.02	2.0	3.3	-1.3
	Zone-III	78	0.008	2.4	4.2	-1.8
GF(HO)- FF(QO)- SF(QO) (DW)	Zone-I	79	0.038	1.7	3.0	-1.3
	Zone-II	79	0.016	2.1	3.3	-1.2
	Zone-III	79	0.004	2.7	4.2	-1.5
GF(HO)- FF(TO)- SF(CW) (DW)	Zone-I	75	0.08	1.4	3.0	-1.6
	Zone-II	75	0.054	1.6	3.3	-1.7
	Zone-III	75	0.036	1.7	4.2	-2.4
GF(HO)- FF(TO)- SF(TO) (DW)	Zone-I	63	0.12	1.2	3.0	-1.8
	Zone-II	63	0.08	1.4	3.3	-1.9
	Zone-III	63	0.04	1.7	4.2	-2.5

Table D-15. T02 Score modifiers for Vertical irregularities SW cases

Typologies	Specifications	District	Median	P[ds]	Equivalent Score	Basic Score	Score Modifier
T01	GF(CW)- FF(CW)- SF(HO) (DW)	Zone-I	72	0.036	2.0	3.0	-0.9
		Zone-II	72	0.016	2.4	3.3	-0.9
		Zone-III	72	0.002	3.3	4.2	-0.9
	GF(CW)- FF(CW)- SF(QO) (DW)	Zone-I	74	0.028	2.2	3.0	-0.8
		Zone-II	74	0.02	2.3	3.3	-1.0
		Zone-III	74	0.01	2.6	4.2	-1.6
	GF(CW)- FF(CW)- SF(TO) (DW)	Zone-I	70	0.02	2.3	3.0	-0.7
		Zone-II	70	0.012	2.5	3.3	-0.8
		Zone-III	70	0.001	3.6	4.2	-0.6
	GF(CW)- FF(HO)- SF(CW) (DW)	Zone-I	75	0.02	2.3	3.0	-0.7
		Zone-II	75	0.01	2.6	3.3	-0.7
		Zone-III	75	0.0012	3.5	4.2	-0.7
		Zone-I	74	0.018	2.3	3.0	-0.6

GF(CW)- FF(HO)- SF(HO) (DW)	Zone-II	74	0.008	2.7	3.3	-0.6
	Zone-III	74	0.0008	3.7	4.2	-0.5
GF(CW)- FF(QO)- SF(CW) (DW)	Zone-I	73	0.02	2.3	3.0	-0.7
	Zone-II	73	0.012	2.5	3.3	-0.8
	Zone-III	73	0.0016	3.4	4.2	-0.8
GF(CW)- FF(QO)- SF(QO) (DW)	Zone-I	78	0.018	2.3	3.0	-0.6
	Zone-II	78	0.004	3.0	3.3	-0.3
	Zone-III	78	0.001	3.6	4.2	-0.6
GF(CW)- FF(TO)- SF(CW) (DW)	Zone-I	65	0.016	2.4	3.0	-0.6
	Zone-II	65	0.006	2.8	3.3	-0.5
	Zone-III	65	0.0012	3.5	4.2	-0.7
GF(CW)- FF(TO)- SF(TO) (DW)	Zone-I	62	0.01	2.6	3.0	-0.4
	Zone-II	62	0.002	3.3	3.3	0.0
	Zone-III	62	0.0006	3.8	4.2	-0.4
GF(HO)- FF(CW)- SF(HO) (DW)	Zone-I	79	0.038	2.0	3.0	-1.0
	Zone-II	79	0.02	2.3	3.3	-1.0
	Zone-III	79	0.01	2.6	4.2	-1.6
GF(HO)- FF(CW)- SF(QO) (DW)	Zone-I	80	0.036	2.0	3.0	-0.9
	Zone-II	80	0.02	2.3	3.3	-1.0
	Zone-III	80	0.01	2.6	4.2	-1.6
GF(HO)- FF(CW)- SF(TO) (DW)	Zone-I	74	0.032	2.1	3.0	-0.9
	Zone-II	74	0.02	2.3	3.3	-1.0
	Zone-III	74	0.01	2.6	4.2	-1.6
GF(HO)- FF(HO)- SF(CW) (DW)	Zone-I	77	0.028	2.2	3.0	-0.8
	Zone-II	77	0.018	2.3	3.3	-0.9
	Zone-III	77	0.004	3.0	4.2	-1.2
GF(HO)- FF(QO)- SF(CW) (DW)	Zone-I	77	0.036	2.0	3.0	-0.9
	Zone-II	77	0.016	2.4	3.3	-0.9
	Zone-III	77	0.0006	3.8	4.2	-0.4
GF(HO)- FF(QO)- SF(QO) (DW)	Zone-I	81	0.03	2.1	3.0	-0.9
	Zone-II	81	0.018	2.3	3.3	-0.9
	Zone-III	81	0.004	3.0	4.2	-1.2
GF(HO)- FF(TO)- SF(CW) (DW)	Zone-I	70	0.036	2.0	3.0	-0.9
	Zone-II	70	0.018	2.3	3.3	-0.9
	Zone-III	70	0.002	3.3	4.2	-0.9
GF(HO)- FF(TO)- SF(TO) (DW)	Zone-I	70	0.036	2.0	3.0	-0.9
	Zone-II	70	0.02	2.3	3.3	-1.0
	Zone-III	70	0.008	2.7	4.2	-1.5

Rapid Visual Screening of School Buildings - Sri Lanka (Pre-Earthquake Analysis)							
School Name: _____			Date: _____				
Address: _____			Latitude: _____		Longitude: _____		
Purpose of the Building: _____		Year Built: _____		School ID: _____	Building ID: _____		
No. Stories: <input type="checkbox"/> Two <input type="checkbox"/> Three	Typology: <input type="checkbox"/> 1 <input type="checkbox"/> 2	Extension/ modification: <input type="checkbox"/> Yes <input type="checkbox"/> No (Highlight in the drawing)					
Foundation: <input type="checkbox"/> Spread Other: _____		Previous Hazard History: _____					
Please Mark the beam and column dimensions							
Side View		Front View			Rear View		
Story Height: _____		No of Bays: Longitudinal: _____ Transverse: _____		Bay Width: Longitudinal: _____ Transverse: _____			
Total Floor Area (Sq.m): _____		Thickness of MI: Exterior _____ Interior _____		Width of MI: Exterior: _____ Interior: _____			
Staircase: No: _____ Location: _____		Storey	Front Side	Middle	Rear Side		
Special Componets: <input type="checkbox"/> Shear Wall <input type="checkbox"/> Taperd (B/C)		GF	<input type="checkbox"/> CW <input type="checkbox"/> QO <input type="checkbox"/> HO <input type="checkbox"/> TO	<input type="checkbox"/> CW <input type="checkbox"/> QO <input type="checkbox"/> HO <input type="checkbox"/> TO	<input type="checkbox"/> CW <input type="checkbox"/> QO <input type="checkbox"/> HO <input type="checkbox"/> TO		
Roof Truss : <input type="checkbox"/> Wood <input type="checkbox"/> Steel Other: _____		FF	<input type="checkbox"/> CW <input type="checkbox"/> QO <input type="checkbox"/> HO <input type="checkbox"/> TO	<input type="checkbox"/> CW <input type="checkbox"/> QO <input type="checkbox"/> HO <input type="checkbox"/> TO	<input type="checkbox"/> CW <input type="checkbox"/> QO <input type="checkbox"/> HO <input type="checkbox"/> TO		
Roof Material: _____		SF	<input type="checkbox"/> CW <input type="checkbox"/> QO <input type="checkbox"/> HO <input type="checkbox"/> TO	<input type="checkbox"/> CW <input type="checkbox"/> QO <input type="checkbox"/> HO <input type="checkbox"/> TO	<input type="checkbox"/> CW <input type="checkbox"/> QO <input type="checkbox"/> HO <input type="checkbox"/> TO		
Opening Window: <input type="checkbox"/> Steel grid <input type="checkbox"/> Wood <input type="checkbox"/> No windows <input type="checkbox"/> Any other: _____							
Building Risk Scores							
Characteristics		Type - 01			Type - 02		
		Zone-I	Zone-II	Zone-III	Zone-I	Zone - II	Zone - III
Basic Score		2.7	3	3.3	3.0	3.3	4.2
Open Ground Storey (OGS)		-1.0	-0.9	-0.8	---	---	---
Vertical Irregularity (VI)	SW	-1.0	-1.1	-1.0	-1.1	-1.2	-1.7
	DW	-1.5	-1.5	-1.3	-1.6	-1.8	-2.5
Plan Irregularity (PI)	SW	-1.0	-0.9	-1.1	-1.0	-1.1	-1.7
	DW	-1.1	-1.2	-1.1	-1.2	-1.3	-1.8
Short columns (SC)		-1.1	-1.1	-1.0	-1.1	-1.1	-1.4
Minimum score (Smin)		1.0	1.0	0.9	1.2	1.2	1.2
Final Score (Level 1)							
Comments:							

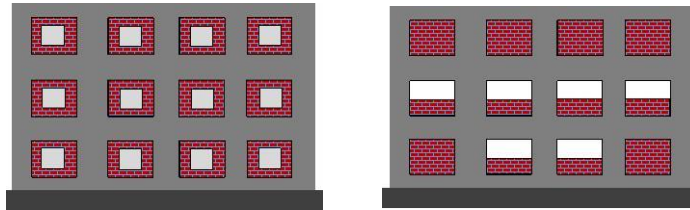
Surveyor Name: _____

Signature: _____

Figure D-1. Proposed RVS and description

Description for score selection

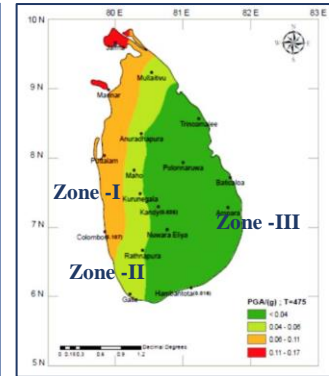
2. Vertical Irregularity



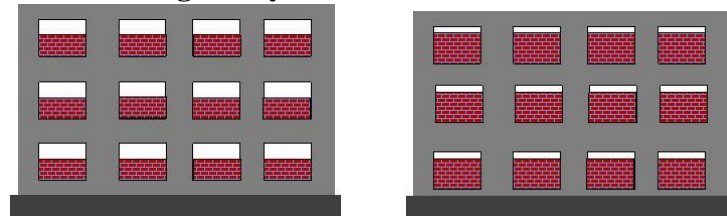
Rear view

Front view

- When the opening size of the walls in the vertical direction is asymmetrical
- The score should be highlighted based on the thickness of the wall

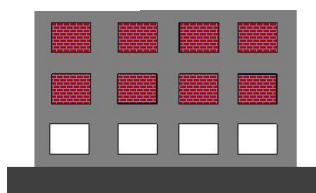


3. Plan Irregularity



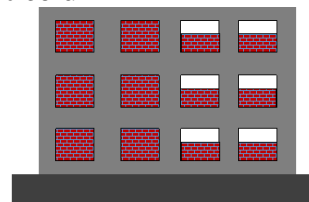
- Both side of the building has various height of the wall
- The score should be highlighted based on the thickness of the wall

1. OGS



- When ground floor has open ground storey

4. Short column



- $\geq 60\%$ short columns in adjacent sides
- It should be selected when there is either plan or vertical irregularity